Search for large missing transverse momentum in association with one top-quark in proton-proton collisions at √s = 13 TeV with the ATLAS detector

The ATLAS Collaboration

DOI
10.1007/JHEP05(2019)041

Publication date
2019

Document Version
Final published version

Published in
Journal of High Energy Physics

Published for SISSA by Springer

Received: *December 28, 2018*
Revised: *April 1, 2019*
Accepted: *April 22, 2019*
Published: *May 7, 2019*

Search for large missing transverse momentum in association with one top-quark in proton–proton collisions at $\sqrt{s} = 13$ TeV with the ATLAS detector

The ATLAS collaboration

E-mail: atlas.publications@cern.ch

Abstract: This paper describes a search for events with one top-quark and large missing transverse momentum in the final state. Data collected during 2015 and 2016 by the ATLAS experiment from 13 TeV proton–proton collisions at the LHC corresponding to an integrated luminosity of 36.1 fb^{-1} are used. Two channels are considered, depending on the leptonic or the hadronic decays of the W boson from the top quark. The obtained results are interpreted in the context of simplified models for dark-matter production and for the single production of a vector-like T quark. In the absence of significant deviations from the Standard Model background expectation, 95% confidence-level upper limits on the corresponding production cross-sections are obtained and these limits are translated into constraints on the parameter space of the models considered.

Keywords: Beyond Standard Model, Dark matter, FCNC Interaction, Hadron-Hadron scattering (experiments), vector-like quarks

ArXiv ePrint: 1812.09743

https://doi.org/10.1007/JHEP05(2019)041

Contents

JHEP05(2019)041

1 Introduction

In spite of its successes in describing the phenomenology of the fundamental particles and the corresponding interactions, the Standard Model (SM) can be considered as a low-energy approximation of a more fundamental theory with new degrees of freedom and symmetries that would become manifest at a higher energy.

One argument supporting the idea that new particles beyond the SM might exist arises from astrophysical measurements, such as the rotational speed of stars in galaxies and gravitational lensing [1–3]. These observations point to the existence of non-light-emitting matter, a dominant fraction of which is of non-baryonic form, usually referred to as dark matter (DM). Even if there are no viable candidates in the SM for particles which could explain DM, proton–proton collisions at the Large Hadron Collider (LHC) may possibly produce new particles that couple both to SM particles and to these DM candidates. While such candidates are not expected to interact significantly with detectors, the SM particles produced in association with the unobserved DM particles could allow these processes to be detected. Search strategies depend on the type of particle or system that is recoiling against the unseen particle. Both ATLAS and CMS have carried out searches for invisible particles produced in association with jets [4–7], photons [8, 9], W or Z bosons [5, 10, 11] and Higgs bosons [12–15], significantly constraining the allowed parameter space for different classes of models predicting DM candidates.

This paper describes a search for the production of invisible particles in association with a single top-quark in proton–proton collisions produced at the LHC with a centre-of-mass energy of $\sqrt{s} = 13$ TeV and detected using the ATLAS detector. Such a final state, commonly referred to as "mono-top", is characterised by a top-quark and significant missing transverse momentum, which is due to the undetected particles. Background contributions from SM processes [16] are expected to be small. In addition, this search is sensitive to specific DM models, since the presence of top-quarks in the final state constrains the flavour structure of the considered couplings [17, 18]. Similar searches were previously conducted by the CDF Collaboration using 7.7 fb^{-1} of Tevatron $p\bar{p}$ collisions at $\sqrt{s} = 1.96$ TeV [19] and by the ATLAS and CMS collaborations using $\sqrt{s} = 8$ TeV [20, 21] and $\sqrt{s} = 13$ TeV [22] LHC data. Searches for new phenomena in events with same-charge leptons and b-tagged jets [23] provide information complementary to the results from mono-top searches and exclude new vector resonances with masses up to 3 TeV, assuming a dark-sector coupling of 1.0 and a coupling to SM particles above 0.3.

A final state with a top-quark and missing transverse momentum can also originate from the single production of new vector-like quarks if these decay into a top-quark and a Z boson that decays invisibly into two neutrinos. Vector-like quarks are colour-triplet spin-1/2 fermions in which, in contrast to the SM quarks, the left- and right-handed components have the same properties under transformations of the electroweak symmetry group $\mathrm{SU(2)_L} \times \mathrm{U(1)_Y}$. Such new particles are predicted in SM extensions, such as Little Higgs [24, 25] and Composite Higgs [26, 27] models, and are expected to mix with SM quarks [28]. In order to preserve gauge invariance, only a limited set of possible representations exist [29, 30] and their electric charge can be $+2/3e$ (T quark), $-1/3e$ (B quark), $+5/3e$ (X quark) or $-4/3e$ (Y quark), with e being the elementary charge. In this paper, only the single production of vector-like T quarks (VLT) via an electroweak interaction is considered. Although couplings of T quarks to first- and second-generation SM quarks are not excluded [31, 32], it is common to assume that they couple exclusively to third-generation SM quarks [33]. Such couplings can be described in terms of $\sin\theta_\mathrm{L}$ [34], where θ_L is the mixing angle of the T quark with the top-quark, or in terms of a generalised coupling κ_T [35, 36]. The T quarks can decay either via the charged current, i.e. $T \rightarrow Wb$, or via flavour-changing neutral currents [37], i.e. $T \rightarrow Zt$ and $T \rightarrow Ht$. The $T \rightarrow Zt \rightarrow \nu\bar{\nu}Wb$ decay is considered in the present search.

The ATLAS and CMS collaborations have sought pair production of T quarks decaying into third-generation quarks in pp collisions at a centre-of-mass energy of 8 TeV [38–41], targeting all three possible decay modes. Searches at 13 TeV have aimed at final states with leptons, targeting the $T \rightarrow Zt$ decay [42, 43], the $T \rightarrow Wb$ decay [44, 45], as well as general single-lepton and fully hadronic final states with boosted bosons [46, 47] and multiple b-

tagged jets [46, 48, 49]. The most stringent mass limit for an isospin singlet T is 1.3 TeV [50]. For such large T masses, the cross-section for single T production may be larger than the pair-production cross-section because of the larger available phase space. Nonetheless, the comparison of single- and pair-production cross-sections depends on the assumed coupling to the SM quarks. Single production of T quarks was sought at 8 TeV [40, 51, 52] by the ATLAS Collaboration. At 13 TeV, the ATLAS and CMS collaborations have sought the decays $T \to Wb$ [53, 54], $T \to Ht$ [55, 56] and $T \to Zt$ [43, 57, 58].

In this paper, two channels for the mono-top signature are considered, targeting the case in which the W boson originating from the top-quark decays into an electron or muon and a neutrino (leptonic channel) and the case in which it decays into a pair of quarks (hadronic channel). These analyses define different signal regions, maximising the signal discovery sensitivity, and control regions, enriched with the dominant background processes. The statistical interpretation of the results is based on a simultaneous fit to the signal and control regions to determine a possible signal contribution and constrain the main backgrounds with data, taking into account experimental and theoretical systematic uncertainties.

The paper is organised as follows. The signal models are introduced in section 2. After a brief introduction to the ATLAS detector, given in section 3, the data samples and samples of simulated signal and background events are described in section 4. The algorithms for the reconstruction and identification of final-state particles are summarised in section 5. Section 6 describes the criteria for the selection of candidate signal events. This section also describes the estimation of the background contribution with the help of dedicated control regions in data. The experimental and theoretical systematic uncertainties (section 7) are taken into account in the statistical interpretation of data, with the results presented in section 8. Concluding remarks are given in section 9.

2 Signal phenomenology

This paper presents a search for two different signals: DM candidates produced in association with top-quarks and single production of vector-like T quarks decaying into a top-quark and a Z boson.

2.1 DM candidates associated with top-quarks

In this search the resonant and non-resonant production of DM particles associated with a top-quark are considered. The non-resonant case, represented in figure 1(a) and figure 1(b), corresponds to a flavour-changing neutral-current interaction, producing a top-quark and a new vector particle V, which in turn decays invisibly into a pair of DM particles. Such a process can be parameterised through a general Lagrangian [16, 59]:

$$\mathcal{L}_{\text{int}} = aV_\mu \bar{u}\gamma^\mu P_{\text{R}} t + g_\chi V_\mu \bar{\chi}\gamma^\mu \chi + \text{h.c.}\,,$$

where a massive vector boson V is coupled to a DM particle (represented by a Dirac fermion χ) with a strength controlled by the parameter g_χ. The term P_{R} is the right-handed chirality projector. The parameter a stands for the coupling constant between the

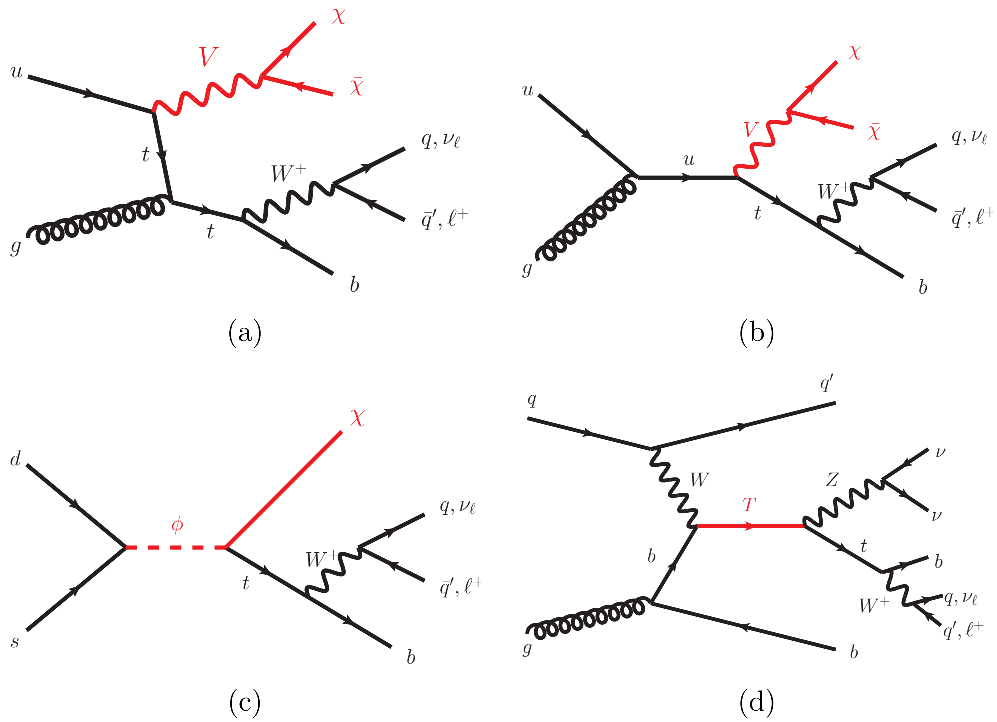

Figure 1. Representative leading-order diagrams corresponding to the signals sought in this paper: non-resonant (a) t-channel and (b) s-channel production of a top-quark in association with a vector boson V which decays into two DM particles; (c) resonant production of a coloured scalar ϕ that decays into a DM particle and a top-quark; and (d) single production of a vector-like T quark decaying into $Zt\,(\rightarrow \nu\bar{\nu}bW)$.

massive vector boson V and the t- and u-quarks, and γ^{μ} are the Dirac matrices. Another possibility is the resonant case, corresponding to the production of a coloured charge-2/3 scalar (ϕ) decaying into a top-quark and a spin-1/2 DM particle (χ) [60]. This process, represented in figure 1(c), is described by the following Lagrangian [16, 59]:

$$\mathcal{L}_{\text{int}} = \lambda\phi\bar{d}^{c}P_{\text{R}}s + y\phi\bar{\chi}P_{\text{R}}t + \text{h.c.}\,,$$

where the parameters λ and y represent the couplings of the charged scalar to the d- and s-quarks and to the top-quark and the DM particle χ, respectively.

2.2 Single production of vector-like T quarks

The single production of T quarks can occur via a charged WTb or a neutral ZTt vertex. However, ZTt production is suppressed because of the required top quark in the initial state. For this reason, ZTt production is not considered in this analysis and single VLT production refers to T production via the WTb vertex throughout this paper. The T quarks can decay into bW, tH and tZ, with the corresponding branching ratios ($\mathcal{B}$) depending on the specific model considered [33, 36].

The specific case of single production of vector-like T quarks decaying into tZ, followed by the Z boson decaying into neutrinos, results in a mono-top signature. As can be seen in figure 1(d), one important difference between DM production and vector-like T-quark production is the presence of additional quarks in the single production of T quarks, which will lead to at least one jet being detected at a small angle relative to the beam line. Similarly to the DM case, the topology of the VLT signal has a distinctive signature, characterised by the presence of a top-quark and missing transverse momentum, arising from the $Z \to \nu\bar{\nu}$ decay (and from the $t \to bW \to \ell\nu$ decay in the single-lepton channel case).

3 ATLAS detector

The ATLAS experiment [61] at the LHC is a multipurpose particle detector with nearly 4π coverage around the collision point.[1] It consists of an inner tracking detector surrounded by a thin superconducting solenoid providing a 2 T axial magnetic field, electromagnetic and hadron calorimeters, and a muon spectrometer. The inner tracking detector covers the pseudorapidity range $|\eta| < 2.5$. It consists of a silicon pixel detector, including the insertable B-layer [62, 63] installed after Run 1 of the LHC, a silicon microstrip detector, and a transition-radiation tracking detector. Lead/liquid-argon (LAr) sampling calorimeters provide electromagnetic (EM) energy measurements with high granularity for $|\eta| < 3.2$. A steel/scintillator-tile hadron calorimeter covers the central pseudorapidity range ($|\eta| < 1.7$). The endcap and forward regions are instrumented with LAr calorimeters for both the EM and hadronic energy measurements up to $|\eta| = 4.9$. The outer part of the detector includes a muon spectrometer with high-precision tracking chambers providing coverage up to $|\eta| = 2.7$, fast detectors for triggering over $|\eta| < 2.4$, and three large air-core toroidal superconducting magnets with eight coils each. A two-level trigger system [64], using custom hardware followed by a software-based trigger level, is used to select events of interest at an average rate of 1 kHz.

4 Data and simulation samples

This analysis is performed using pp collision data recorded at a centre-of-mass energy of $\sqrt{s} = 13$ TeV with the ATLAS detector during 2015 and 2016 in the periods when the LHC was operating with 25 ns bunch spacing and with an average number of collisions per bunch crossing $\langle\mu\rangle$ of around 23. Only periods in which all detector components necessary for this analysis were functional are considered, resulting in a data sample with a total integrated luminosity of 36.1 fb^{-1}.

In the single-lepton channel, events are required to pass at least one of the single-muon or single-electron triggers [64]. The triggers require a p_{T} of at least 20 GeV (26 GeV) for muons and 24 GeV (26 GeV) for electrons for the 2015 (2016) data sets, and also have requirements on lepton reconstruction and isolation. These are complemented by triggers

[1] ATLAS uses a right-handed coordinate system with its origin at the nominal interaction point (IP) in the centre of the detector and the z-axis along the beam pipe. The x-axis points from the IP to the centre of the LHC ring, and the y-axis points upwards. Cylindrical coordinates (r, ϕ) are used in the transverse plane, ϕ being the azimuthal angle around the z-axis. The pseudorapidity is defined in terms of the polar angle θ as $\eta = -\ln\tan(\theta/2)$. Angular distance is measured in units of $\Delta R \equiv \sqrt{(\Delta\eta)^2 + (\Delta\phi)^2}$.

JHEP05(2019)041

with higher p_{T} thresholds and relaxed isolation and identification requirements to ensure maximum efficiency at higher lepton p_{T}. In the hadronic channel, events are considered if they are accepted by triggers that select events with high missing transverse momentum, with online thresholds of 70 GeV in 2015 and 90 GeV to 110 GeV in 2016.

For all signal and background processes of interest, Monte Carlo (MC) events were simulated.

Signal events for both the resonant and non-resonant DM scenarios were generated according to a simplified model [65] described in section 1, implemented in MadGraph5_aMC@NLOv2.3.2 [66] through FeynRules 2.0 [67, 68]. Such generation was done at leading order (LO) using the NNPDF3.0LO [69] parton distribution function (PDF) set. Parton showering, hadronisation and underlying-event modelling were handled using the Pythia 8.212 [70] event generator with the A14 [71] set of tuned parameters, using the NNPDF2.3LO PDF set [72]. Signal samples for the resonant model were generated assuming a DM mass of $m_\chi = 10$ GeV and a range of the new scalar masses, m_ϕ, between 1 TeV and 5 TeV, representing two different kinematic regimes. The kinematic distributions predicted by the model have only a small dependence on the coupling parameters and therefore all samples were generated using a coupling constant of $\lambda = 0.2$ and a mixing parameter of $y = 0.4$. The remaining kinematic dependence on the different couplings and masses was accounted for by means of a reweighting procedure (see section 8 for details). Similarly, the signal samples for the non-resonant model were generated for values of m_V between 500 GeV and 3 TeV, corresponding to the expected sensitivity of the analysis, and a benchmark DM mass $m_\chi = 1$ GeV. The values of the couplings were set to $a = 0.5$ and $g_\chi = 1.0$. The kinematic effect of changing the coupling values was taken into account by using the previously mentioned reweighting procedure. The samples were normalised to the theoretical LO cross-sections, computed with MadGraph5_aMC@NLO.

The single production of T quarks was generated using the Feynrules 2.0 implementation of a general model [35] interfaced to MadGraph5_aMC@NLOv2.3.2. The NNPDF2.3 LO PDF set and Pythia 8.212 with the A14 set of tuned parameters were used. Since the current analysis targets a final state with large missing transverse momentum, only the $T \to Zt$ decay, with Z decaying invisibly, was considered, as represented in figure 1(d). Samples were generated for T masses in the range from 700 to 2000 GeV with a benchmark coupling of $\kappa_T = 0.5$ in the WTb production vertex. Additional samples were generated with alternative values of $\kappa_T = 0.1$ and 1.0 in order to study the effect of a varying T-quark width on kinematic distributions. The samples were normalised to the next-to-leading-order (NLO) cross-section by correcting the LO cross-sections calculated with MadGraph5_aMC@NLO for the difference between the NLO and LO cross-sections reported for the neutral single-T production process via a ZTt coupling [36]. For large values of the coupling the narrow-width approximation used in the cross-section calculation does not apply, so the cross-sections were corrected to include width effects, using a reweighting procedure similar to that previously mentioned, in order to account for the corresponding kinematic effects.

For the background samples, several matrix element (ME) event generators were combined with parton shower and hadronisation programs. Powheg-Box v2 [73–79] interfaced to Pythia 8.210 using the A14 set of tuned parameters was used to simulate $t\bar{t}$ production at NLO. Single top production was generated at NLO with Powheg-Box v1 for the t-, Wt- and s-channels and at LO with MadGraph5_aMC@NLO for the tZq process, interfaced to Pythia 6.428 [80]. The CTEQ6L1 PDF set [81] and the Perugia 2012 set of tuned parameters [82] were used in the parton shower, hadronisation, and underlying-event simulation. The CT10f4 (CT10) PDF set [83] was used in the matrix element calculations for the t-channel (Wt- and s- channels). To model the $W+$jets and $Z+$jets background the Sherpa v2.2.1 [84] generator was used. Matrix elements were calculated for up to two partons at NLO and up to four partons at LO using the Comix [85] and OpenLoops [86] ME generators, and merged with the Sherpa parton shower [87] according to the ME+PS@NLO prescription [88]. The NNPDF3.0 next-to-NLO (NNLO) PDF set [89] was used in conjunction with a Sherpa parton shower tuning from the authors. Diboson processes were simulated with Powheg-Box v2 interfaced to Pythia 8.186. The CT10nlo PDF set was used for the hard process while the CTEQ6L1 PDF set was used for the parton shower. For the simulation of $t\bar{t}$ events with additional bosons $t\bar{t}+X$ ($X = W$, Z, Higgs), MadGraph5_aMC@NLO v2.3.2 interfaced to Pythia 8.186 was used at NLO in QCD. Non-perturbative effects were modelled with the AZNLO set of tuned parameters [90].

The considered cross-sections for the dominant backgrounds, $t\bar{t}$ and $W/Z+$jets, were evaluated at NNLO in quantum chromodynamics (QCD) [91, 92]. The calculation for $t\bar{t}$ also includes next-to-next-to-leading logarithmic soft gluon terms.

The EvtGen v1.2.0 program [93] was used to simulate properties of the bottom and charmed hadron decays except for samples generated with Sherpa. All simulated samples except the DM non-resonant signal in the leptonic channel and $t\bar{t}+X$ processes were processed with the full simulation of the ATLAS detector [94] using Geant4 [95]. Additional samples used in the estimation of systematic uncertainties were instead produced using Atlfast2 [96], in which a parameterised detector simulation was used for the calorimeter responses. This simulation was also used for the generation of the DM non-resonant signal in the leptonic channel and $t\bar{t}+X$ processes. All samples were simulated with a varying number of minimum-bias interactions generated with Pythia 8.186 using the A2 set of tuned parameters [97], overlaid on the hard-scattering event to account for the multiple pp interactions in the same or nearby bunch crossings (pile-up). Simulated events were corrected using per-event weights to describe the distribution of the average number of interactions per proton bunch-crossing as observed in data.

5 Event reconstruction and object selection

Events are required to have at least one vertex candidate with at least two tracks with $p_{\mathrm{T}} > 400\,\mathrm{MeV}$. The primary vertex is taken to be the vertex candidate with the largest sum of squared transverse momenta of all associated tracks.

Electron candidates are reconstructed from an isolated electromagnetic calorimeter energy deposit matched to a track in the inner detector passing tight likelihood-based requirements [98]. They are required to have a transverse energy $E_{\mathrm{T}} > 30\,\mathrm{GeV}$ and pseudorapidity $|\eta| < 2.47$, with the transition region between the barrel and endcap electromagnetic

JHEP05(2019)041

calorimeters, $1.37 < |\eta| < 1.52$, excluded. Electron candidates must have a track satisfying requirements of $|d_0|/\sigma_{d_0} < 5$ for the transverse impact parameter significance relative to the beamline and $|\Delta z_0 \sin\theta| < 0.5$ mm for the longitudinal impact parameter calculated relative to the primary vertex. Furthermore, electrons must satisfy isolation requirements based on inner detector tracks and topological clusters in the calorimeter [99], with an isolation efficiency of 90% (99%) for electrons from $Z \to ee$ decays with $p_{\mathrm{T}} = 25(60)$ GeV. Correction factors are applied to simulated electrons to take into account the small differences in reconstruction, identification, and isolation efficiencies between data and MC simulation.

Muon candidates are reconstructed by combining tracks reconstructed in the inner detector with matching tracks reconstructed in the muon spectrometer, and are required to satisfy $p_{\mathrm{T}} > 30$ GeV and $|\eta| < 2.5$ [100]. Muon candidates must satisfy requirements of $|d_0|/\sigma_{d_0} < 3$ and $|\Delta z_0 \sin\theta| < 0.5$ mm for the transverse impact parameter significance and the longitudinal impact parameter, respectively. An isolation requirement based on inner detector tracks and topological clusters in the calorimeters is imposed, which achieves an isolation efficiency of 90% (99%) for muons from $Z \to \mu\mu$ decays with $p_{\mathrm{T}} = 25(60)$ GeV. Similarly to electrons, correction factors are applied to muons to account for the small differences between data and simulation [100].

Jets are reconstructed from topological clusters of energy deposited in the calorimeter [99] using the anti-k_t algorithm [101] with a radius parameter of 0.4 (1.0) for small-R (large-R) jets, as implemented in the FastJet package [102].

Small-R jets are calibrated using an energy- and η-dependent simulation-based calibration scheme with corrections derived from data [103]. Jets are accepted within the fiducial region $|\eta| < 2.5$ and $p_{\mathrm{T}} > 30$ GeV ($p_{\mathrm{T}} > 25$ GeV) for the leptonic (hadronic) analysis. In the hadronic channel this threshold has been relaxed to increase forward-jet acceptance. Forward jets in the region $2.5 < |\eta| < 4.5$ are also considered in the vector-like T-quark search analysis. Quality criteria are imposed to reject events that contain any jets arising from non-collision sources or detector noise [104]. To reduce the contribution from jets associated with pile-up, jets with $p_{\mathrm{T}} < 60$ GeV and $|\eta| < 2.4$ must satisfy a criterion that matches them to the hard-scatter vertex using information from tracks reconstructed in the inner tracking detector [105].

To prevent double counting of electron energy deposits as small-R jets, the closest jet with distance $\Delta R_{y,\phi} \equiv \sqrt{(\Delta y)^2 + (\Delta\phi)^2} < 0.2$ from a reconstructed electron is removed. If the nearest surviving jet is within $\Delta R_{y,\phi} = 0.4$ of the electron, the electron is discarded to ensure it is sufficiently separated from nearby jet activity. Jets with fewer than three tracks and distance $\Delta R_{y,\phi} < 0.2$ from a muon are removed to reduce the number of jet fakes from muons depositing energy in the calorimeters. Muons with a distance $\Delta R_{y,\phi} < 0.4$ from any of the surviving jets are removed to avoid contamination due to non-prompt muons from heavy-flavour hadron decays.

Large-R jets are trimmed [106] to mitigate the impact of initial-state radiation, underlying-event activity and pile-up. The jet energy and pseudorapidity are further calibrated to account for residual detector effects using energy- and η-dependent calibration factors derived from simulation, with uncertainties derived from data [107]. Trimmed large-

JHEP05(2019)041

R jets are considered if they fulfil $p_{\mathrm{T}} > 250\,\mathrm{GeV}$ and $|\eta| < 2.0$. To identify large-R jets that are more likely to have originated from hadronically decaying top-quarks than from the fragmentation of other quarks and gluons, jet substructure information is exploited.

In the trimming procedure, sub-jets, with radius $R_{\mathrm{sub}} = 0.2$, are clustered starting from the large-R jet constituents using a k_t algorithm. A sub-jet is retained only if it contains at least 5% of the total large-R jet transverse momentum, thereby removing the soft constituents from the large-R jet. A top-tagging algorithm [108] is applied, corresponding to a loose working point with an approximately constant top-tagging efficiency of 80% above p_{T} of 400 GeV. The algorithm depends on the calibrated jet mass, measured from clusters in the calorimeter, and the N-subjetiness ratio τ_{32} [109]. The N-subjetiness τ_N [109] expresses how well a jet can be described as containing N or fewer sub-jets. The ratio $\tau_{32} = \tau_3/\tau_2$ allows discrimination between jets containing a three-prong structure and jets containing a two-prong structure.

In addition to calorimeter-based jets, jets reconstructed from inner detector tracks using the anti-k_t algorithm with a radius parameter of 0.2 are also used in the hadronic channel, following a similar strategy as in [110]. They are referred to as track-based jets and are required to satisfy $p_{\mathrm{T}} > 10\,\mathrm{GeV}$ and $|\eta| < 2.5$.

Small-R calorimeter-based and track-based jets with $|\eta| < 2.5$ are b-tagged as likely to contain b-hadrons using multivariate techniques which exploit the long lifetime of b-hadrons and large invariant mass of their decay products relative to c- and light hadrons [111, 112]. The working point used provides an average tagging efficiency of 70% for b-jets and a rejection factor of 12.2 (7.1) against calorimeter-based (track-based) jets initiated by c-quarks and 381 (120) against calorimeter-based (track-based) jets initiated by light-flavour quarks, in simulated $t\bar{t}$ events. Correction factors are derived and applied to correct for the small differences in b-quark selection efficiency between data and MC simulation [111, 113, 114].

The missing transverse momentum is calculated as the negative vector sum of the transverse momenta of particles in the event, and its magnitude is denoted $E_{\mathrm{T}}^{\mathrm{miss}}$. In addition to the identified jets, electrons, muons, hadronically decaying τ-leptons and photons, a track-based soft term is included in the $E_{\mathrm{T}}^{\mathrm{miss}}$ calculation by considering tracks associated with the hard-scattering vertex in the event which are not also associated with an identified jet, electron, muon, hadronically decaying τ-lepton, or photon [115, 116].

6 Event selection and background estimation

The experimental signature of mono-top events expected in the DM (resonant and non-resonant) and vector-like T-quark models considered is the presence of a top-quark and significant missing transverse momentum, as seen in section 2. For the case of single VLT production, at least one additional forward jet is also expected.

The leptonic channel is only considered in order to target the non-resonant DM model. In this model, the u-quark-initiated production of top-quarks is favoured over anti-top-quark production, due to the PDF structure of the proton. Therefore, positively charged leptons are favoured in the final state. Events that pass preselection are required to contain exactly one positively charged lepton and one b-tagged jet with $p_{\mathrm{T}} > 30\,\mathrm{GeV}$. In order to reduce the number of multijet background events, which are characterised by low $E_{\mathrm{T}}^{\mathrm{miss}}$ and low W boson transverse mass[2] m_{T}^{W}, it is also required that $E_{\mathrm{T}}^{\mathrm{miss}} > 50\,\mathrm{GeV}$ and $m_{\mathrm{T}}^{W} + E_{\mathrm{T}}^{\mathrm{miss}} > 60\,\mathrm{GeV}$.

In the hadronic channel, because of the large expected Lorentz boost of the top-quarks produced in the signal events, the top-quark decay products can be collimated into a large-R jet. This signature is used in both the non-resonant and resonant DM models and the VLT models. Preselected events are then required to contain zero leptons, one large-R jet with $p_{\mathrm{T}} > 250\,\mathrm{GeV}$ and $|\eta| < 2.0$. In order to suppress the multijet background contribution, $E_{\mathrm{T}}^{\mathrm{miss}} > 200\,\mathrm{GeV}$ is also required.

6.1 Signal region definition

The signal region selection is optimised for the different considered benchmarks with simulated data, using variables tested and found to be well-modelled. In the optimisation the sensitivity is estimated by performing a fit to the shape of the most discriminating observable including systematic uncertainties (see section 8 for details). These observables are $E_{\mathrm{T}}^{\mathrm{miss}}$ in the leptonic channel and the transverse mass of the top-tagged large-R jet (J) and the $E_{\mathrm{T}}^{\mathrm{miss}}$ system, $m_{\mathrm{T}}(E_{\mathrm{T}}^{\mathrm{miss}}, J)$[3], in the hadronic channel. For the tested mass hypothesis, the resulting best-performing selections lead to three signal regions: 1L-DM-SR for the non-resonant DM search in the leptonic channel and 0L-DM-SR and 0L-VLT-SR targeting the search in the hadronic channel for DM and VLT quarks, respectively.

In the leptonic channel, the mono-top signal is enhanced in regions of phase space characterised by high m_{T}^{W} values. In addition, the lepton and b-tagged jet are closer to each other when originating from the decay of a top-quark than in the case of $W+$jets and multijet background events. Hence, in addition to the preselection described previously, the region 1L-DM-SR is defined by requiring $m_{\mathrm{T}}^{W} > 260\,\mathrm{GeV}$ and $|\Delta\phi(\ell, b)| < 1.2$.

In the hadronic channel, events in 0L-DM-SR and 0L-VLT-SR are required to contain exactly one top-tagged large-R jet with $p_{\mathrm{T}} > 250\,\mathrm{GeV}$ and one b-tagged track-based jet, in addition to the preselection criteria. The distance between the top-tagged large-R jet and the $E_{\mathrm{T}}^{\mathrm{miss}}$ in the transverse plane, $\Delta\Phi(E_{\mathrm{T}}^{\mathrm{miss}}, J)$, is required to fulfil $\Delta\Phi(E_{\mathrm{T}}^{\mathrm{miss}}, J) \geq \pi/2$ since for signal events they are more likely to be produced back-to-back. In order to suppress background events due to fake $E_{\mathrm{T}}^{\mathrm{miss}}$ mostly coming from jet mis-reconstruction in multijet production, the asymmetry between $E_{\mathrm{T}}^{\mathrm{miss}}$ and the p_{T} of the top-tagged large-R jet defined as $\Omega = (E_{\mathrm{T}}^{\mathrm{miss}} - p_{\mathrm{T}}(J))/(E_{\mathrm{T}}^{\mathrm{miss}} + p_{\mathrm{T}}(J))$ is required to be $\Omega > -0.3$. The multijet background is additionally suppressed by requiring the minimum distance between

[2] The transverse mass of the lepton and $E_{\mathrm{T}}^{\mathrm{miss}}$ system is defined as $m_{\mathrm{T}}^{W} = \sqrt{2p_{\mathrm{T}}(\ell)E_{\mathrm{T}}^{\mathrm{miss}}(1-\cos\Delta\phi(p_{\mathrm{T}}(\ell), E_{\mathrm{T}}^{\mathrm{miss}}))}$, where $p_{\mathrm{T}}(\ell)$ denotes the modulus of the lepton transverse momentum, and $\Delta\phi(p_{\mathrm{T}}(\ell), E_{\mathrm{T}}^{\mathrm{miss}})$ the azimuthal angle between the missing transverse momentum and the lepton directions.

[3] The transverse mass of the large-R jet and $E_{\mathrm{T}}^{\mathrm{miss}}$ is defined as $m_{\mathrm{T}}(E_{\mathrm{T}}^{\mathrm{miss}}, \mathrm{J}) = \sqrt{m(\mathrm{J})^2 + 2E_{\mathrm{T}}^{\mathrm{miss}} \cdot \left(E_{\mathrm{T(J)}} - p_{\mathrm{T}}(\mathrm{J})\cos(\Phi(\mathrm{J}) - \Phi(E_{\mathrm{T}}^{\mathrm{miss}}))\right)}$, where $m_{\mathrm{T}}(\mathrm{J})$ is the reconstructed invariant mass of the calibrated calorimeter-cluster constituents of a large-R jet and $E_{\mathrm{T}}(\mathrm{J})$ is the projection of its energy in the transverse plane.

JHEP05(2019)041

the $E_{\mathrm{T}}^{\mathrm{miss}}$ and any small-R jet in the transverse plane to be $\Delta\Phi_{\mathrm{min}} > 1.0$. The signal region 0L-VLT-SR is defined by requiring in addition at least one forward jet with $p_{\mathrm{T}} > 25$ GeV. The signal region requirements are summarised in table 1.

6.2 Background estimation

Dedicated control regions enriched in the dominant backgrounds are included in the fit to constrain these backgrounds with data. Multijet production background is estimated from data, while the rest of background processes are taken from simulation.

The dominant background in the signal regions is due to $t\bar{t}$ production in both channels, representing 78% of the total background in the leptonic and 55% (64%) in the DM (VLT) hadronic channels. This is followed by contributions from $W+$jets (13%) and single top production (6.8%) in the leptonic channel and from $W+$jets and $Z+$jets production, at the level of 12% (13%) for $W+$jets and 14% (15%) for $Z+$jets in the DM (VLT) signal regions, in the hadronic channel. A minor background in the signal region with a non-negligible contribution in the control regions is multijet production. The rest of the backgrounds considered in the analysis are diboson production as well as $t\bar{t}$ production in association with a Z, W or Higgs boson.

The estimation of the multijet background is in particularly important in the control regions used to estimate the main backgrounds. In the leptonic channel the multijet background originates from either misidentification of a jet as a lepton candidate (fake lepton) or from the presence of a non-prompt lepton (e.g., from a semileptonic b- or c-hadron decay) that passes the isolation requirement. The shape and the normalisation of the relevant distributions in multijet events and related systematic uncertainties are estimated using a matrix method in the electron channel and the anti-muon method in the muon channel [117]. The matrix method exploits differences in efficiencies to pass loose or tight quality requirements [98] between prompt leptons, obtained from W and Z decays, and non-prompt or fake lepton candidates, from the misidentification of photons or jets. These efficiencies are measured in dedicated control regions. The prompt lepton efficiencies are measured as a function of the p_{T} of the leading jet and the angular distance between the lepton and its nearest jet, while the non-prompt or fake efficiencies are parameterised in terms of the p_{T} of the leading jet, the angle in the transverse plane between the lepton and the $E_{\mathrm{T}}^{\mathrm{miss}}$ and the b-tagged jet multiplicity. Multijet background events containing non-prompt muons are modelled with the anti-muon method using a sample of events enriched in non-isolated muons [117]. Most of these events originate from b- or c-hadron decays in jets. These events pass the kinematic requirements of the selections described in section 5. Only some of the muon identification criteria are modified, ensuring there is no overlap with the signal selection. The normalisation is determined using a binned maximum-likelihood fit to the number of events observed in data in a control region dominated by multijet events. This region is defined with the preselection criteria, but removing the requirement on $E_{\mathrm{T}}^{\mathrm{miss}}$ and requiring $m_{\mathrm{T}}^{W} < 60$ GeV.

In the hadronic channel the estimation of the multijet background is performed using a set of control regions (B,C and D) dominated by multijet background and defined to be orthogonal to the considered signal region (0L-DM-SR or 0L-VLT-SR). The shape of the

Selections (leptonic channel)	1L-DM-SR	1L-TCR	1L-WCR
Number of leptons	$= 1$	$= 1$	$= 1$
$p_{\mathrm{T}}(\ell)$ [GeV]	> 30	> 30	> 30
Lepton charge	> 0	> 0	> 0
Number of jets	$= 1$	$= 2$	$= 1$
Number of b-tagged jets	$= 1$	$= 2$	$= 1$
p_{T}(b-tagged jet) [GeV]	> 30	> 30	> 30
$E_{\mathrm{T}}^{\mathrm{miss}}$ [GeV]	> 50	> 50	> 50
$m_{\mathrm{T}}^{W} + E_{\mathrm{T}}^{\mathrm{miss}}$ [GeV]	> 60	> 60	> 60
m_{T}^{W} [GeV]	> 260	$60 < m_{\mathrm{T}}^{W} < 100$	$60 < m_{\mathrm{T}}^{W} < 100$
$\lvert\Delta\phi(\ell, b)\rvert$	< 1.2	—	—
Selections (hadronic channel)	**0L-DM-SR 0L-VLT-SR**	**0L-TCR**	**0L-VCR**
Number of forward jets	$= 0$ (0L-DM-SR) ≥ 1 (0L-VLT-SR)	—	—
Number of leptons	$= 0$	$= 0$	$= 0$
$E_{\mathrm{T}}^{\mathrm{miss}}$ [GeV]	> 200	> 200	> 200
Number of large-R jets	≥ 1	≥ 1	≥ 1
Number of top-tagged jets	≥ 1	≥ 1	≥ 1
$\Delta\Phi(E_{\mathrm{T}}^{\mathrm{miss}}, J)$	$> \frac{\pi}{2}$	$> \frac{\pi}{2}$	$> \frac{\pi}{2}$
Number of track-jets	≥ 1	≥ 1	≥ 1
Number of b-tagged track-jets	$= 1$	≥ 2	$= 0$
Veto jet (masked tile-calo)	—	applied	—
$\Omega = \frac{E_{\mathrm{T}}^{\mathrm{miss}} - p_{\mathrm{T}}(J)}{E_{\mathrm{T}}^{\mathrm{miss}} + p_{\mathrm{T}}(J)}$	> -0.3	> -0.3	> -0.3
$\Delta\Phi_{\mathrm{min}}(E_{\mathrm{T}}^{\mathrm{miss}}, \text{calo jets})$	> 1.0	$0.2 < \Delta\Phi_{\mathrm{min}} < 1.0$	> 1.0

Table 1. Overview of the event selections used to define the signal and control regions.

multijet background is estimated from the control region B, which differs from the signal region by requiring zero top-tagged large-R jets. This shape is normalised by a factor which is calculated as the ratio of the numbers of multijet events in regions C and D. Region C (region D) differs from the signal region (B region) by requiring $\Delta\Phi(E_{\mathrm{T}}^{\mathrm{miss}}, J) < \pi/2$.

In regions B and D, with zero top-tagged large-R jets, J is a large-R jet chosen randomly from the selected large-R jets. The multijet contribution in these control regions is determined from the difference between data and the residual contribution of other background processes evaluated from simulation assuming the theoretical predictions for the corresponding cross-sections.

The control regions are defined to be orthogonal to each other and to the signal region. They are required to fulfil the preselection criteria. In the leptonic channel, control regions enriched in $t\bar{t}$ and $W+$jets processes are used (referred to as 1L-TCR and 1L-WCR, respectively). In the hadronic channel, a control region enriched in $t\bar{t}$ production (referred to as 0L-TCR) and a region enriched in both the $W+$jets and $Z+$jets processes (referred to as 0L-VCR) are defined.

The control regions in the leptonic channel, 1L-TCR and 1L-WCR, are defined by modifying the requirement on m_{T}^{W} to a window around the W mass, 60 GeV $< m_{\mathrm{T}}^{W} <$

100 GeV, and removing the requirement on $|\Delta\phi(\ell, b)|$. For the 1L-TCR, events are also required to contain a second b-tagged jet. The $t\bar{t}$ control region in the hadronic channel, 0L-TCR, is defined by requiring two b-tagged track-based jets and the minimum distance between the $E_{\mathrm{T}}^{\mathrm{miss}}$ and any small-R jet in the transverse plane to satisfy $\Delta\Phi_{\mathrm{min}} < 1$ (in order to reduce the signal contribution) and $\Delta\Phi_{\mathrm{min}} > 0.2$ in order to suppress the multijet background). Events with calorimeter-based jets located close to disabled modules of the hadronic calorimeter are vetoed. In the 0L-VCR control region a veto on b-tagged track-based jets is applied.

Table 1 details the control region selection in comparison with the signal region requirements. A comparison of the observed and expected distributions for $E_{\mathrm{T}}^{\mathrm{miss}}$ and $m_{\mathrm{T}}(E_{\mathrm{T}}^{\mathrm{miss}}, J)$ in the control regions is shown in figure 2 for the leptonic and hadronic channel, respectively. The expectations in the leptonic (hadronic) channel are obtained from a fit of the background-only hypothesis to data in the 1L (0L) control regions, where the normalisations of the $t\bar{t}$ and $W+$jets ($t\bar{t}$ and W/Z +jets) processes are treated as nuisance parameters in the fit (see section 8 for details of the fit).

7 Systematic uncertainties

The normalisation and shapes of the signal and background estimates are affected by systematic uncertainties from experimental sources and theoretical predictions. Each source of uncertainty is included as a nuisance parameter in the likelihood fit that determines the possible signal contribution. The analysis is limited by statistical uncertainties, thus the inclusion of systematic uncertainties leads to only a small degradation of the expected sensitivity.

The sources of experimental uncertainty include the uncertainty in the lepton trigger, identification and isolation efficiencies, the lepton energy and momentum scale and resolution [98–100], the $E_{\mathrm{T}}^{\mathrm{miss}}$ trigger and track-based soft-term scale and resolution [115, 116], the jet pile-up rejection requirement, energy scale and resolution [118], resolutions for relevant large-R jet properties (mass, transverse momentum and the N-subjetiness ratio τ_{32}), the b-tagging efficiency [111, 112], the pile-up reweighting, and the luminosity.

The uncertainty in the combined 2015+2016 integrated luminosity is 2.1%, derived following a methodology similar to that detailed in ref. [119], using a calibration of the luminosity scale through x–y beam-separation scans and using the LUCID-2 detector for the baseline luminosity measurements [120]. This systematic uncertainty is applied to all backgrounds and signals that are estimated using MC events, which are normalised to the measured integrated luminosity.

Theoretical cross-section uncertainties are applied to the normalisation of the simulated processes. Additional shape uncertainties stemming from theoretical estimations are calculated by comparing samples simulated with different assumptions and are estimated for the dominant backgrounds.

Uncertainties in the modelling of the $t\bar{t}$ and t-channel single top background come from the choice of NLO-matching method, the parton shower and hadronisation modelling, and the amount of additional gluon radiation. The NLO-matching uncertainty is estimated by comparing events produced with Powheg-Box and MadGraph5_aMC@NLO [66], both

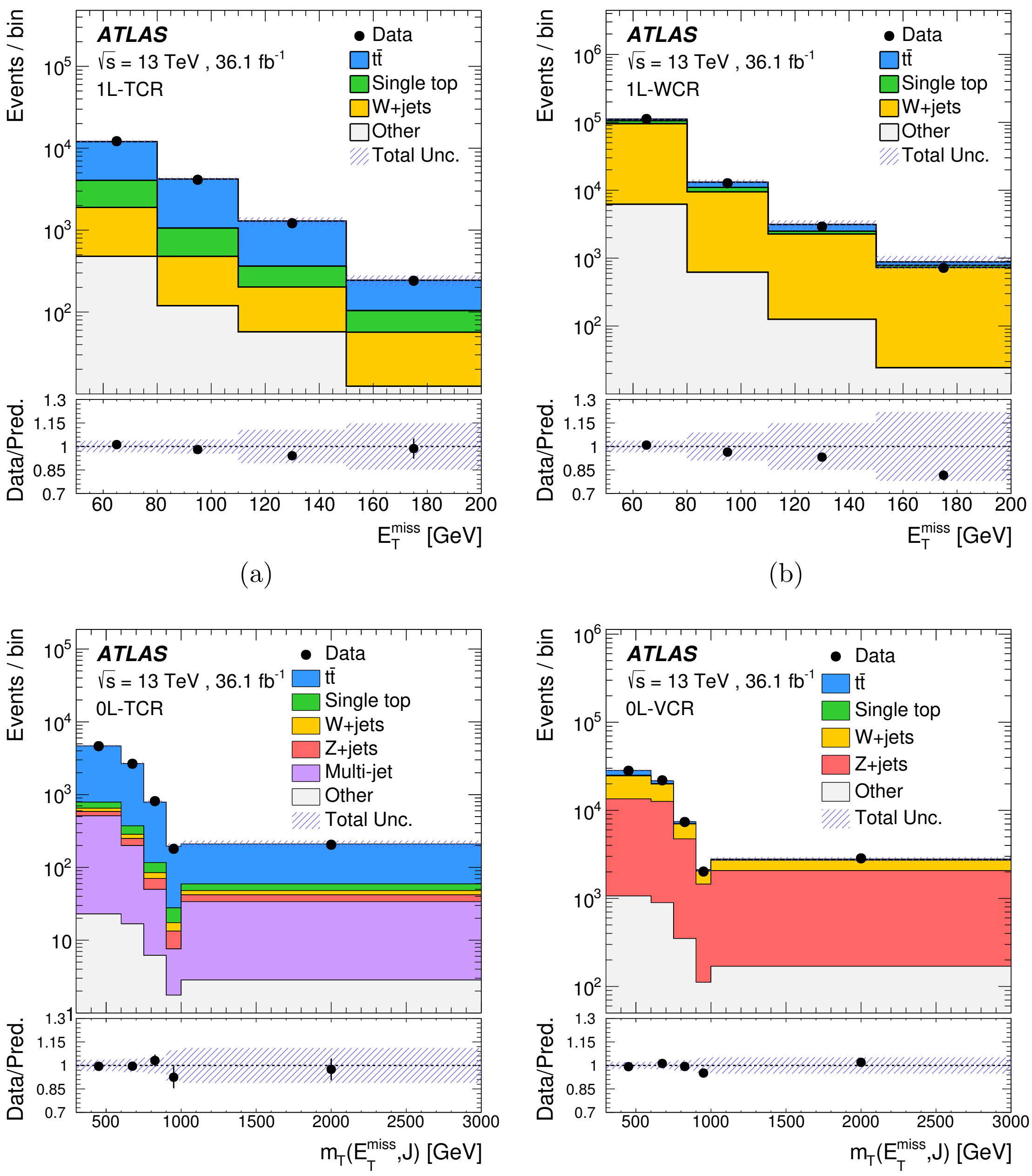

Figure 2. Comparison of data and SM prediction for the E_T^{miss} distribution in (a) the $t\bar{t}$ and (b) W+jets control regions; and for the transverse mass of the top-tagged large-R jet and E_T^{miss} system, $m_T(E_T^{miss}, J)$, distribution in the (c) $t\bar{t}$ and (d) W/Z +jet control regions used for the dark-matter search ((a) and (b)) and vector-like T-quark search ((c) and (d)). Other backgrounds in the 1L regions include multi-jet, Z+jets and diboson contributions, while in the 0L regions it is composed of diboson, $t\bar{t}$ +X and multi-jet contributions. The expectations in the leptonic (hadronic) channel are obtained from a fit of the background-only hypothesis to data in the 1L (0L) control regions, where the normalisations of the $t\bar{t}$ and W+jets ($t\bar{t}$ and W/Z +jets) processes are treated as nuisance parameters in the fit. The error bands include statistical and systematic uncertainties. The last bin contains the overflow events.

interfaced with Herwig++ [121]. The parton shower, hadronisation, and underlying-event model uncertainty is estimated by comparing two parton shower models, Pythia and Herwig++, while keeping the same hard-scatter matrix element generator. Variations of the amount of additional gluon radiation are estimated by comparing simulated samples with enhanced or reduced radiation and different values of tunable parameters related to additional radiation [122]. The choice of scheme to account for the interference between the Wt and $t\bar{t}$ processes constitutes another source of systematic uncertainty that is estimated by comparing samples using either the diagram removal scheme or the diagram subtraction scheme [123].

Modelling uncertainties affecting the shape of the W/Z +jets background are estimated in the hadronic channel, where these processes constitute an important background. An uncertainty in the modelling of W/Z +jets is estimated by comparing the nominal simulation with a MadGraph5_aMC@NLO simulation in which matrix elements were calculated at LO for up to four partons. In addition, the effects of independently varying the scales for the renormalisation, factorisation, and resummation by factors of 0.5 and 2 are used. Since the W/Z +jets background is constrained by a control region with a veto on b-tagged jets, an additional uncertainty related to the b-flavour content in the W/Z +jets background is taken into account by varying the number of events containing b-hadrons by 50% [124, 125]. Uncertainties in the modelling of the signal samples have been evaluated for signal points close to the expected exclusion mass limits and found to be negligible.

The effects of parton distribution function (PDF) uncertainties on the acceptance of the $t\bar{t}$ and W/Z +jets backgrounds are estimated following the PDF4LHC prescription [126].

The systematic uncertainty of 50% associated with the data-driven modelling of the multijet events is estimated in the leptonic channel, based on comparisons of the rates obtained using alternative methods, as described in previous analyses [117]. In the case of the hadronic channel, this systematic is derived from a closure test of the data-driven method in a multijet-dominated validation region using simulated dijet samples.

A breakdown of the effects of the various sources of systematic uncertainty on the background prediction is presented in table 2 and table 3 for the two searches. The relative effects on the background yields in the signal region after the simultaneous fit to data in the signal and control regions are shown. The dominant background modelling uncertainties are due to the modelling of single top Wt production for the leptonic channel and the modelling of the b-flavour content in the W/Z +jets backgrounds.

8 Results

In order to test for the presence of a signal, a simultaneous fit to data in the signal and control regions is performed. The fit is based on a profile-likelihood technique, where systematic uncertainties are allowed to vary as Gaussian-distributed nuisance parameters (NP) and subsequently acquire their best-fit values. Additionally, the dominant backgrounds are constrained by treating their normalisation as NP in the fit. The calculation of confidence

	1L-DM-SR		0L-DM-SR					
	non-$t\bar{t}$	$t\bar{t}$	$t\bar{t}$	Single top	W+jets	Z+jets	Multijet	Other
b-tagging	4.8	4.6	4.1	2.9	9.2	7.7	—	8.0
$E_{\mathrm{T}}^{\mathrm{miss}}$	12	1.1	2.2	2.1	2.2	2.2	3.0	2.0
Large-R jets	—	—	9.0	9.5	13	13	—	12
Small-R jets	9.9	7.0	1.3	2.9	1.0	0.5	—	1.0
Lepton	1.2	0.8	< 0.1	< 0.1	< 0.1	< 0.1	—	< 0.1
Luminosity	2.0	2.1	2.1	2.1	2.3	2.2	—	2.1
Pile-up	5.3	1.4	0.3	0.3	0.8	1.2	—	1.4
Background modelling	15	14	8.9	5.3	27	27	110	1.0
Total systematic	18	12	6.8	13	32	31	89	16

Table 2. Relative effect (in %) of various sources of systematic uncertainty on the predicted background yields in the signal regions used for the dark-matter search, obtained after the fit to data. Individual sources of uncertainties are correlated, and their sum in quadrature is not necessarily equal to the total background uncertainty.

	0L-VLT-SR				
	$t\bar{t}$	Single top	W+jets	Z+jets	Other
b-tagging	3.9	3.2	11	7.7	8.4
$E_{\mathrm{T}}^{\mathrm{miss}}$	1.4	1.9	0.8	0.5	0.3
Large-R jets	11	12	15	13	13
Small-R jets	7.3	7.8	7.6	8.3	11
Lepton	< 0.1	< 0.1	< 0.1	< 0.1	< 0.1
Luminosity	2.2	2.3	2.4	2.1	2.2
Pile-up	1.3	2.9	4.7	4.1	5.1
Background modelling	14	6.1	28	26	2.7
Total systematic	7.9	15.5	21	19	19.5

Table 3. Relative effect (in %) of various sources of systematic uncertainty on the predicted background yields in the signal region used for the vector-like T-quark search, obtained after the fit to data. Individual sources of uncertainties are correlated, and their sum in quadrature is not necessarily equal to the total background uncertainty.

intervals and hypothesis testing is performed using a frequentist method as implemented in RooStats [127] using the asymptotic approximation [128].

The $E_{\mathrm{T}}^{\mathrm{miss}}$ distribution is used in the 1L signal region and the number of events is used instead in the control regions, while for the case of the 0L regions the distribution of the transverse mass of the top-tagged large-R jet and $E_{\mathrm{T}}^{\mathrm{miss}}$ system, $m_{\mathrm{T}}(E_{\mathrm{T}}^{\mathrm{miss}}, J)$, is used in signal and control regions. For each of the three fits the binning of the distributions is optimised separately to obtain the highest expected sensitivity. For the testing of the non-resonant DM signal, both the 1L and 0L regions are used simultaneously in the fit (two signal regions and four control regions). For the resonant DM and VLT tests the fits are performed in the corresponding 0L regions, one signal region and two control regions for each fit. Uncertainties due to the limited size of the simulated samples are taken into account in each bin of the fitted distributions. Nuisance parameters accounting for systematic uncertainties are not considered in the fit if they have an impact on either normalisation or shape which is below 1%. The systematic uncertainties are symmetrised

JHEP05(2019)041

	1L-DM-SR	1L-TCR	1L-WCR	0L-DM-SR	0L-VLT-SR	0L-TCR	0L-VCR
$t\bar{t}$	390 ± 140	$12\,300 \pm 3100$	8400 ± 1700	$10\,200 \pm 2900$	3700 ± 1200	7000 ± 1700	6100 ± 1800
Single top	66 ± 21	2930 ± 760	$12\,200 \pm 1700$	1020 ± 260	356 ± 97	274 ± 71	890 ± 250
W+jets	34.2 ± 8.4	1890 ± 640	$92\,000 \pm 24\,000$	2240 ± 900	770 ± 310	147 ± 87	$28\,000 \pm 12\,000$
Z+jets	0.40 ± 0.86	112 ± 49	3410 ± 990	2700 ± 1100	850 ± 360	139 ± 83	$27\,000 \pm 11\,000$
Other	14 ± 15	640 ± 880	$7000 \pm 10\,000$	530 ± 190	89 ± 28	1060 ± 640	2730 ± 760
Total Background	500 ± 140	$17\,900 \pm 3400$	$123\,000 \pm 26\,000$	$16\,600 \pm 4500$	5800 ± 1700	8600 ± 2000	$66\,000 \pm 22\,000$
Data	511	17 662	127 286	15 781	5454	8493	62 304
R DM $m_\phi = 1$ TeV	—	—	—	$11\,300 \pm 1300$	—	56 ± 13	8100 ± 1600
R DM $m_\phi = 2$ TeV	—	—	—	469 ± 83	—	4.3 ± 1.1	349 ± 86
NR DM $m_\phi = 1$ TeV	165 ± 23	1.02 ± 0.47	20.2 ± 2.8	2090 ± 280	—	29.0 ± 5.9	1600 ± 320
NR DM $m_\phi = 2$ TeV	6.5 ± 2.7	0.027 ± 0.013	0.496 ± 0.097	95 ± 13	—	1.08 ± 0.21	75 ± 15
VLT $m_{\mathrm{VLT}} = 0.9$ TeV	—	—	—	—	112 ± 20	21.0 ± 5.3	76 ± 17

Table 4. Numbers of events observed in the signal and control regions, together with the estimated SM backgrounds before the fit to data. The uncertainties include statistical and systematic uncertainties. The expected numbers of events for benchmark signals normalised to the theoretical prediction are also shown. The benchmark signals correspond to: the non-resonant (NR) DM model with $m_V = 1$ TeV and 2 TeV, $m_\chi = 1$ GeV, $a = 0.5$ and $g_\chi = 1$; the resonant (R) DM model with $m_\phi = 1$ TeV and 2 TeV, $m_\chi = 10$ GeV, $\lambda = 0.2$ and $y = 0.4$; and a VLT with a mass of 0.9 TeV.

and also smoothed if the bin-to-bin statistical variation is significant. Most uncertainties are found to be neither significantly constrained nor pulled from their initial values. Small variations are observed in the $t\bar{t}$ modelling and multijet background uncertainties due to the mis-modelling observed in the shape of the transverse momentum distribution of top-quarks [129, 130]. Small variations are also observed in the large-R jet and Z/W +jets modelling uncertainties. The results of the fit show that the data are compatible with the background-only hypothesis.

The numbers of events observed in the signal and control regions are presented in table 4, together with the backgrounds estimated prior to the simultaneous fit. The distribution of the observable used in the fit ($E_{\mathrm{T}}^{\mathrm{miss}}$ or $m_{\mathrm{T}}(E_{\mathrm{T}}^{\mathrm{miss}}, J)$) in the signal regions for data and the fitted SM expectation under the background-only hypothesis are shown in figure 3. In these plots, the expected contribution from a benchmark signal is also shown for comparison. No significant excess above the SM expectation is found in any of the signal regions.

Since there is no evidence of a signal, expected and observed upper limits on the signal cross-section as a function of the V mass for the non-resonant model, the mass of the scalar particle ϕ for the resonant model and the VLT mass are derived at 95% confidence level (CL) and are shown in figure 4. Comparing the cross-section limits with the theoretical expectation, lower limits on the invisible particle and VLT masses can be derived. The LO values of the cross-section for non-resonant (resonant) DM production are evaluated using MadGraph5_aMC@NLO, as detailed in section 4, assuming $m_\chi = 1$ GeV, $a = 0.5$ and $g_\chi = 1$ ($m_\chi = 10$ GeV, $\lambda = 0.2$ and $y = 0.4$). For the VLT interpretation, the single-T production cross-section is taken from the NLO calculations for $c_W = 1$, with the coupling c_W defined in ref. [36]. The narrow-width approximation is used [36]. For the current analysis, it was checked using dedicated Monte Carlo samples that the chirality of

JHEP05(2019)041

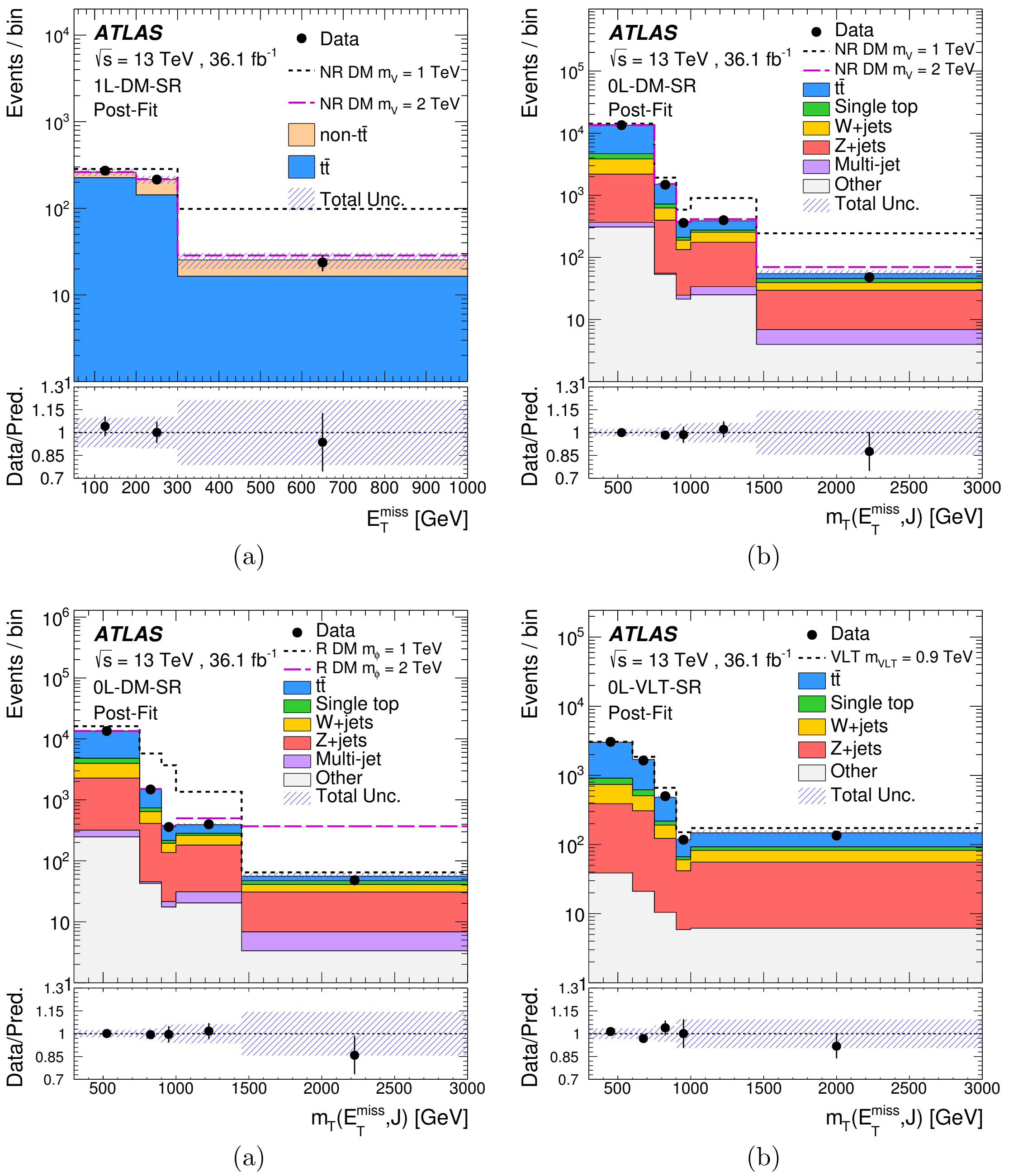

Figure 3. Comparison of data and fitted expectations for the $E_{\mathrm{T}}^{\mathrm{miss}}$ and the transverse mass of the top-tagged large-R jet and $E_{\mathrm{T}}^{\mathrm{miss}}$ system, $m_{\mathrm{T}}(E_{\mathrm{T}}^{\mathrm{miss}}, J)$, distributions in the signal regions. Other backgrounds in the 1L regions include multi-jet, Z+jets and diboson contributions, while in the 0L regions it is composed of diboson and $t\bar{t}+X$ contributions. The background-only hypothesis is used in the fit: (a) and (b) including the 1L and 0L DM signal regions as well as the 1L and 0L control regions; (c) 0L DM signal and control regions; (d) 0L VLT signal and control regions. The error bands include statistical and systematic uncertainties. The expected shape of a benchmark signal normalised to the theoretical prediction is added on top of the SM prediction. The benchmark signals correspond to: the non-resonant (NR) DM model with $m_V = 1$ TeV and 2 TeV, $m_\chi = 1$ GeV, $a = 0.5$ and $g_\chi = 1$; the resonant (R) DM model with $m_\phi = 1$ TeV and 2 TeV, $m_\chi = 10$ GeV, $\lambda = 0.2$ and $y = 0.4$; and a VLT with a mass of 0.9 TeV.

JHEP05(2019)041

the coupling has negligible impact on the considered observables. The cross-section is also corrected for width effects calculated with MadGraph5_aMC@NLO, assuming that the ratio of NLO to LO cross-sections remains approximately the same for a non-vanishing T-quark width. The computed cross-section is then multiplied by the value of $\mathcal{B}(T \to Zt)$ in the singlet model, which is $\approx 25\%$ in the range of VLT masses investigated in this analysis. The considered benchmark coupling of $\kappa_T = 0.5$ corresponds to $c_W = 0.45$. The observed (expected) mass limits at 95% CL are 2.0 (1.9) TeV and 3.4 (3.3) TeV for the non-resonant and resonant dark-matter models, respectively. For the VLT case, there is no observed or expected mass exclusion for the considered reference benchmark coupling.

Two-dimensional exclusion regions in the planes formed by the mediator masses, the DM particle mass, and couplings between the DM, the new heavy particle and the SM fermions are obtained by reweighting the events using the transverse momentum from the vector sum of the momenta of the DM candidates. This procedure is validated with dedicated samples and allows reproduction of the correct event kinematics for the masses and couplings required for the multidimensional scans. The observed (expected) 95% CL upper limit contours for the signal strength $\sigma/\sigma_{\text{theory}}$ are shown in figures 5(a)–5(c) for the non-resonant model, in which σ is the observed (expected) limit on the model cross-section at a given point of the parameter space and σ_{theory} is the predicted cross-section in the model at the same point. The corresponding results for the resonant model are shown in figures 5(d) and 5(e). Since a reweighting procedure was used to obtain the required signal points, the results shown in figure 5 include a systematic uncertainty in the signal normalisation associated with this procedure. This uncertainty was estimated from dedicated MC samples to be 10% and 25% for the non-resonant and resonant case, respectively, by comparing reweighted samples with those generated with the corresponding signal masses and couplings.

The limited sensitivity of the current analysis to single VLT production for low T masses (cf. figure 4(c)) implies that there is also less sensitivity to the corresponding coupling. This can be seen in figure 6(a), which shows the expected and observed 95% CL upper limits on c_W, taken as the sum in quadrature of the left- and right-handed couplings $c_{\text{L},W}$ and $c_{\text{R},W}$, as a function of the VLT mass. Nonetheless, the sensitivity remains approximately constant for masses up to 1.4 TeV. A singlet T, which corresponds to $\mathcal{B}(T \to Zt) \approx 25\%$ over the mass range studied in this analysis, was assumed. The obtained limits on c_W can also be translated into expected and observed 95% CL upper limits for the mixing angle of a singlet T with the SM top-quark, as shown in figure 6(b). For these results, a signal reweighting procedure was adopted in order to take into account the width effects induced by the variation of the c_W coupling. The systematic uncertainty in the signal normalisation was estimated to be 3% from dedicated MC samples and was considered when deriving the limits shown in figure 6. In the range $m(T) > 1.1$ TeV, the obtained exclusion limit on the c_W coupling improves on the previous results [43].

JHEP05(2019)041

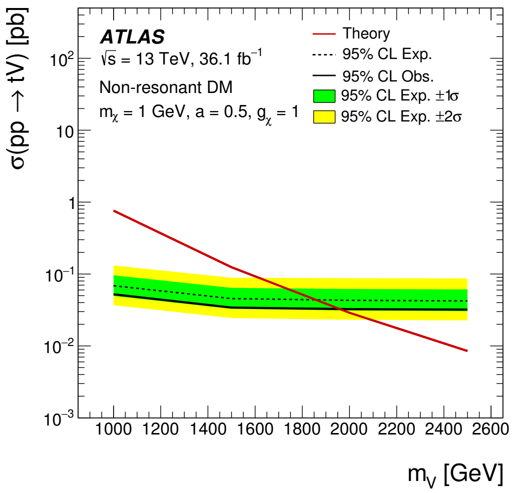

(a)

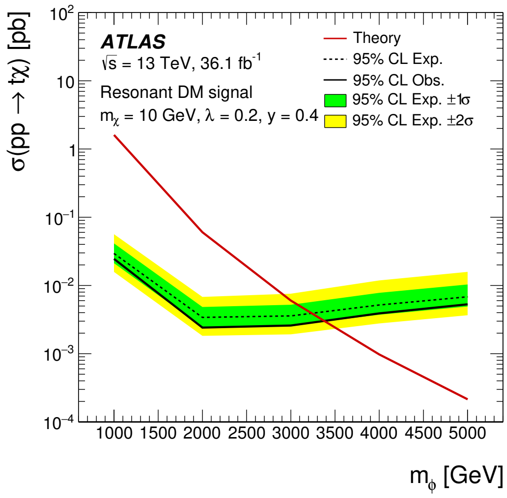

(b)

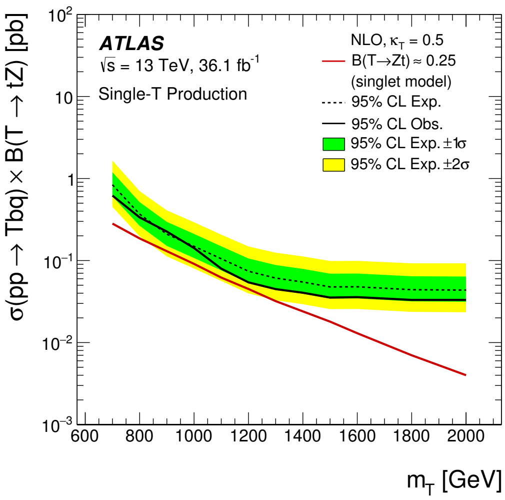

(c)

Figure 4. 95% CL upper limits on the signal cross-section as a function of (a) the V mass in the non-resonant (NR) model, (b) the mass of the scalar particle ϕ in the resonant (R) model and (c) the VLT mass. LO values for the production cross-section were computed for the non-resonant (resonant) DM production modes assuming $m_\chi = 1$ GeV, $a = 0.5$ and $g_\chi = 1$ ($m_\chi = 10$ GeV, $\lambda = 0.2$ and $y = 0.4$).

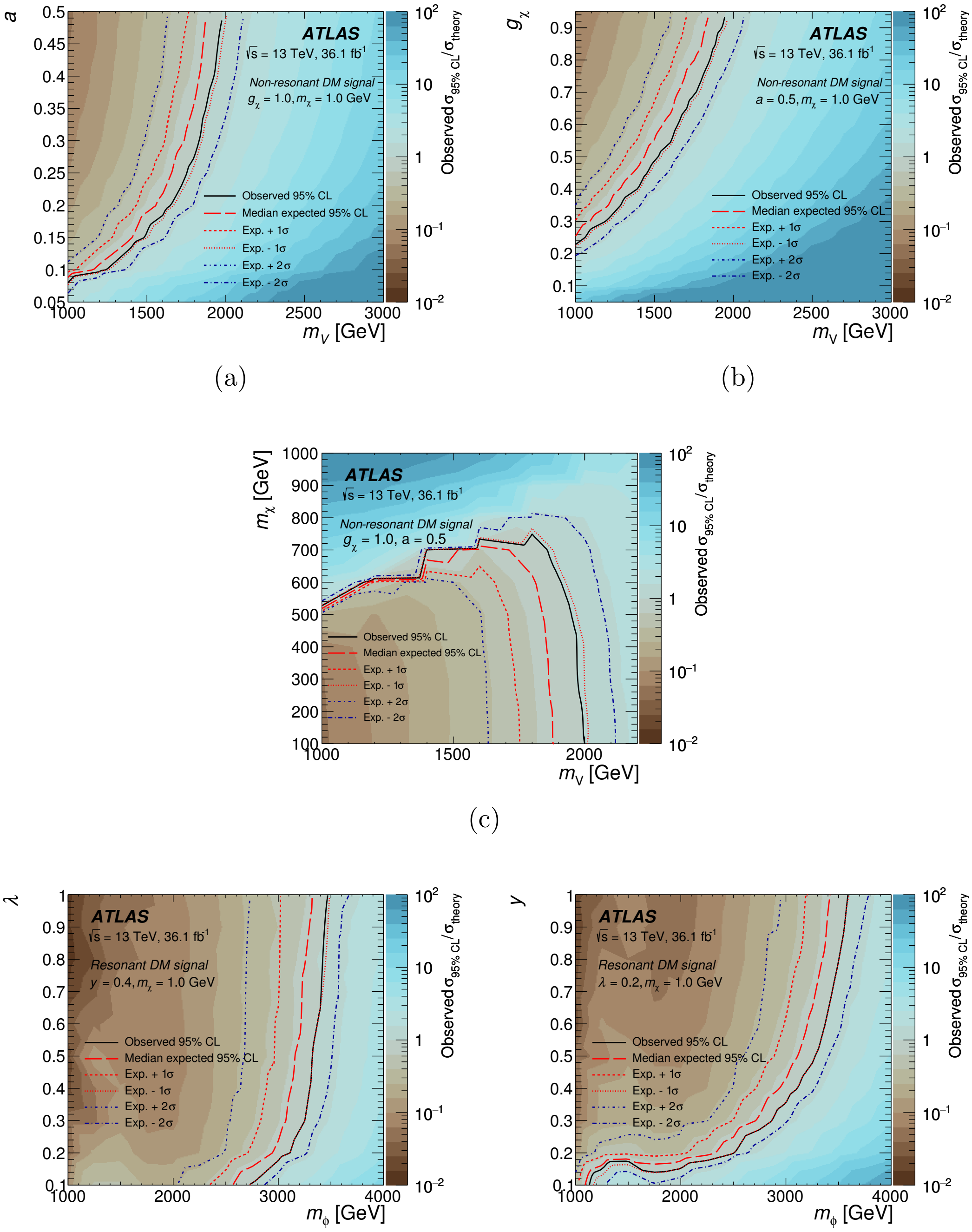

Figure 5. The 95% CL upper limit contours on the signal strength $\sigma/\sigma_{\text{theory}}$ are shown for the non-resonant (NR) and resonant (R) DM production models. Non-resonant model: (a) V mass vs a; (b) V mass vs g_χ and (c) V mass vs mass of the DM candidate χ. Resonant model: (d) mass of the scalar ϕ vs λ; (e) mass of the scalar ϕ vs y. The solid (dashed) lines correspond to the observed (median expected and corresponding $\pm 1\sigma$ and $\pm 2\sigma$ bands) limits for $\sigma/\sigma_{\text{theory}} = 1$. The predicted cross-sections were computed with MadGraph5_aMC@NLO.

JHEP05(2019)041

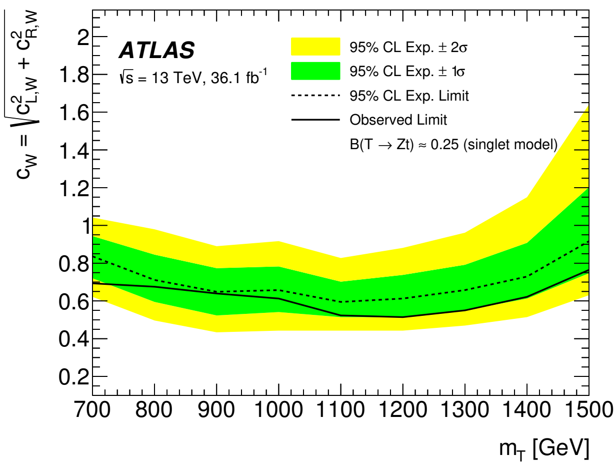

(a)

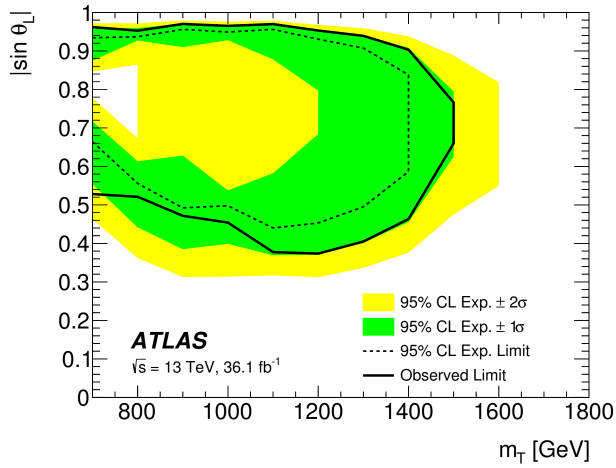

(b)

Figure 6. Expected and observed 95% CL limits from the combination of the single-production channels on (a) the coupling of the T quark to SM particles, $c_W = \sqrt{c_{\mathrm{L},W}^2 + c_{\mathrm{R},W}^2}$ assuming a singlet T, corresponding to a $\mathcal{B}$ of $\approx 25\%$; and (b) the absolute value of $\sin\theta_{\mathrm{L}}$, with θ_{L} being the mixing angle of a singlet T with the SM top-quark.

9 Conclusions

This analysis seeks anomalous production of events with large $E_{\mathrm{T}}^{\mathrm{miss}}$ and a single top-quark in LHC pp data at $\sqrt{s} = 13$ TeV collected by the ATLAS detector in 2015 and 2016, corresponding to an integrated luminosity of 36.1 fb^{-1}. No deviations with respect to SM predictions are observed and 95% CL upper limits on the production cross-section of three BSM processes are obtained: resonant and non-resonant production of dark matter (DM) in association with single top-quarks, and single production of vector-like T quarks decaying into $tZ(\to \nu\bar{\nu})$.

These limits are also interpreted in terms of the excluded regions in the parameter space of the considered BSM scenarios. For DM production in the non-resonant scenario, masses of a new vector particle coupling to the DM candidate up to 2 TeV are excluded at 95% CL for $m_\chi = 1$ GeV, $g_\chi = 1.0$ and $a = 0.5$, while in the resonant case, masses of a new scalar particle coupling to DM up to 3.4 TeV are excluded at 95% CL for $m_\chi = 10$ GeV, $y = 0.4$ and $\lambda = 0.2$. For the production of T singlets, couplings of these new quarks to top-quarks and W bosons, c_W, above 0.7 are excluded for $m_T = 1.4$ TeV and below.

A Event yields in the signal and control regions after the fit to data

The numbers of events observed in the signal and control regions are presented in tables 5, 6 and 7, together with the backgrounds estimated in the simultaneous fit to data in the corresponding regions under the background-only hypothesis. In table 5, 1L and 0L DM signal regions as well as the 1L and 0L control regions are included in the fit. table 6 includes 0L DM signal and control regions, while VLT signal and control regions are considered for table 7.

Leptonic channel	1L-DM-SR	1L-TCR	1L-WCR
$t\bar{t}$	385 ± 41	12 100 ± 2000	8470 ± 800
Non-$t\bar{t}$	117 ± 17	5540 ± 960	119 000 ± 26 000
Total	502 ± 62	17 700 ± 3100	127 000 ± 26 000
Data	511	17 662	127 286
Hadronic channel	**0L-DM-SR**	**0L-TCR**	**0L-VCR**
$t\bar{t}$	9900 ± 870	7160 ± 620	5900 ± 250
Single top	990 ± 110	273 ± 36	879 ± 98
W+jets	2050 ± 520	119 ± 65	23 100 ± 4900
Z+jets	2460 ± 460	135 ± 61	29 900 ± 4600
Multijet	87 ± 90	760 ± 350	0 ± 0
Other	328 ± 41	50.1 ± 5.6	2670 ± 310
Total	15 800 ± 1200	8490 ± 760	62 400 ± 1500
Data	15 781	8493	62 304

Table 5. Numbers of events observed in the signal and control regions used for the non-resonant dark-matter search, together with the estimated SM backgrounds in the fit to data, under the background-only hypothesis. The uncertainties include statistical and systematic uncertainties. The uncertainties in the individual backgrounds are correlated, and do not necessarily add in quadrature to the total background uncertainty.

JHEP05(2019)041

	0L-DM-SR	0L-TCR	0L-VCR
$t\bar{t}$	9690 ± 620	7110 ± 460	5710 ± 580
Single top	990 ± 110	282 ± 40	870 ± 110
W+jets	2070 ± 540	121 ± 67	$23\,000 \pm 5000$
Z+jets	2610 ± 530	149 ± 61	$30\,100 \pm 4700$
Other	330 ± 44	51.4 ± 6.1	2670 ± 310
Multijet	92 ± 88	800 ± 360	0 ± 0
Total	$15\,800 \pm 370$	8510 ± 280	$62\,300 \pm 1400$
Data	15 781	8493	62 304

Table 6. Numbers of events observed in the signal and control regions used for the resonant dark-matter search, together with the estimated SM backgrounds in the fit to data, under the background-only hypothesis. The uncertainties include statistical and systematic uncertainties. The uncertainties in the individual backgrounds are correlated, and do not necessarily add in quadrature to the total background uncertainty.

	0L-VLT-SR	0L-TCR	0L-VCR
$t\bar{t}$	3560 ± 280	7160 ± 370	5310 ± 740
Single top	323 ± 45	278 ± 37	820 ± 120
W+jets	660 ± 200	126 ± 72	$21\,900 \pm 5900$
Z+jets	830 ± 180	160 ± 64	$31\,800 \pm 4800$
Other	82 ± 14	800 ± 320	2590 ± 340
Total	5460 ± 160	8530 ± 270	$62\,300 \pm 1400$
Data	5454	8493	62 304

Table 7. Numbers of events observed in the signal and control regions used for the vector-like T-quark search, together with the estimated SM backgrounds in the fit to data, under the background-only hypothesis. The uncertainties include statistical and systematic uncertainties. The uncertainties in the individual backgrounds are correlated, and do not necessarily add in quadrature to the total background uncertainty.

Acknowledgments

We thank CERN for the very successful operation of the LHC, as well as the support staff from our institutions without whom ATLAS could not be operated efficiently.

We acknowledge the support of ANPCyT, Argentina; YerPhI, Armenia; ARC, Australia; BMWFW and FWF, Austria; ANAS, Azerbaijan; SSTC, Belarus; CNPq and FAPESP, Brazil; NSERC, NRC and CFI, Canada; CERN; CONICYT, Chile; CAS, MOST and NSFC, China; COLCIENCIAS, Colombia; MSMT CR, MPO CR and VSC CR, Czech Republic; DNRF and DNSRC, Denmark; IN2P3-CNRS, CEA-DRF/IRFU, France; SRNSFG, Georgia; BMBF, HGF, and MPG, Germany; GSRT, Greece; RGC, Hong Kong SAR, China; ISF and Benoziyo Center, Israel; INFN, Italy; MEXT and JSPS, Japan; CNRST, Morocco; NWO, Netherlands; RCN, Norway; MNiSW and NCN, Poland; FCT, Portugal; MNE/IFA, Romania; MES of Russia and NRC KI, Russian Federation; JINR;

JHEP05(2019)041

MESTD, Serbia; MSSR, Slovakia; ARRS and MIZŠ, Slovenia; DST/NRF, South Africa; MINECO, Spain; SRC and Wallenberg Foundation, Sweden; SERI, SNSF and Cantons of Bern and Geneva, Switzerland; MOST, Taiwan; TAEK, Turkey; STFC, United Kingdom; DOE and NSF, United States of America. In addition, individual groups and members have received support from BCKDF, CANARIE, CRC and Compute Canada, Canada; COST, ERC, ERDF, Horizon 2020, and Marie Skłodowska-Curie Actions, European Union; Investissements d' Avenir Labex and Idex, ANR, France; DFG and AvH Foundation, Germany; Herakleitos, Thales and Aristeia programmes co-financed by EU-ESF and the Greek NSRF, Greece; BSF-NSF and GIF, Israel; CERCA Programme Generalitat de Catalunya, Spain; The Royal Society and Leverhulme Trust, United Kingdom.

The crucial computing support from all WLCG partners is acknowledged gratefully, in particular from CERN, the ATLAS Tier-1 facilities at TRIUMF (Canada), NDGF (Denmark, Norway, Sweden), CC-IN2P3 (France), KIT/GridKA (Germany), INFN-CNAF (Italy), NL-T1 (Netherlands), PIC (Spain), ASGC (Taiwan), RAL (U.K.) and BNL (U.S.A.), the Tier-2 facilities worldwide and large non-WLCG resource providers. Major contributors of computing resources are listed in ref. [131].

References

[1] V. Trimble, *Existence and nature of dark matter in the universe*, *Ann. Rev. Astron. Astrophys.* **25** (1987) 425.

[2] G. Bertone, D. Hooper and J. Silk, *Particle dark matter: evidence, candidates and constraints*, *Phys. Rept.* **405** (2005) 279 [hep-ph/0404175] [INSPIRE].

[3] J.L. Feng, *Dark matter candidates from particle physics and methods of detection*, *Ann. Rev. Astron. Astrophys.* **48** (2010) 495 [arXiv:1003.0904] [INSPIRE].

[4] ATLAS collaboration, *Search for dark matter and other new phenomena in events with an energetic jet and large missing transverse momentum using the ATLAS detector*, *JHEP* **01** (2018) 126 [arXiv:1711.03301] [INSPIRE].

[5] CMS collaboration, *Search for dark matter produced with an energetic jet or a hadronically decaying W or Z boson at $\sqrt{s} = 13$ TeV*, *JHEP* **07** (2017) 014 [arXiv:1703.01651] [INSPIRE].

[6] ATLAS collaboration, *Search for dark matter produced in association with bottom or top quarks in $\sqrt{s} = 13$ TeV pp collisions with the ATLAS detector*, *Eur. Phys. J.* **C 78** (2018) 18 [arXiv:1710.11412] [INSPIRE].

[7] ATLAS collaboration, *Search for top-squark pair production in final states with one lepton, jets and missing transverse momentum using 36 fb^{-1} of $\sqrt{s} = 13$ TeV pp collision data with the ATLAS detector*, *JHEP* **06** (2018) 108 [arXiv:1711.11520] [INSPIRE].

[8] ATLAS collaboration, *Search for dark matter at $\sqrt{s} = 13$ TeV in final states containing an energetic photon and large missing transverse momentum with the ATLAS detector*, *Eur. Phys. J.* **C 77** (2017) 393 [arXiv:1704.03848] [INSPIRE].

[9] CMS collaboration, *Search for new physics in the monophoton final state in proton-proton collisions at $\sqrt{s} = 13$ TeV*, JHEP **10** (2017) 073 [arXiv:1706.03794] [INSPIRE].

[10] ATLAS collaboration, *Search for dark matter in events with a hadronically decaying vector boson and missing transverse momentum in pp collisions at $\sqrt{s} = 13$ TeV with the ATLAS detector*, JHEP **10** (2018) 180 [arXiv:1807.11471] [INSPIRE].

[11] ATLAS collaboration, *Search for an invisibly decaying Higgs boson or dark matter candidates produced in association with a Z boson in pp collisions at $\sqrt{s} = 13$ TeV with the ATLAS detector*, Phys. Lett. **B 776** (2018) 318 [arXiv:1708.09624] [INSPIRE].

[12] ATLAS collaboration, *Search for dark matter produced in association with a Higgs boson decaying to $b\bar{b}$ using 36 fb^{-1} of pp collisions at $\sqrt{s} = 13$ TeV with the ATLAS detector*, Phys. Rev. Lett. **119** (2017) 181804 [arXiv:1707.01302] [INSPIRE].

[13] ATLAS collaboration, *Search for dark matter in association with a Higgs boson decaying to two photons at $\sqrt{s} = 13$ TeV with the ATLAS detector*, Phys. Rev. **D 96** (2017) 112004 [arXiv:1706.03948] [INSPIRE].

[14] CMS collaboration, *Search for associated production of dark matter with a Higgs boson decaying to $b\bar{b}$ or $\gamma\gamma$ at $\sqrt{s} = 13$ TeV*, JHEP **10** (2017) 180 [arXiv:1703.05236] [INSPIRE].

[15] CMS collaboration, *Search for dark matter produced in association with a Higgs boson decaying to $\gamma\gamma$ or $\tau^+\tau^-$ at $\sqrt{s} = 13$ TeV*, JHEP **09** (2018) 046 [arXiv:1806.04771] [INSPIRE].

[16] J. Andrea, B. Fuks and F. Maltoni, *Monotops at the LHC*, Phys. Rev. **D 84** (2011) 074025 [arXiv:1106.6199] [INSPIRE].

[17] T. Lin, E.W. Kolb and L.-T. Wang, *Probing dark matter couplings to top and bottom quarks at the LHC*, Phys. Rev. **D 88** (2013) 063510 [arXiv:1303.6638] [INSPIRE].

[18] G. Cacciapaglia et al., *LHC constraints and potential on resonant monotop production*, Eur. Phys. J. **C 79** (2019) 174 [arXiv:1811.03626] [INSPIRE].

[19] CDF collaboration, *Search for a dark matter candidate produced in association with a single top quark in $p\bar{p}$ collisions at $\sqrt{s} = 1.96$ TeV*, Phys. Rev. Lett. **108** (2012) 201802 [arXiv:1202.5653] [INSPIRE].

[20] CMS collaboration, *Search for monotop signatures in proton-proton collisions at $\sqrt{s} = 8$ TeV*, Phys. Rev. Lett. **114** (2015) 101801 [arXiv:1410.1149] [INSPIRE].

[21] ATLAS collaboration, *Search for invisible particles produced in association with single-top-quarks in proton-proton collisions at $\sqrt{s} = 8$ TeV with the ATLAS detector*, Eur. Phys. J. **C 75** (2015) 79 [arXiv:1410.5404] [INSPIRE].

[22] CMS collaboration, *Search for dark matter in events with energetic, hadronically decaying top quarks and missing transverse momentum at $\sqrt{s} = 13$ TeV*, JHEP **06** (2018) 027 [arXiv:1801.08427] [INSPIRE].

[23] ATLAS collaboration, *Search for new phenomena in events with same-charge leptons and b-jets in pp collisions at $\sqrt{s} = 13$ TeV with the ATLAS detector*, JHEP **12** (2018) 039 [arXiv:1807.11883] [INSPIRE].

[24] N. Arkani-Hamed, A.G. Cohen, E. Katz and A.E. Nelson, *The littlest Higgs*, JHEP **07** (2002) 034 [hep-ph/0206021] [INSPIRE].

[25] M. Schmaltz and D. Tucker-Smith, *Little Higgs review*, Ann. Rev. Nucl. Part. Sci. **55** (2005) 229 [hep-ph/0502182] [INSPIRE].

[26] D.B. Kaplan, H. Georgi and S. Dimopoulos, *Composite Higgs scalars*, Phys. Lett. **B 136** (1984) 187.

[27] K. Agashe, R. Contino and A. Pomarol, *The minimal composite Higgs model*, Nucl. Phys. **B 719** (2005) 165 [hep-ph/0412089] [INSPIRE].

[28] F. del Aguila and M.J. Bowick, *The possibility of new fermions with $\Delta I = 0$ mass*, Nucl. Phys. **B 224** (1983) 107 [INSPIRE].

[29] F. del Aguila, M. Pérez-Victoria and J. Santiago, *Effective description of quark mixing*, Phys. Lett. **B 492** (2000) 98 [hep-ph/0007160] [INSPIRE].

[30] F. del Aguila, M. Pérez-Victoria and J. Santiago, *Observable contributions of new exotic quarks to quark mixing*, JHEP **09** (2000) 011 [hep-ph/0007316] [INSPIRE].

[31] A. Atre, M. Carena, T. Han and J. Santiago, *Heavy quarks above the top at the Tevatron*, Phys. Rev. **D 79** (2009) 054018 [arXiv:0806.3966] [INSPIRE].

[32] A. Atre et al., *Model-independent searches for new quarks at the LHC*, JHEP **08** (2011) 080 [arXiv:1102.1987] [INSPIRE].

[33] J.A. Aguilar-Saavedra, *Identifying top partners at LHC*, JHEP **11** (2009) 030 [arXiv:0907.3155] [INSPIRE].

[34] J.A. Aguilar-Saavedra, R. Benbrik, S. Heinemeyer and M. Pérez-Victoria, *Handbook of vectorlike quarks: mixing and single production*, Phys. Rev. **D 88** (2013) 094010 [arXiv:1306.0572] [INSPIRE].

[35] M. Buchkremer, G. Cacciapaglia, A. Deandrea and L. Panizzi, *Model independent framework for searches of top partners*, Nucl. Phys. **B 876** (2013) 376 [arXiv:1305.4172] [INSPIRE].

[36] O. Matsedonskyi, G. Panico and A. Wulzer, *On the interpretation of top partners searches*, JHEP **12** (2014) 097 [arXiv:1409.0100] [INSPIRE].

[37] F. del Aguila, L. Ametller, G.L. Kane and J. Vidal, *Vector like fermion and standard Higgs production at hadron colliders*, Nucl. Phys. **B 334** (1990) 1 [INSPIRE].

[38] ATLAS collaboration, *Search for production of vector-like quark pairs and of four top quarks in the lepton-plus-jets final state in pp collisions at $\sqrt{s} = 8$ TeV with the ATLAS detector*, JHEP **08** (2015) 105 [arXiv:1505.04306] [INSPIRE].

[39] ATLAS collaboration, *Analysis of events with b-jets and a pair of leptons of the same charge in pp collisions at $\sqrt{s} = 8$ TeV with the ATLAS detector*, JHEP **10** (2015) 150 [arXiv:1504.04605] [INSPIRE].

[40] ATLAS collaboration, *Search for pair and single production of new heavy quarks that decay to a Z boson and a third-generation quark in pp collisions at $\sqrt{s} = 8$ TeV with the ATLAS detector*, JHEP **11** (2014) 104 [arXiv:1409.5500] [INSPIRE].

[41] CMS collaboration, *Search for vector-like charge 2/3 T quarks in proton-proton collisions at $\sqrt{s} = 8$ TeV*, Phys. Rev. **D 93** (2016) 012003 [arXiv:1509.04177] [INSPIRE].

[42] ATLAS collaboration, *Search for pair production of vector-like top quarks in events with one lepton, jets and missing transverse momentum in $\sqrt{s} = 13$ TeV pp collisions with the ATLAS detector*, JHEP **08** (2017) 052 [arXiv:1705.10751] [INSPIRE].

[43] ATLAS collaboration, *Search for pair- and single-production of vector-like quarks in final states with at least one Z boson decaying into a pair of electrons or muons in pp collision data collected with the ATLAS detector at $\sqrt{s} = 13$ TeV*, Phys. Rev. **D 98** (2018) 112010 [arXiv:1806.10555] [INSPIRE].

[44] ATLAS collaboration, *Search for pair production of heavy vector-like quarks decaying to high-p_T W bosons and b quarks in the lepton-plus-jets final state in pp collisions at $\sqrt{s} = 13$ TeV with the ATLAS detector*, JHEP **10** (2017) 141 [arXiv:1707.03347] [INSPIRE].

JHEP05(2019)041

[45] CMS collaboration, *Search for pair production of vector-like quarks in the $bW\bar{b}W$ channel from proton-proton collisions at $\sqrt{s} = 13$ TeV*, Phys. Lett. **B 779** (2018) 82 [arXiv:1710.01539] [INSPIRE].

[46] CMS collaboration, *Search for pair production of vector-like T and B quarks in single-lepton final states using boosted jet substructure in proton-proton collisions at $\sqrt{s} = 13$ TeV*, JHEP **11** (2017) 085 [arXiv:1706.03408] [INSPIRE].

[47] ATLAS collaboration, *Search for pair production of heavy vector-like quarks decaying into hadronic final states in pp collisions at $\sqrt{s} = 13$ TeV with the ATLAS detector*, Phys. Rev. **D 98** (2018) 092005 [arXiv:1808.01771] [INSPIRE].

[48] ATLAS collaboration, *Search for pair production of up-type vector-like quarks and for four-top-quark events in final states with multiple b-jets with the ATLAS detector*, JHEP **07** (2018) 089 [arXiv:1803.09678] [INSPIRE].

[49] CMS collaboration, *Search for vector-like T and B quark pairs in final states with leptons at $\sqrt{s} = 13$ TeV*, JHEP **08** (2018) 177 [arXiv:1805.04758] [INSPIRE].

[50] ATLAS collaboration, *Combination of the searches for pair-produced vector-like partners of the third-generation quarks at $\sqrt{s} = 13$ TeV with the ATLAS detector*, Phys. Rev. Lett. **121** (2018) 211801 [arXiv:1808.02343] [INSPIRE].

[51] ATLAS collaboration, *Search for single production of vector-like quarks decaying into Wb in pp collisions at $\sqrt{s} = 8$ TeV with the ATLAS detector*, Eur. Phys. J. **C 76** (2016) 442 [arXiv:1602.05606] [INSPIRE].

[52] ATLAS collaboration, *Search for the production of single vector-like and excited quarks in the Wt final state in pp collisions at $\sqrt{s} = 8$ TeV with the ATLAS detector*, JHEP **02** (2016) 110 [arXiv:1510.02664] [INSPIRE].

[53] CMS collaboration, *Search for single production of vector-like quarks decaying into a b quark and a W boson in proton-proton collisions at $\sqrt{s} = 13$ TeV*, Phys. Lett. **B 772** (2017) 634 [arXiv:1701.08328] [INSPIRE].

[54] CMS collaboration, *Search for a heavy resonance decaying to a top quark and a vector-like top quark at $\sqrt{s} = 13$ TeV*, JHEP **09** (2017) 053 [arXiv:1703.06352] [INSPIRE].

[55] CMS collaboration, *Search for electroweak production of a vector-like quark decaying to a top quark and a Higgs boson using boosted topologies in fully hadronic final states*, JHEP **04** (2017) 136 [arXiv:1612.05336] [INSPIRE].

[56] CMS collaboration, *Search for single production of a heavy vector-like T quark decaying to a Higgs boson and a top quark with a lepton and jets in the final state*, Phys. Lett. **B 771** (2017) 80 [arXiv:1612.00999] [INSPIRE].

[57] CMS collaboration, *Search for single production of a vector-like T quark decaying to a Z boson and a top quark in proton-proton collisions at $\sqrt{s} = 13$ TeV*, Phys. Lett. **B 781** (2018) 574 [arXiv:1708.01062] [INSPIRE].

[58] CMS collaboration, *Search for single production of vector-like quarks decaying to a Z boson and a top or a bottom quark in proton-proton collisions at $\sqrt{s} = 13$ TeV*, JHEP **05** (2017) 029 [arXiv:1701.07409] [INSPIRE].

[59] D. Abercrombie et al., *Dark matter benchmark models for early LHC run-2 searches: report of the ATLAS/CMS dark matter forum*, arXiv:1507.00966 [INSPIRE].

[60] J. Wang, C.S. Li, D.Y. Shao and H. Zhang, *Search for the signal of monotop production at the early LHC*, Phys. Rev. **D 86** (2012) 034008 [arXiv:1109.5963] [INSPIRE].

JHEP05(2019)041

[61] ATLAS collaboration, *The ATLAS experiment at the CERN Large Hadron Collider*, 2008 *JINST* **3** S08003 [INSPIRE].

[62] ATLAS collaboration, *ATLAS insertable b-layer technical design report*, ATLAS-TDR-19 (2010).

[63] ATLAS IBL collaboration, *Production and integration of the ATLAS insertable B-layer*, 2018 *JINST* **13** T05008 [arXiv:1803.00844] [INSPIRE].

[64] ATLAS collaboration, *Performance of the ATLAS trigger system in 2015*, *Eur. Phys. J.* **C 77** (2017) 317 [arXiv:1611.09661] [INSPIRE].

[65] I. Boucheneb, G. Cacciapaglia, A. Deandrea and B. Fuks, *Revisiting monotop production at the LHC*, *JHEP* **01** (2015) 017 [arXiv:1407.7529] [INSPIRE].

[66] J. Alwall et al., *The automated computation of tree-level and next-to-leading order differential cross sections and their matching to parton shower simulations*, *JHEP* **07** (2014) 079 [arXiv:1405.0301] [INSPIRE].

[67] A. Alloul et al., *FeynRules 2.0 — A complete toolbox for tree-level phenomenology*, *Comput. Phys. Commun.* **185** (2014) 2250 [arXiv:1310.1921] [INSPIRE].

[68] C. Degrande et al., *UFO — The Universal FeynRules Output*, *Comput. Phys. Commun.* **183** (2012) 1201 [arXiv:1108.2040] [INSPIRE].

[69] NNPDF collaboration, *Parton distributions for the LHC run II*, *JHEP* **04** (2015) 040 [arXiv:1410.8849] [INSPIRE].

[70] T. Sjöstrand, S. Mrenna and P.Z. Skands, *A brief introduction to PYTHIA 8.1*, *Comput. Phys. Commun.* **178** (2008) 852 [arXiv:0710.3820] [INSPIRE].

[71] ATLAS collaboration, *ATLAS run 1 PYTHIA8 tunes*, ATL-PHYS-PUB-2014-021 (2014).

[72] R.D. Ball et al., *Parton distributions with LHC data*, *Nucl. Phys.* **B 867** (2013) 244 [arXiv:1207.1303] [INSPIRE].

[73] P. Nason, *A new method for combining NLO QCD with shower Monte Carlo algorithms*, *JHEP* **11** (2004) 040 [hep-ph/0409146] [INSPIRE].

[74] S. Frixione, P. Nason and C. Oleari, *Matching NLO QCD computations with parton shower simulations: the POWHEG method*, *JHEP* **11** (2007) 070 [arXiv:0709.2092] [INSPIRE].

[75] S. Alioli, P. Nason, C. Oleari and E. Re, *A general framework for implementing NLO calculations in shower Monte Carlo programs: the POWHEG BOX*, *JHEP* **06** (2010) 043 [arXiv:1002.2581] [INSPIRE].

[76] S. Frixione, P. Nason and G. Ridolfi, *A positive-weight next-to-leading-order Monte Carlo for heavy flavour hadroproduction*, *JHEP* **09** (2007) 126 [arXiv:0707.3088] [INSPIRE].

[77] R. Frederix, E. Re and P. Torrielli, *Single-top t-channel hadroproduction in the four-flavour scheme with POWHEG and aMC@NLO*, *JHEP* **09** (2012) 130 [arXiv:1207.5391] [INSPIRE].

[78] E. Re, *Single-top Wt-channel production matched with parton showers using the POWHEG method*, *Eur. Phys. J.* **C 71** (2011) 1547 [arXiv:1009.2450] [INSPIRE].

[79] S. Alioli, P. Nason, C. Oleari and E. Re, *NLO single-top production matched with shower in POWHEG: s- and t-channel contributions*, *JHEP* **09** (2009) 111 [*Erratum ibid.* **02** (2010) 011] [arXiv:0907.4076] [INSPIRE].

[80] T. Sjöstrand, S. Mrenna and P.Z. Skands, *PYTHIA 6.4 physics and manual*, *JHEP* **05** (2006) 026 [hep-ph/0603175] [INSPIRE].

JHEP05(2019)041

[81] J. Pumplin et al., *New generation of parton distributions with uncertainties from global QCD analysis*, *JHEP* **07** (2002) 012 [hep-ph/0201195] [INSPIRE].

[82] P.Z. Skands, *Tuning Monte Carlo generators: the Perugia tunes*, *Phys. Rev.* **D 82** (2010) 074018 [arXiv:1005.3457] [INSPIRE].

[83] H.-L. Lai et al., *New parton distributions for collider physics*, *Phys. Rev.* **D 82** (2010) 074024 [arXiv:1007.2241] [INSPIRE].

[84] T. Gleisberg et al., *Event generation with SHERPA 1.1*, *JHEP* **02** (2009) 007 [arXiv:0811.4622] [INSPIRE].

[85] T. Gleisberg and S. Hoeche, *Comix, a new matrix element generator*, *JHEP* **12** (2008) 039 [arXiv:0808.3674] [INSPIRE].

[86] F. Cascioli, P. Maierhofer and S. Pozzorini, *Scattering amplitudes with open loops*, *Phys. Rev. Lett.* **108** (2012) 111601 [arXiv:1111.5206] [INSPIRE].

[87] S. Schumann and F. Krauss, *A parton shower algorithm based on Catani-Seymour dipole factorisation*, *JHEP* **03** (2008) 038 [arXiv:0709.1027] [INSPIRE].

[88] S. Hoeche, F. Krauss, M. Schonherr and F. Siegert, *QCD matrix elements + parton showers: the NLO case*, *JHEP* **04** (2013) 027 [arXiv:1207.5030] [INSPIRE].

[89] NNPDF collaboration, *Parton distributions for the LHC Run II*, *JHEP* **04** (2015) 040 [arXiv:1410.8849] [INSPIRE].

[90] ATLAS collaboration, *Measurement of the Z/γ^* boson transverse momentum distribution in pp collisions at $\sqrt{s} = 7$ TeV with the ATLAS detector*, *JHEP* **09** (2014) 145 [arXiv:1406.3660] [INSPIRE].

[91] M. Czakon and A. Mitov, *Top++: a program for the calculation of the top-pair cross-section at hadron colliders*, *Comput. Phys. Commun.* **185** (2014) 2930 [arXiv:1112.5675] [INSPIRE].

[92] S. Catani et al., *Vector boson production at hadron colliders: a fully exclusive QCD calculation at NNLO*, *Phys. Rev. Lett.* **103** (2009) 082001 [arXiv:0903.2120] [INSPIRE].

[93] D.J. Lange, *The EvtGen particle decay simulation package*, *Nucl. Instrum. Meth.* **A 462** (2001) 152 [INSPIRE].

[94] ATLAS collaboration, *The ATLAS simulation infrastructure*, *Eur. Phys. J.* **C 70** (2010) 823 [arXiv:1005.4568] [INSPIRE].

[95] GEANT4 collaboration, *GEANT4: a simulation toolkit*, *Nucl. Instrum. Meth.* **A 506** (2003) 250 [INSPIRE].

[96] ATLAS collaboration, *The simulation principle and performance of the ATLAS fast calorimeter simulation FastCaloSim*, ATL-PHYS-PUB-2010-013 (2010).

[97] ATLAS collaboration, *Summary of ATLAS PYTHIA 8 tunes*, ATL-PHYS-PUB-2012-003 (2012).

[98] ATLAS collaboration, *Electron efficiency measurements with the ATLAS detector using the 2015 LHC proton-proton collision data*, ATLAS-CONF-2016-024 (2016).

[99] ATLAS collaboration, *Topological cell clustering in the ATLAS calorimeters and its performance in LHC Run 1*, *Eur. Phys. J.* **C 77** (2017) 490 [arXiv:1603.02934] [INSPIRE].

[100] ATLAS collaboration, *Muon reconstruction performance of the ATLAS detector in proton–proton collision data at $\sqrt{s} = 13$ TeV*, *Eur. Phys. J.* **C 76** (2016) 292 [arXiv:1603.05598] [INSPIRE].

[101] M. Cacciari, G.P. Salam and G. Soyez, *The anti-k_t jet clustering algorithm*, *JHEP* **04** (2008) 063 [arXiv:0802.1189] [INSPIRE].

[102] M. Cacciari, G.P. Salam and G. Soyez, *FastJet user manual*, *Eur. Phys. J.* **C 72** (2012) 1896 [arXiv:1111.6097] [INSPIRE].

[103] ATLAS collaboration, *Jet calibration and systematic uncertainties for jets reconstructed in the ATLAS detector at $\sqrt{s} = 13$ TeV*, ATL-PHYS-PUB-2015-015 (2015).

[104] ATLAS collaboration, *Selection of jets produced in 13TeV proton-proton collisions with the ATLAS detector*, ATLAS-CONF-2015-029 (2015).

[105] ATLAS collaboration, *Tagging and suppression of pileup jets with the ATLAS detector*, ATLAS-CONF-2014-018 (2014).

[106] D. Krohn, J. Thaler and L.-T. Wang, *Jet trimming*, *JHEP* **02** (2010) 084 [arXiv:0912.1342] [INSPIRE].

[107] ATLAS collaboration, *In-situ measurements of the ATLAS large-radius jet response in* 13 *TeV pp collisions*, ATLAS-CONF-2017-063 (2017).

[108] ATLAS collaboration, *Boosted hadronic top identification at ATLAS for early* 13 *TeV data*, ATL-PHYS-PUB-2015-053 (2015).

[109] J. Thaler and K. Van Tilburg, *Identifying boosted objects with N-subjettiness*, *JHEP* **03** (2011) 015 [arXiv:1011.2268] [INSPIRE].

[110] ATLAS collaboration, *Search for heavy particles decaying into top-quark pairs using lepton-plus-jets events in proton–proton collisions at $\sqrt{s} = 13$ TeV with the ATLAS detector*, *Eur. Phys. J.* **C 78** (2018) 565 [arXiv:1804.10823] [INSPIRE].

[111] ATLAS collaboration, *Performance of b-jet identification in the ATLAS experiment*, 2016 *JINST* **11** P04008 [arXiv:1512.01094] [INSPIRE].

[112] ATLAS collaboration, *Optimisation of the ATLAS b-tagging performance for the 2016 LHC Run*, ATL-PHYS-PUB-2016-012 (2016).

[113] ATLAS collaboration, *Calibration of light-flavour jet b-tagging rates on ATLAS proton-proton collision data at $\sqrt{s} = 13$ TeV*, ATLAS-CONF-2018-006 (2018).

[114] ATLAS collaboration, *Measurement of b-tagging Efficiency of c-jets in $t\bar{t}$ Events Using a Likelihood Approach with the ATLAS Detector*, ATLAS-CONF-2018-001 (2018).

[115] ATLAS collaboration, *Expected performance of missing transverse momentum reconstruction for the ATLAS detector at $\sqrt{s} = 13$ TeV*, ATL-PHYS-PUB-2015-023 (2015).

[116] ATLAS collaboration, *Performance of missing transverse momentum reconstruction for the ATLAS detector in the first proton-proton collisions at at $\sqrt{s} = 13$ TeV*, ATL-PHYS-PUB-2015-027 (2015).

[117] ATLAS collaboration, *Estimation of non-prompt and fake lepton backgrounds in final states with top quarks produced in proton-proton collisions at $\sqrt{s} = 8$ TeV with the ATLAS Detector*, ATLAS-CONF-2014-058 (1951336).

[118] ATLAS collaboration, *Jet energy scale measurements and their systematic uncertainties in proton-proton collisions at $\sqrt{s} = 13$ TeV with the ATLAS detector*, *Phys. Rev.* **D 96** (2017) 072002 [arXiv:1703.09665] [INSPIRE].

[119] ATLAS collaboration, *Luminosity determination in pp collisions at $\sqrt{s} = 8$ TeV using the ATLAS detector at the LHC*, *Eur. Phys. J.* **C 76** (2016) 653 [arXiv:1608.03953] [INSPIRE].

[120] G. Avoni et al., *The new LUCID-2 detector for luminosity measurement and monitoring in ATLAS*, 2018 *JINST* **13** P07017 [INSPIRE].

[121] M. Bahr et al., *HERWIG++ physics and manual*, *Eur. Phys. J.* **C 58** (2008) 639 [arXiv:0803.0883] [INSPIRE].

[122] ATLAS collaboration, *Comparison of Monte Carlo generator predictions to ATLAS measurements of top pair production at* 7 *TeV*, ATL-PHYS-PUB-2015-002 (2015).

[123] S. Frixione et al., *Single-top hadroproduction in association with a W boson*, *JHEP* **07** (2008) 029 [arXiv:0805.3067] [INSPIRE].

[124] ATLAS collaboration, *Analysis of the Wtb vertex from the measurement of triple-differential angular decay rates of single top quarks produced in the t-channel at* $\sqrt{s} = 8$ *TeV with the ATLAS detector*, *JHEP* **12** (2017) 017 [arXiv:1707.05393] [INSPIRE].

[125] ATLAS collaboration, *Measurement of the cross-section for W boso production in association with b-jets in pp collisions at* $\sqrt{s} = 7$ *TeV with the ATLAS detector*, *JHEP* **06** (2013) 084 [arXiv:1302.2929] [INSPIRE].

[126] J. Butterworth et al., *PDF4LHC recommendations for LHC Run II*, *J. Phys.* **G 43** (2016) 023001 [arXiv:1510.03865] [INSPIRE].

[127] W. Verkerke and D. Kirkby, *The RooFit toolkit for data modeling*, (2003).

[128] G. Cowan, K. Cranmer, E. Gross and O. Vitells, *Asymptotic formulae for likelihood-based tests of new physics*, *Eur. Phys. J.* **C 71** (2011) 1554 [*Erratum ibid.* **C 73** (2013) 2501] [arXiv:1007.1727] [INSPIRE].

[129] ATLAS collaboration, *Measurements of top-quark pair differential cross-sections in the lepton+jets channel in pp collisions at* $\sqrt{s} = 13$ *TeV using the ATLAS detector*, *JHEP* **11** (2017) 191 [arXiv:1708.00727] [INSPIRE].

[130] ATLAS collaboration, *Measurements of* $t\bar{t}$ *differential cross-sections of highly boosted top quarks decaying to all-hadronic final states in pp collisions at* $\sqrt{s} = 13$ *TeV using the ATLAS detector*, *Phys. Rev.* **D 98** (2018) 012003 [arXiv:1801.02052] [INSPIRE].

[131] ATLAS collaboration, *ATLAS computing acknowledgements*, ATL-GEN-PUB-2016-002 (2016).

The ATLAS collaboration

M. Aaboud[34d], G. Aad[99], B. Abbott[125], O. Abdinov[13,*], B. Abeloos[129], D.K. Abhayasinghe[91], S.H. Abidi[164], O.S. AbouZeid[39], N.L. Abraham[153], H. Abramowicz[158], H. Abreu[157], Y. Abulaiti[6], B.S. Acharya[64a,64b,p], S. Adachi[160], L. Adam[97], L. Adamczyk[81a], J. Adelman[119], M. Adersberger[112], A. Adiguzel[12c,ai], T. Adye[141], A.A. Affolder[143], Y. Afik[157], C. Agheorghiesei[27c], J.A. Aguilar-Saavedra[137f,137a,ah], F. Ahmadov[77,af], G. Aielli[71a,71b], S. Akatsuka[83], T.P.A. Åkesson[94], E. Akilli[52], A.V. Akimov[108], G.L. Alberghi[23b,23a], J. Albert[173], P. Albicocco[49], M.J. Alconada Verzini[86], S. Alderweireldt[117], M. Aleksa[35], I.N. Aleksandrov[77], C. Alexa[27b], T. Alexopoulos[10], M. Alhroob[125], B. Ali[139], G. Alimonti[66a], J. Alison[36], S.P. Alkire[145], C. Allaire[129], B.M.M. Allbrooke[153], B.W. Allen[128], P.P. Allport[21], A. Aloisio[67a,67b], A. Alonso[39], F. Alonso[86], C. Alpigiani[145], A.A. Alshehri[55], M.I. Alstaty[99], B. Alvarez Gonzalez[35], D. Álvarez Piqueras[171], M.G. Alviggi[67a,67b], B.T. Amadio[18], Y. Amaral Coutinho[78b], A. Ambler[101], L. Ambroz[132], C. Amelung[26], D. Amidei[103], S.P. Amor Dos Santos[137a,137c], S. Amoroso[44], C.S. Amrouche[52], F. An[76], C. Anastopoulos[146], L.S. Ancu[52], N. Andari[142], T. Andeen[11], C.F. Anders[59b], J.K. Anders[20], K.J. Anderson[36], A. Andreazza[66a,66b], V. Andrei[59a], C.R. Anelli[173], S. Angelidakis[37], I. Angelozzi[118], A. Angerami[38], A.V. Anisenkov[120b,120a], A. Annovi[69a], C. Antel[59a], M.T. Anthony[146], M. Antonelli[49], D.J.A. Antrim[168], F. Anulli[70a], M. Aoki[79], J.A. Aparisi Pozo[171], L. Aperio Bella[35], G. Arabidze[104], J.P. Araque[137a], V. Araujo Ferraz[78b], R. Araujo Pereira[78b], A.T.H. Arce[47], R.E. Ardell[91], F.A. Arduh[86], J-F. Arguin[107], S. Argyropoulos[75], A.J. Armbruster[35], L.J. Armitage[90], A. Armstrong[168], O. Arnaez[164], H. Arnold[118], M. Arratia[31], O. Arslan[24], A. Artamonov[109,*], G. Artoni[132], S. Artz[97], S. Asai[160], N. Asbah[57], E.M. Asimakopoulou[169], L. Asquith[153], K. Assamagan[29], R. Astalos[28a], R.J. Atkin[32a], M. Atkinson[170], N.B. Atlay[148], K. Augsten[139], G. Avolio[35], R. Avramidou[58a], M.K. Ayoub[15a], A.M. Azoulay[165b], G. Azuelos[107,av], A.E. Baas[59a], M.J. Baca[21], H. Bachacou[142], K. Bachas[65a,65b], M. Backes[132], P. Bagnaia[70a,70b], M. Bahmani[82], H. Bahrasemani[149], A.J. Bailey[171], J.T. Baines[141], M. Bajic[39], C. Bakalis[10], O.K. Baker[180], P.J. Bakker[118], D. Bakshi Gupta[8], S. Balaji[154], E.M. Baldin[120b,120a], P. Balek[177], F. Balli[142], W.K. Balunas[134], J. Balz[97], E. Banas[82], A. Bandyopadhyay[24], S. Banerjee[178,l], A.A.E. Bannoura[179], L. Barak[158], W.M. Barbe[37], E.L. Barberio[102], D. Barberis[53b,53a], M. Barbero[99], T. Barillari[113], M-S. Barisits[35], J. Barkeloo[128], T. Barklow[150], R. Barnea[157], S.L. Barnes[58c], B.M. Barnett[141], R.M. Barnett[18], Z. Barnovska-Blenessy[58a], A. Baroncelli[72a], G. Barone[29], A.J. Barr[132], L. Barranco Navarro[171], F. Barreiro[96], J. Barreiro Guimarães da Costa[15a], R. Bartoldus[150], A.E. Barton[87], P. Bartos[28a], A. Basalaev[135], A. Bassalat[129], R.L. Bates[55], S.J. Batista[164], S. Batlamous[34e], J.R. Batley[31], M. Battaglia[143], M. Bauce[70a,70b], F. Bauer[142], K.T. Bauer[168], H.S. Bawa[150,n], J.B. Beacham[123], T. Beau[133], P.H. Beauchemin[167], P. Bechtle[24], H.C. Beck[51], H.P. Beck[20,s], K. Becker[50], M. Becker[97], C. Becot[44], A. Beddall[12d], A.J. Beddall[12a], V.A. Bednyakov[77], M. Bedognetti[118], C.P. Bee[152], T.A. Beermann[74], M. Begalli[78b], M. Begel[29], A. Behera[152], J.K. Behr[44], A.S. Bell[92], G. Bella[158], L. Bellagamba[23b], A. Bellerive[33], M. Bellomo[157], P. Bellos[9], K. Belotskiy[110], N.L. Belyaev[110], O. Benary[158,*], D. Benchekroun[34a], M. Bender[112], N. Benekos[10], Y. Benhammou[158], E. Benhar Noccioli[180], J. Benitez[75], D.P. Benjamin[47], M. Benoit[52], J.R. Bensinger[26], S. Bentvelsen[118], L. Beresford[132], M. Beretta[49], D. Berge[44], E. Bergeaas Kuutmann[169], N. Berger[5], B. Bergmann[139], L.J. Bergsten[26], J. Beringer[18], S. Berlendis[7], N.R. Bernard[100], G. Bernardi[133], C. Bernius[150], F.U. Bernlochner[24], T. Berry[91], P. Berta[97], C. Bertella[15a], G. Bertoli[43a,43b], I.A. Bertram[87], G.J. Besjes[39], O. Bessidskaia Bylund[179], M. Bessner[44], N. Besson[142], A. Bethani[98], S. Bethke[113], A. Betti[24], A.J. Bevan[90], J. Beyer[113], R. Bi[136], R.M. Bianchi[136], O. Biebel[112], D. Biedermann[19], R. Bielski[35],

JHEP05(2019)041

K. Bierwagen[97], N.V. Biesuz[69a,69b], M. Biglietti[72a], T.R.V. Billoud[107], M. Bindi[51], A. Bingul[12d],
C. Bini[70a,70b], S. Biondi[23b,23a], M. Birman[177], T. Bisanz[51], J.P. Biswal[158], C. Bittrich[46],
D.M. Bjergaard[47], J.E. Black[150], K.M. Black[25], T. Blazek[28a], I. Bloch[44], C. Blocker[26], A. Blue[55],
U. Blumenschein[90], Dr. Blunier[144a], G.J. Bobbink[118], V.S. Bobrovnikov[120b,120a], S.S. Bocchetta[94],
A. Bocci[47], D. Boerner[179], D. Bogavac[112], A.G. Bogdanchikov[120b,120a], C. Bohm[43a],
V. Boisvert[91], P. Bokan[169], T. Bold[81a], A.S. Boldyrev[111], A.E. Bolz[59b], M. Bomben[133],
M. Bona[90], J.S. Bonilla[128], M. Boonekamp[142], A. Borisov[121], G. Borissov[87], J. Bortfeldt[35],
D. Bortoletto[132], V. Bortolotto[71a,71b], D. Boscherini[23b], M. Bosman[14], J.D. Bossio Sola[30],
K. Bouaouda[34a], J. Boudreau[136], E.V. Bouhova-Thacker[87], D. Boumediene[37], C. Bourdarios[129],
S.K. Boutle[55], A. Boveia[123], J. Boyd[35], D. Boye[32b,ap], I.R. Boyko[77], A.J. Bozson[91], J. Bracinik[21],
N. Brahimi[99], A. Brandt[8], G. Brandt[179], O. Brandt[59a], F. Braren[44], U. Bratzler[161], B. Brau[100],
J.E. Brau[128], W.D. Breaden Madden[55], K. Brendlinger[44], L. Brenner[44], R. Brenner[169],
S. Bressler[177], B. Brickwedde[97], D.L. Briglin[21], D. Britton[55], D. Britzger[113], I. Brock[24],
R. Brock[104], G. Brooijmans[38], T. Brooks[91], W.K. Brooks[144b], E. Brost[119], J.H Broughton[21],
P.A. Bruckman de Renstrom[82], D. Bruncko[28b], A. Bruni[23b], G. Bruni[23b], L.S. Bruni[118],
S. Bruno[71a,71b], B.H. Brunt[31], M. Bruschi[23b], N. Bruscino[136], P. Bryant[36], L. Bryngemark[44],
T. Buanes[17], Q. Buat[35], P. Buchholz[148], A.G. Buckley[55], I.A. Budagov[77], M.K. Bugge[131],
F. Bührer[50], O. Bulekov[110], D. Bullock[8], T.J. Burch[119], S. Burdin[88], C.D. Burgard[118],
A.M. Burger[5], B. Burghgrave[119], K. Burka[82], S. Burke[141], I. Burmeister[45], J.T.P. Burr[132],
V. Büscher[97], E. Buschmann[51], P. Bussey[55], J.M. Butler[25], C.M. Buttar[55], J.M. Butterworth[92],
P. Butti[35], W. Buttinger[35], A. Buzatu[155], A.R. Buzykaev[120b,120a], G. Cabras[23b,23a],
S. Cabrera Urbán[171], D. Caforio[139], H. Cai[170], V.M.M. Cairo[2], O. Cakir[4a], N. Calace[52],
P. Calafiura[18], A. Calandri[99], G. Calderini[133], P. Calfayan[63], G. Callea[55], L.P. Caloba[78b],
S. Calvente Lopez[96], D. Calvet[37], S. Calvet[37], T.P. Calvet[152], M. Calvetti[69a,69b],
R. Camacho Toro[133], S. Camarda[35], D. Camarero Munoz[96], P. Camarri[71a,71b], D. Cameron[131],
R. Caminal Armadans[100], C. Camincher[35], S. Campana[35], M. Campanelli[92], A. Camplani[39],
A. Campoverde[148], V. Canale[67a,67b], M. Cano Bret[58c], J. Cantero[126], T. Cao[158], Y. Cao[170],
M.D.M. Capeans Garrido[35], I. Caprini[27b], M. Caprini[27b], M. Capua[40b,40a], R.M. Carbone[38],
R. Cardarelli[71a], F.C. Cardillo[146], I. Carli[140], T. Carli[35], G. Carlino[67a], B.T. Carlson[136],
L. Carminati[66a,66b], R.M.D. Carney[43a,43b], S. Caron[117], E. Carquin[144b], S. Carrá[66a,66b],
G.D. Carrillo-Montoya[35], D. Casadei[32b], M.P. Casado[14,g], A.F. Casha[164], D.W. Casper[168],
R. Castelijn[118], F.L. Castillo[171], V. Castillo Gimenez[171], N.F. Castro[137a,137e], A. Catinaccio[35],
J.R. Catmore[131], A. Cattai[35], J. Caudron[24], V. Cavaliere[29], E. Cavallaro[14], D. Cavalli[66a],
M. Cavalli-Sforza[14], V. Cavasinni[69a,69b], E. Celebi[12b], F. Ceradini[72a,72b], L. Cerda Alberich[171],
A.S. Cerqueira[78a], A. Cerri[153], L. Cerrito[71a,71b], F. Cerutti[18], A. Cervelli[23b,23a], S.A. Cetin[12b],
A. Chafaq[34a], D. Chakraborty[119], S.K. Chan[57], W.S. Chan[118], Y.L. Chan[61a], J.D. Chapman[31],
B. Chargeishvili[156b], D.G. Charlton[21], C.C. Chau[33], C.A. Chavez Barajas[153], S. Che[123],
A. Chegwidden[104], S. Chekanov[6], S.V. Chekulaev[165a], G.A. Chelkov[77,au], M.A. Chelstowska[35],
C. Chen[58a], C.H. Chen[76], H. Chen[29], J. Chen[58a], J. Chen[38], S. Chen[134], S.J. Chen[15c],
X. Chen[15b,at], Y. Chen[80], Y-H. Chen[44], H.C. Cheng[103], H.J. Cheng[15d], A. Cheplakov[77],
E. Cheremushkina[121], R. Cherkaoui El Moursli[34e], E. Cheu[7], K. Cheung[62], T.J.A. Chevalérias[142],
L. Chevalier[142], V. Chiarella[49], G. Chiarelli[69a], G. Chiodini[65a], A.S. Chisholm[35,21], A. Chitan[27b],
I. Chiu[160], Y.H. Chiu[173], M.V. Chizhov[77], K. Choi[63], A.R. Chomont[129], S. Chouridou[159],
Y.S. Chow[118], V. Christodoulou[92], M.C. Chu[61a], J. Chudoba[138], A.J. Chuinard[101],
J.J. Chwastowski[82], L. Chytka[127], D. Cinca[45], V. Cindro[89], I.A. Cioară[24], A. Ciocio[18],
F. Cirotto[67a,67b], Z.H. Citron[177], M. Citterio[66a], A. Clark[52], M.R. Clark[38], P.J. Clark[48],
C. Clement[43a,43b], Y. Coadou[99], M. Cobal[64a,64c], A. Coccaro[53b], J. Cochran[76], H. Cohen[158],
A.E.C. Coimbra[177], L. Colasurdo[117], B. Cole[38], A.P. Colijn[118], J. Collot[56], P. Conde Muiño[137a,i],

E. Coniavitis[50], S.H. Connell[32b], I.A. Connelly[98], S. Constantinescu[27b], F. Conventi[67a,aw], A.M. Cooper-Sarkar[132], F. Cormier[172], K.J.R. Cormier[164], L.D. Corpe[92], M. Corradi[70a,70b], E.E. Corrigan[94], F. Corriveau[101,ad], A. Cortes-Gonzalez[35], M.J. Costa[171], F. Costanza[5], D. Costanzo[146], G. Cottin[31], G. Cowan[91], B.E. Cox[98], J. Crane[98], K. Cranmer[122], S.J. Crawley[55], R.A. Creager[134], G. Cree[33], S. Crépé-Renaudin[56], F. Crescioli[133], M. Cristinziani[24], V. Croft[122], G. Crosetti[40b,40a], A. Cueto[96], T. Cuhadar Donszelmann[146], A.R. Cukierman[150], S. Czekierda[82], P. Czodrowski[35], M.J. Da Cunha Sargedas De Sousa[58b], C. Da Via[98], W. Dabrowski[81a], T. Dado[28a,y], S. Dahbi[34e], T. Dai[103], F. Dallaire[107], C. Dallapiccola[100], M. Dam[39], G. D'amen[23b,23a], J. Damp[97], J.R. Dandoy[134], M.F. Daneri[30], N.P. Dang[178,l], N.D Dann[98], M. Danninger[172], V. Dao[35], G. Darbo[53b], S. Darmora[8], O. Dartsi[5], A. Dattagupta[128], T. Daubney[44], S. D'Auria[66a,66b], W. Davey[24], C. David[44], T. Davidek[140], D.R. Davis[47], E. Dawe[102], I. Dawson[146], K. De[8], R. De Asmundis[67a], A. De Benedetti[125], M. De Beurs[118], S. De Castro[23b,23a], S. De Cecco[70a,70b], N. De Groot[117], P. de Jong[118], H. De la Torre[104], F. De Lorenzi[76], A. De Maria[69a,69b], D. De Pedis[70a], A. De Salvo[70a], U. De Sanctis[71a,71b], M. De Santis[71a,71b], A. De Santo[153], K. De Vasconcelos Corga[99], J.B. De Vivie De Regie[129], C. Debenedetti[143], D.V. Dedovich[77], N. Dehghanian[3], M. Del Gaudio[40b,40a], J. Del Peso[96], Y. Delabat Diaz[44], D. Delgove[129], F. Deliot[142], C.M. Delitzsch[7], M. Della Pietra[67a,67b], D. Della Volpe[52], A. Dell'Acqua[35], L. Dell'Asta[25], M. Delmastro[5], C. Delporte[129], P.A. Delsart[56], D.A. DeMarco[164], S. Demers[180], M. Demichev[77], S.P. Denisov[121], D. Denysiuk[118], L. D'Eramo[133], D. Derendarz[82], J.E. Derkaoui[34d], F. Derue[133], P. Dervan[88], K. Desch[24], C. Deterre[44], K. Dette[164], M.R. Devesa[30], P.O. Deviveiros[35], A. Dewhurst[141], S. Dhaliwal[26], F.A. Di Bello[52], A. Di Ciaccio[71a,71b], L. Di Ciaccio[5], W.K. Di Clemente[134], C. Di Donato[67a,67b], A. Di Girolamo[35], G. Di Gregorio[69a,69b], B. Di Micco[72a,72b], R. Di Nardo[100], K.F. Di Petrillo[57], R. Di Sipio[164], D. Di Valentino[33], C. Diaconu[99], M. Diamond[164], F.A. Dias[39], T. Dias Do Vale[137a], M.A. Diaz[144a], J. Dickinson[18], E.B. Diehl[103], J. Dietrich[19], S. Díez Cornell[44], A. Dimitrievska[18], J. Dingfelder[24], F. Dittus[35], F. Djama[99], T. Djobava[156b], J.I. Djuvsland[59a], M.A.B. Do Vale[78c], M. Dobre[27b], D. Dodsworth[26], C. Doglioni[94], J. Dolejsi[140], Z. Dolezal[140], M. Donadelli[78d], J. Donini[37], A. D'onofrio[90], M. D'Onofrio[88], J. Dopke[141], A. Doria[67a], M.T. Dova[86], A.T. Doyle[55], E. Drechsler[51], E. Dreyer[149], T. Dreyer[51], Y. Du[58b], F. Dubinin[108], M. Dubovsky[28a], A. Dubreuil[52], E. Duchovni[177], G. Duckeck[112], A. Ducourthial[133], O.A. Ducu[107,x], D. Duda[113], A. Dudarev[35], A.C. Dudder[97], E.M. Duffield[18], L. Duflot[129], M. Dührssen[35], C. Dülsen[179], M. Dumancic[177], A.E. Dumitriu[27b,e], A.K. Duncan[55], M. Dunford[59a], A. Duperrin[99], H. Duran Yildiz[4a], M. Düren[54], A. Durglishvili[156b], D. Duschinger[46], B. Dutta[44], D. Duvnjak[1], M. Dyndal[44], S. Dysch[98], B.S. Dziedzic[82], C. Eckardt[44], K.M. Ecker[113], R.C. Edgar[103], T. Eifert[35], G. Eigen[17], K. Einsweiler[18], T. Ekelof[169], M. El Kacimi[34c], R. El Kosseifi[99], V. Ellajosyula[99], M. Ellert[169], F. Ellinghaus[179], A.A. Elliot[90], N. Ellis[35], J. Elmsheuser[29], M. Elsing[35], D. Emeliyanov[141], A. Emerman[38], Y. Enari[160], J.S. Ennis[175], M.B. Epland[47], J. Erdmann[45], A. Ereditato[20], S. Errede[170], M. Escalier[129], C. Escobar[171], O. Estrada Pastor[171], A.I. Etienvre[142], E. Etzion[158], H. Evans[63], A. Ezhilov[135], M. Ezzi[34e], F. Fabbri[55], L. Fabbri[23b,23a], V. Fabiani[117], G. Facini[92], R.M. Faisca Rodrigues Pereira[137a], R.M. Fakhrutdinov[121], S. Falciano[70a], P.J. Falke[5], S. Falke[5], J. Faltova[140], Y. Fang[15a], M. Fanti[66a,66b], A. Farbin[8], A. Farilla[72a], E.M. Farina[68a,68b], T. Farooque[104], S. Farrell[18], S.M. Farrington[175], P. Farthouat[35], F. Fassi[34e], P. Fassnacht[35], D. Fassouliotis[9], M. Faucci Giannelli[48], A. Favareto[53b,53a], W.J. Fawcett[31], L. Fayard[129], O.L. Fedin[135,q], W. Fedorko[172], M. Feickert[41], S. Feigl[131], L. Feligioni[99], C. Feng[58b], E.J. Feng[35], M. Feng[47], M.J. Fenton[55], A.B. Fenyuk[121], L. Feremenga[8], J. Ferrando[44], A. Ferrari[169], P. Ferrari[118], R. Ferrari[68a], D.E. Ferreira de Lima[59b], A. Ferrer[171], D. Ferrere[52], C. Ferretti[103], F. Fiedler[97], A. Filipčič[89], F. Filthaut[117], K.D. Finelli[25], M.C.N. Fiolhais[137a,137c,a], L. Fiorini[171], C. Fischer[14], W.C. Fisher[104], N. Flaschel[44], I. Fleck[148], P. Fleischmann[103], R.R.M. Fletcher[134], T. Flick[179], B.M. Flierl[112], L.M. Flores[134], L.R. Flores Castillo[61a], F.M. Follega[73a,73b], N. Fomin[17], G.T. Forcolin[73a,73b], A. Formica[142], F.A. Förster[14], A.C. Forti[98], A.G. Foster[21], D. Fournier[129], H. Fox[87], S. Fracchia[146], P. Francavilla[69a,69b], M. Franchini[23b,23a], S. Franchino[59a], D. Francis[35], L. Franconi[143], M. Franklin[57], M. Frate[168], M. Fraternali[68a,68b], A.N. Fray[90], D. Freeborn[92], S.M. Fressard-Batraneanu[35], B. Freund[107], W.S. Freund[78b], E.M. Freundlich[45], D.C. Frizzell[125], D. Froidevaux[35], J.A. Frost[132], C. Fukunaga[161], E. Fullana Torregrosa[171], T. Fusayasu[114], J. Fuster[171], O. Gabizon[157], A. Gabrielli[23b,23a], A. Gabrielli[18], G.P. Gach[81a], S. Gadatsch[52], P. Gadow[113], G. Gagliardi[53b,53a], L.G. Gagnon[107], C. Galea[27b], B. Galhardo[137a,137c], E.J. Gallas[132], B.J. Gallop[141], P. Gallus[139], G. Galster[39], R. Gamboa Goni[90], K.K. Gan[123], S. Ganguly[177], J. Gao[58a], Y. Gao[88], Y.S. Gao[150,n], C. García[171], J.E. García Navarro[171], J.A. García Pascual[15a], M. Garcia-Sciveres[18], R.W. Gardner[36], N. Garelli[150], S. Gargiulo[50], V. Garonne[131], K. Gasnikova[44], A. Gaudiello[53b,53a], G. Gaudio[68a], I.L. Gavrilenko[108], A. Gavrilyuk[109], C. Gay[172], G. Gaycken[24], E.N. Gazis[10], C.N.P. Gee[141], J. Geisen[51], M. Geisen[97], M.P. Geisler[59a], K. Gellerstedt[43a,43b], C. Gemme[53b], M.H. Genest[56], C. Geng[103], S. Gentile[70a,70b], S. George[91], D. Gerbaudo[14], G. Gessner[45], S. Ghasemi[148], M. Ghasemi Bostanabad[173], M. Ghneimat[24], B. Giacobbe[23b], S. Giagu[70a,70b], N. Giangiacomi[23b,23a], P. Giannetti[69a], A. Giannini[67a,67b], S.M. Gibson[91], M. Gignac[143], D. Gillberg[33], G. Gilles[179], D.M. Gingrich[3,av], M.P. Giordani[64a,64c], F.M. Giorgi[23b], P.F. Giraud[142], P. Giromini[57], G. Giugliarelli[64a,64c], D. Giugni[66a], F. Giuli[132], M. Giulini[59b], S. Gkaitatzis[159], I. Gkialas[9,k], E.L. Gkougkousis[14], P. Gkountoumis[10], L.K. Gladilin[111], C. Glasman[96], J. Glatzer[14], P.C.F. Glaysher[44], A. Glazov[44], M. Goblirsch-Kolb[26], J. Godlewski[82], S. Goldfarb[102], T. Golling[52], D. Golubkov[121], A. Gomes[137a,137b], R. Goncalves Gama[78a], R. Gonçalo[137a], G. Gonella[50], L. Gonella[21], A. Gongadze[77], F. Gonnella[21], J.L. Gonski[57], S. González de la Hoz[171], S. Gonzalez-Sevilla[52], L. Goossens[35], P.A. Gorbounov[109], H.A. Gordon[29], B. Gorini[35], E. Gorini[65a,65b], A. Gorišek[89], A.T. Goshaw[47], C. Gössling[45], M.I. Gostkin[77], C.A. Gottardo[24], C.R. Goudet[129], D. Goujdami[34c], A.G. Goussiou[145], N. Govender[32b,c], C. Goy[5], E. Gozani[157], I. Grabowska-Bold[81a], P.O.J. Gradin[169], E.C. Graham[88], J. Gramling[168], E. Gramstad[131], S. Grancagnolo[19], V. Gratchev[135], P.M. Gravila[27f], F.G. Gravili[65a,65b], C. Gray[55], H.M. Gray[18], Z.D. Greenwood[93,ak], C. Grefe[24], K. Gregersen[94], I.M. Gregor[44], P. Grenier[150], K. Grevtsov[44], N.A. Grieser[125], J. Griffiths[8], A.A. Grillo[143], K. Grimm[150,b], S. Grinstein[14,z], Ph. Gris[37], J.-F. Grivaz[129], S. Groh[97], E. Gross[177], J. Grosse-Knetter[51], G.C. Grossi[93], Z.J. Grout[92], C. Grud[103], A. Grummer[116], L. Guan[103], W. Guan[178], J. Guenther[35], A. Guerguichon[129], F. Guescini[165a], D. Guest[168], R. Gugel[50], B. Gui[123], T. Guillemin[5], S. Guindon[35], U. Gul[55], C. Gumpert[35], J. Guo[58c], W. Guo[103], Y. Guo[58a,t], Z. Guo[99], R. Gupta[44], S. Gurbuz[12c], G. Gustavino[125], B.J. Gutelman[157], P. Gutierrez[125], C. Gutschow[92], C. Guyot[142], M.P. Guzik[81a], C. Gwenlan[132], C.B. Gwilliam[88], A. Haas[122], C. Haber[18], H.K. Hadavand[8], N. Haddad[34e], A. Hadef[58a], S. Hageböck[24], M. Hagihara[166], H. Hakobyan[181,*], M. Haleem[174], J. Haley[126], G. Halladjian[104], G.D. Hallewell[99], K. Hamacher[179], P. Hamal[127], K. Hamano[173], A. Hamilton[32a], G.N. Hamity[146], K. Han[58a,aj], L. Han[58a], S. Han[15d], K. Hanagaki[79,v], M. Hance[143], D.M. Handl[112], B. Haney[134], R. Hankache[133], P. Hanke[59a], E. Hansen[94], J.B. Hansen[39], J.D. Hansen[39], M.C. Hansen[24], P.H. Hansen[39], E.C. Hanson[98], K. Hara[166], A.S. Hard[178], T. Harenberg[179], S. Harkusha[105], P.F. Harrison[175], N.M. Hartmann[112], Y. Hasegawa[147], A. Hasib[48], S. Hassani[142], S. Haug[20], R. Hauser[104], L. Hauswald[46], L.B. Havener[38], M. Havranek[139], C.M. Hawkes[21], R.J. Hawkings[35], D. Hayden[104], C. Hayes[152], C.P. Hays[132], J.M. Hays[90], H.S. Hayward[88], S.J. Haywood[141], M.P. Heath[48], V. Hedberg[94], L. Heelan[8], S. Heer[24], K.K. Heidegger[50], J. Heilman[33], S. Heim[44], T. Heim[18], B. Heinemann[44,aq], J.J. Heinrich[112], L. Heinrich[122], C. Heinz[54], J. Hejbal[138], L. Helary[35], A. Held[172], S. Hellesund[131],

JHEP05(2019)041

C.M. Helling[143], S. Hellman[43a,43b], C. Helsens[35], R.C.W. Henderson[87], Y. Heng[178], S. Henkelmann[172], A.M. Henriques Correia[35], G.H. Herbert[19], H. Herde[26], V. Herget[174], Y. Hernández Jiménez[32c], H. Herr[97], M.G. Herrmann[112], T. Herrmann[46], G. Herten[50], R. Hertenberger[112], L. Hervas[35], T.C. Herwig[134], G.G. Hesketh[92], N.P. Hessey[165a], A. Higashida[160], S. Higashino[79], E. Higón-Rodriguez[171], K. Hildebrand[36], E. Hill[173], J.C. Hill[31], K.K. Hill[29], K.H. Hiller[44], S.J. Hillier[21], M. Hils[46], I. Hinchliffe[18], M. Hirose[130], D. Hirschbuehl[179], B. Hiti[89], O. Hladik[138], D.R. Hlaluku[32c], X. Hoad[48], J. Hobbs[152], N. Hod[165a], M.C. Hodgkinson[146], A. Hoecker[35], M.R. Hoeferkamp[116], F. Hoenig[112], D. Hohn[24], D. Hohov[129], T.R. Holmes[36], M. Holzbock[112], M. Homann[45], S. Honda[166], T. Honda[79], T.M. Hong[136], A. Hönle[113], B.H. Hooberman[170], W.H. Hopkins[128], Y. Horii[115], P. Horn[46], A.J. Horton[149], L.A. Horyn[36], J-Y. Hostachy[56], A. Hostiuc[145], S. Hou[155], A. Hoummada[34a], J. Howarth[98], J. Hoya[86], M. Hrabovsky[127], J. Hrdinka[35], I. Hristova[19], J. Hrivnac[129], A. Hrynevich[106], T. Hryn'ova[5], P.J. Hsu[62], S.-C. Hsu[145], Q. Hu[29], S. Hu[58c], Y. Huang[15a], Z. Hubacek[139], F. Hubaut[99], M. Huebner[24], F. Huegging[24], T.B. Huffman[132], M. Huhtinen[35], R.F.H. Hunter[33], P. Huo[152], A.M. Hupe[33], N. Huseynov[77,af], J. Huston[104], J. Huth[57], R. Hyneman[103], G. Iacobucci[52], G. Iakovidis[29], I. Ibragimov[148], L. Iconomidou-Fayard[129], Z. Idrissi[34e], P. Iengo[35], R. Ignazzi[39], O. Igonkina[118,ab], R. Iguchi[160], T. Iizawa[52], Y. Ikegami[79], M. Ikeno[79], D. Iliadis[159], N. Ilic[117], F. Iltzsche[46], G. Introzzi[68a,68b], M. Iodice[72a], K. Iordanidou[38], V. Ippolito[70a,70b], M.F. Isacson[169], N. Ishijima[130], M. Ishino[160], M. Ishitsuka[162], W. Islam[126], C. Issever[132], S. Istin[157], F. Ito[166], J.M. Iturbe Ponce[61a], R. Iuppa[73a,73b], A. Ivina[177], H. Iwasaki[79], J.M. Izen[42], V. Izzo[67a], P. Jacka[138], P. Jackson[1], R.M. Jacobs[24], V. Jain[2], G. Jäkel[179], K.B. Jakobi[97], K. Jakobs[50], S. Jakobsen[74], T. Jakoubek[138], D.O. Jamin[126], R. Jansky[52], J. Janssen[24], M. Janus[51], P.A. Janus[81a], G. Jarlskog[94], N. Javadov[77,af], T. Javůrek[35], M. Javurkova[50], F. Jeanneau[142], L. Jeanty[18], J. Jejelava[156a,ag], A. Jelinskas[175], P. Jenni[50,d], J. Jeong[44], N. Jeong[44], S. Jézéquel[5], H. Ji[178], J. Jia[152], H. Jiang[76], Y. Jiang[58a], Z. Jiang[150,r], S. Jiggins[50], F.A. Jimenez Morales[37], J. Jimenez Pena[171], S. Jin[15c], A. Jinaru[27b], O. Jinnouchi[162], H. Jivan[32c], P. Johansson[146], K.A. Johns[7], C.A. Johnson[63], W.J. Johnson[145], K. Jon-And[43a,43b], R.W.L. Jones[87], S.D. Jones[153], S. Jones[7], T.J. Jones[88], J. Jongmanns[59a], P.M. Jorge[137a,137b], J. Jovicevic[165a], X. Ju[18], J.J. Junggeburth[113], A. Juste Rozas[14,z], A. Kaczmarska[82], M. Kado[129], H. Kagan[123], M. Kagan[150], T. Kaji[176], E. Kajomovitz[157], C.W. Kalderon[94], A. Kaluza[97], S. Kama[41], A. Kamenshchikov[121], L. Kanjir[89], Y. Kano[160], V.A. Kantserov[110], J. Kanzaki[79], B. Kaplan[122], L.S. Kaplan[178], D. Kar[32c], M.J. Kareem[165b], E. Karentzos[10], S.N. Karpov[77], Z.M. Karpova[77], V. Kartvelishvili[87], A.N. Karyukhin[121], L. Kashif[178], R.D. Kass[123], A. Kastanas[43a,43b], Y. Kataoka[160], C. Kato[58d,58c], J. Katzy[44], K. Kawade[80], K. Kawagoe[85], T. Kawamoto[160], G. Kawamura[51], E.F. Kay[88], V.F. Kazanin[120b,120a], R. Keeler[173], R. Kehoe[41], J.S. Keller[33], E. Kellermann[94], J.J. Kempster[21], J. Kendrick[21], O. Kepka[138], S. Kersten[179], B.P. Kerševan[89], S. Ketabchi Haghighat[164], R.A. Keyes[101], M. Khader[170], F. Khalil-Zada[13], A. Khanov[126], A.G. Kharlamov[120b,120a], T. Kharlamova[120b,120a], E.E. Khoda[172], A. Khodinov[163], T.J. Khoo[52], E. Khramov[77], J. Khubua[156b], S. Kido[80], M. Kiehn[52], C.R. Kilby[91], Y.K. Kim[36], N. Kimura[64a,64c], O.M. Kind[19], B.T. King[88], D. Kirchmeier[46], J. Kirk[141], A.E. Kiryunin[113], T. Kishimoto[160], D. Kisielewska[81a], V. Kitali[44], O. Kivernyk[5], E. Kladiva[28b,*], T. Klapdor-Kleingrothaus[50], M.H. Klein[103], M. Klein[88], U. Klein[88], K. Kleinknecht[97], P. Klimek[119], A. Klimentov[29], T. Klingl[24], T. Klioutchnikova[35], F.F. Klitzner[112], P. Kluit[118], S. Kluth[113], E. Kneringer[74], E.B.F.G. Knoops[99], A. Knue[50], A. Kobayashi[160], D. Kobayashi[85], T. Kobayashi[160], M. Kobel[46], M. Kocian[150], P. Kodys[140], P.T. Koenig[24], T. Koffas[33], E. Koffeman[118], N.M. Köhler[113], T. Koi[150], M. Kolb[59b], I. Koletsou[5], T. Kondo[79], N. Kondrashova[58c], K. Köneke[50], A.C. König[117], T. Kono[79], R. Konoplich[122,am], V. Konstantinides[92], N. Konstantinidis[92], B. Konya[94], R. Kopeliansky[63], S. Koperny[81a],

K. Korcyl[82], K. Kordas[159], G. Koren[158], A. Korn[92], I. Korolkov[14], E.V. Korolkova[146], N. Korotkova[111], O. Kortner[113], S. Kortner[113], T. Kosek[140], V.V. Kostyukhin[24], A. Kotwal[47], A. Koulouris[10], A. Kourkoumeli-Charalampidi[68a,68b], C. Kourkoumelis[9], E. Kourlitis[146], V. Kouskoura[29], A.B. Kowalewska[82], R. Kowalewski[173], T.Z. Kowalski[81a], C. Kozakai[160], W. Kozanecki[142], A.S. Kozhin[121], V.A. Kramarenko[111], G. Kramberger[89], D. Krasnopevtsev[58a], M.W. Krasny[133], A. Krasznahorkay[35], D. Krauss[113], J.A. Kremer[81a], J. Kretzschmar[88], P. Krieger[164], K. Krizka[18], K. Kroeninger[45], H. Kroha[113], J. Kroll[138], J. Kroll[134], J. Krstic[16], U. Kruchonak[77], H. Krüger[24], N. Krumnack[76], M.C. Kruse[47], T. Kubota[102], S. Kuday[4b], J.T. Kuechler[179], S. Kuehn[35], A. Kugel[59a], F. Kuger[174], T. Kuhl[44], V. Kukhtin[77], R. Kukla[99], Y. Kulchitsky[105], S. Kuleshov[144b], Y.P. Kulinich[170], M. Kuna[56], T. Kunigo[83], A. Kupco[138], T. Kupfer[45], O. Kuprash[158], H. Kurashige[80], L.L. Kurchaninov[165a], Y.A. Kurochkin[105], A. Kurova[110], M.G. Kurth[15d], E.S. Kuwertz[35], M. Kuze[162], J. Kvita[127], T. Kwan[101], A. La Rosa[113], J.L. La Rosa Navarro[78d], L. La Rotonda[40b,40a], F. La Ruffa[40b,40a], C. Lacasta[171], F. Lacava[70a,70b], J. Lacey[44], D.P.J. Lack[98], H. Lacker[19], D. Lacour[133], E. Ladygin[77], R. Lafaye[5], B. Laforge[133], T. Lagouri[32c], S. Lai[51], S. Lammers[63], W. Lampl[7], E. Lançon[29], U. Landgraf[50], M.P.J. Landon[90], M.C. Lanfermann[52], V.S. Lang[44], J.C. Lange[51], R.J. Langenberg[35], A.J. Lankford[168], F. Lanni[29], K. Lantzsch[24], A. Lanza[68a], A. Lapertosa[53b,53a], S. Laplace[133], J.F. Laporte[142], T. Lari[66a], F. Lasagni Manghi[23b,23a], M. Lassnig[35], T.S. Lau[61a], A. Laudrain[129], M. Lavorgna[67a,67b], M. Lazzaroni[66a,66b], B. Le[102], O. Le Dortz[133], E. Le Guirriec[99], E.P. Le Quilleuc[142], M. LeBlanc[7], T. LeCompte[6], F. Ledroit-Guillon[56], C.A. Lee[29], G.R. Lee[144a], L. Lee[57], S.C. Lee[155], B. Lefebvre[101], M. Lefebvre[173], F. Legger[112], C. Leggett[18], K. Lehmann[149], N. Lehmann[179], G. Lehmann Miotto[35], W.A. Leight[44], A. Leisos[159,w], M.A.L. Leite[78d], R. Leitner[140], D. Lellouch[177], K.J.C. Leney[92], T. Lenz[24], B. Lenzi[35], R. Leone[7], S. Leone[69a], C. Leonidopoulos[48], G. Lerner[153], C. Leroy[107], R. Les[164], A.A.J. Lesage[142], C.G. Lester[31], M. Levchenko[135], J. Levêque[5], D. Levin[103], L.J. Levinson[177], D. Lewis[90], B. Li[15b], B. Li[103], C-Q. Li[58a,al], H. Li[58a], H. Li[58b], L. Li[58c], M. Li[15a], Q. Li[15d], Q.Y. Li[58a], S. Li[58d,58c], X. Li[58c], Y. Li[148], Z. Liang[15a], B. Liberti[71a], A. Liblong[164], K. Lie[61c], S. Liem[118], A. Limosani[154], C.Y. Lin[31], K. Lin[104], T.H. Lin[97], R.A. Linck[63], J.H. Lindon[21], B.E. Lindquist[152], A.L. Lionti[52], E. Lipeles[134], A. Lipniacka[17], M. Lisovyi[59b], T.M. Liss[170,as], A. Lister[172], A.M. Litke[143], J.D. Little[8], B. Liu[76], B.L Liu[6], H.B. Liu[29], H. Liu[103], J.B. Liu[58a], J.K.K. Liu[132], K. Liu[133], M. Liu[58a], P. Liu[18], Y. Liu[15a], Y.L. Liu[58a], Y.W. Liu[58a], M. Livan[68a,68b], A. Lleres[56], J. Llorente Merino[15a], S.L. Lloyd[90], C.Y. Lo[61b], F. Lo Sterzo[41], E.M. Lobodzinska[44], P. Loch[7], T. Lohse[19], K. Lohwasser[146], M. Lokajicek[138], J.D. Long[170], R.E. Long[87], L. Longo[65a,65b], K.A. Looper[123], J.A. Lopez[144b], I. Lopez Paz[98], A. Lopez Solis[146], J. Lorenz[112], N. Lorenzo Martinez[5], M. Losada[22], P.J. Lösel[112], A. Lösle[50], X. Lou[44], X. Lou[15a], A. Lounis[129], J. Love[6], P.A. Love[87], J.J. Lozano Bahilo[171], H. Lu[61a], M. Lu[58a], Y.J. Lu[62], H.J. Lubatti[145], C. Luci[70a,70b], A. Lucotte[56], C. Luedtke[50], F. Luehring[63], I. Luise[133], L. Luminari[70a], B. Lund-Jensen[151], M.S. Lutz[100], P.M. Luzi[133], D. Lynn[29], R. Lysak[138], E. Lytken[94], F. Lyu[15a], V. Lyubushkin[77], T. Lyubushkina[77], H. Ma[29], L.L. Ma[58b], Y. Ma[58b], G. Maccarrone[49], A. Macchiolo[113], C.M. Macdonald[146], J. Machado Miguens[134,137b], D. Madaffari[171], R. Madar[37], W.F. Mader[46], A. Madsen[44], N. Madysa[46], J. Maeda[80], K. Maekawa[160], S. Maeland[17], T. Maeno[29], M. Maerker[46], A.S. Maevskiy[111], V. Magerl[50], D.J. Mahon[38], C. Maidantchik[78b], T. Maier[112], A. Maio[137a,137b,137d], O. Majersky[28a], S. Majewski[128], Y. Makida[79], N. Makovec[129], B. Malaescu[133], Pa. Malecki[82], V.P. Maleev[135], F. Malek[56], U. Mallik[75], D. Malon[6], C. Malone[31], S. Maltezos[10], S. Malyukov[35], J. Mamuzic[171], G. Mancini[49], I. Mandić[89], J. Maneira[137a], L. Manhaes de Andrade Filho[78a], J. Manjarres Ramos[46], K.H. Mankinen[94], A. Mann[112], A. Manousos[74], B. Mansoulie[142], J.D. Mansour[15a], M. Mantoani[51], S. Manzoni[66a,66b], A. Marantis[159], G. Marceca[30], L. March[52], L. Marchese[132], G. Marchiori[133], M. Marcisovsky[138],

C. Marcon[94], C.A. Marin Tobon[35], M. Marjanovic[37], D.E. Marley[103], F. Marroquim[78b], Z. Marshall[18], M.U.F Martensson[169], S. Marti-Garcia[171], C.B. Martin[123], T.A. Martin[175], V.J. Martin[48], B. Martin dit Latour[17], M. Martinez[14,z], V.I. Martinez Outschoorn[100], S. Martin-Haugh[141], V.S. Martoiu[27b], A.C. Martyniuk[92], A. Marzin[35], L. Masetti[97], T. Mashimo[160], R. Mashinistov[108], J. Masik[98], A.L. Maslennikov[120b,120a], L.H. Mason[102], L. Massa[71a,71b], P. Massarotti[67a,67b], P. Mastrandrea[5], A. Mastroberardino[40b,40a], T. Masubuchi[160], P. Mättig[179], J. Maurer[27b], B. Maček[89], S.J. Maxfield[88], D.A. Maximov[120b,120a], R. Mazini[155], I. Maznas[159], S.M. Mazza[143], G. Mc Goldrick[164], S.P. Mc Kee[103], A. McCarn[103], T.G. McCarthy[113], L.I. McClymont[92], W.P. McCormack[18], E.F. McDonald[102], J.A. Mcfayden[35], G. Mchedlidze[51], M.A. McKay[41], K.D. McLean[173], S.J. McMahon[141], P.C. McNamara[102], C.J. McNicol[175], R.A. McPherson[173,ad], J.E. Mdhluli[32c], Z.A. Meadows[100], S. Meehan[145], T.M. Megy[50], S. Mehlhase[112], A. Mehta[88], T. Meideck[56], B. Meirose[42], D. Melini[171,h], B.R. Mellado Garcia[32c], J.D. Mellenthin[51], M. Melo[28a], F. Meloni[44], A. Melzer[24], S.B. Menary[98], E.D. Mendes Gouveia[137a], L. Meng[88], X.T. Meng[103], A. Mengarelli[23b,23a], S. Menke[113], E. Meoni[40b,40a], S. Mergelmeyer[19], S.A.M. Merkt[136], C. Merlassino[20], P. Mermod[52], L. Merola[67a,67b], C. Meroni[66a], F.S. Merritt[36], A. Messina[70a,70b], J. Metcalfe[6], A.S. Mete[168], C. Meyer[134], J. Meyer[157], J-P. Meyer[142], H. Meyer Zu Theenhausen[59a], F. Miano[153], R.P. Middleton[141], L. Mijović[48], G. Mikenberg[177], M. Mikestikova[138], M. Mikuž[89], M. Milesi[102], A. Milic[164], D.A. Millar[90], D.W. Miller[36], A. Milov[177], D.A. Milstead[43a,43b], A.A. Minaenko[121], M. Miñano Moya[171], I.A. Minashvili[156b], A.I. Mincer[122], B. Mindur[81a], M. Mineev[77], Y. Minegishi[160], Y. Ming[178], L.M. Mir[14], A. Mirto[65a,65b], K.P. Mistry[134], T. Mitani[176], J. Mitrevski[112], V.A. Mitsou[171], M. Mittal[58c], A. Miucci[20], P.S. Miyagawa[146], A. Mizukami[79], J.U. Mjörnmark[94], T. Mkrtchyan[181], M. Mlynarikova[140], T. Moa[43a,43b], K. Mochizuki[107], P. Mogg[50], S. Mohapatra[38], S. Molander[43a,43b], R. Moles-Valls[24], M.C. Mondragon[104], K. Mönig[44], J. Monk[39], E. Monnier[99], A. Montalbano[149], J. Montejo Berlingen[35], F. Monticelli[86], S. Monzani[66a], N. Morange[129], D. Moreno[22], M. Moreno Llácer[35], P. Morettini[53b], M. Morgenstern[118], S. Morgenstern[46], D. Mori[149], M. Morii[57], M. Morinaga[176], V. Morisbak[131], A.K. Morley[35], G. Mornacchi[35], A.P. Morris[92], J.D. Morris[90], L. Morvaj[152], P. Moschovakos[10], M. Mosidze[156b], H.J. Moss[146], J. Moss[150,o], K. Motohashi[162], R. Mount[150], E. Mountricha[35], E.J.W. Moyse[100], S. Muanza[99], F. Mueller[113], J. Mueller[136], R.S.P. Mueller[112], D. Muenstermann[87], G.A. Mullier[94], F.J. Munoz Sanchez[98], P. Murin[28b], W.J. Murray[175,141], A. Murrone[66a,66b], M. Muškinja[89], C. Mwewa[32a], A.G. Myagkov[121,an], J. Myers[128], M. Myska[139], B.P. Nachman[18], O. Nackenhorst[45], K. Nagai[132], K. Nagano[79], Y. Nagasaka[60], M. Nagel[50], E. Nagy[99], A.M. Nairz[35], Y. Nakahama[115], K. Nakamura[79], T. Nakamura[160], I. Nakano[124], H. Nanjo[130], F. Napolitano[59a], R.F. Naranjo Garcia[44], R. Narayan[11], D.I. Narrias Villar[59a], I. Naryshkin[135], T. Naumann[44], G. Navarro[22], R. Nayyar[7], H.A. Neal[103,*], P.Y. Nechaeva[108], T.J. Neep[142], A. Negri[68a,68b], M. Negrini[23b], S. Nektarijevic[117], C. Nellist[51], M.E. Nelson[132], S. Nemecek[138], P. Nemethy[122], M. Nessi[35,f], M.S. Neubauer[170], M. Neumann[179], P.R. Newman[21], T.Y. Ng[61c], Y.S. Ng[19], H.D.N. Nguyen[99], T. Nguyen Manh[107], E. Nibigira[37], R.B. Nickerson[132], R. Nicolaidou[142], D.S. Nielsen[39], J. Nielsen[143], N. Nikiforou[11], V. Nikolaenko[121,an], I. Nikolic-Audit[133], K. Nikolopoulos[21], P. Nilsson[29], Y. Ninomiya[79], A. Nisati[70a], N. Nishu[58c], R. Nisius[113], I. Nitsche[45], T. Nitta[176], T. Nobe[160], Y. Noguchi[83], M. Nomachi[130], I. Nomidis[133], M.A. Nomura[29], T. Nooney[90], M. Nordberg[35], N. Norjoharuddeen[132], T. Novak[89], O. Novgorodova[46], R. Novotny[139], L. Nozka[127], K. Ntekas[168], E. Nurse[92], F. Nuti[102], F.G. Oakham[33,av], H. Oberlack[113], J. Ocariz[133], A. Ochi[80], I. Ochoa[38], J.P. Ochoa-Ricoux[144a], K. O'Connor[26], S. Oda[85], S. Odaka[79], S. Oerdek[51], A. Oh[98], S.H. Oh[47], C.C. Ohm[151], H. Oide[53b,53a], M.L. Ojeda[164], H. Okawa[166], Y. Okazaki[83], Y. Okumura[160], T. Okuyama[79], A. Olariu[27b], L.F. Oleiro Seabra[137a], S.A. Olivares Pino[144a], D. Oliveira Damazio[29], J.L. Oliver[1], M.J.R. Olsson[36], A. Olszewski[82], J. Olszowska[82], D.C. O'Neil[149], A. Onofre[137a,137e], K. Onogi[115], P.U.E. Onyisi[11], H. Oppen[131], M.J. Oreglia[36], G.E. Orellana[86], Y. Oren[158], D. Orestano[72a,72b], N. Orlando[61b], A.A. O'Rourke[44], R.S. Orr[164], B. Osculati[53b,53a,*], V. O'Shea[55], R. Ospanov[58a], G. Otero y Garzon[30], H. Otono[85], M. Ouchrif[34d], F. Ould-Saada[131], A. Ouraou[142], Q. Ouyang[15a], M. Owen[55], R.E. Owen[21], V.E. Ozcan[12c], N. Ozturk[8], J. Pacalt[127], H.A. Pacey[31], K. Pachal[149], A. Pacheco Pages[14], L. Pacheco Rodriguez[142], C. Padilla Aranda[14], S. Pagan Griso[18], M. Paganini[180], G. Palacino[63], S. Palazzo[48], S. Palestini[35], M. Palka[81b], D. Pallin[37], I. Panagoulias[10], C.E. Pandini[35], J.G. Panduro Vazquez[91], P. Pani[35], G. Panizzo[64a,64c], L. Paolozzi[52], T.D. Papadopoulou[10], K. Papageorgiou[9,k], A. Paramonov[6], D. Paredes Hernandez[61b], S.R. Paredes Saenz[132], B. Parida[163], T.H. Park[33], A.J. Parker[87], K.A. Parker[44], M.A. Parker[31], F. Parodi[53b,53a], J.A. Parsons[38], U. Parzefall[50], V.R. Pascuzzi[164], J.M.P. Pasner[143], E. Pasqualucci[70a], S. Passaggio[53b], F. Pastore[91], P. Pasuwan[43a,43b], S. Pataraia[97], J.R. Pater[98], A. Pathak[178,l], T. Pauly[35], B. Pearson[113], M. Pedersen[131], L. Pedraza Diaz[117], R. Pedro[137a,137b], S.V. Peleganchuk[120b,120a], O. Penc[138], C. Peng[15d], H. Peng[58a], B.S. Peralva[78a], M.M. Perego[129], A.P. Pereira Peixoto[137a], D.V. Perepelitsa[29], F. Peri[19], L. Perini[66a,66b], H. Pernegger[35], S. Perrella[67a,67b], V.D. Peshekhonov[77,*], K. Peters[44], R.F.Y. Peters[98], B.A. Petersen[35], T.C. Petersen[39], E. Petit[56], A. Petridis[1], C. Petridou[159], P. Petroff[129], M. Petrov[132], F. Petrucci[72a,72b], M. Pettee[180], N.E. Pettersson[100], A. Peyaud[142], R. Pezoa[144b], T. Pham[102], F.H. Phillips[104], P.W. Phillips[141], M.W. Phipps[170], G. Piacquadio[152], E. Pianori[18], A. Picazio[100], M.A. Pickering[132], R.H. Pickles[98], R. Piegaia[30], J.E. Pilcher[36], A.D. Pilkington[98], M. Pinamonti[71a,71b], J.L. Pinfold[3], M. Pitt[177], L. Pizzimento[71a,71b], M.-A. Pleier[29], V. Pleskot[140], E. Plotnikova[77], D. Pluth[76], P. Podberezko[120b,120a], R. Poettgen[94], R. Poggi[52], L. Poggioli[129], I. Pogrebnyak[104], D. Pohl[24], I. Pokharel[51], G. Polesello[68a], A. Poley[18], A. Policicchio[70a,70b], R. Polifka[35], A. Polini[23b], C.S. Pollard[44], V. Polychronakos[29], D. Ponomarenko[110], L. Pontecorvo[35], G.A. Popeneciu[27d], D.M. Portillo Quintero[133], S. Pospisil[139], K. Potamianos[44], I.N. Potrap[77], C.J. Potter[31], H. Potti[11], T. Poulsen[94], J. Poveda[35], T.D. Powell[146], M.E. Pozo Astigarraga[35], P. Pralavorio[99], S. Prell[76], D. Price[98], M. Primavera[65a], S. Prince[101], N. Proklova[110], K. Prokofiev[61c], F. Prokoshin[144b], S. Protopopescu[29], J. Proudfoot[6], M. Przybycien[81a], A. Puri[170], P. Puzo[129], J. Qian[103], Y. Qin[98], A. Quadt[51], M. Queitsch-Maitland[44], A. Qureshi[1], P. Rados[102], F. Ragusa[66a,66b], G. Rahal[95], J.A. Raine[52], S. Rajagopalan[29], A. Ramirez Morales[90], T. Rashid[129], S. Raspopov[5], M.G. Ratti[66a,66b], D.M. Rauch[44], F. Rauscher[112], S. Rave[97], B. Ravina[146], I. Ravinovich[177], J.H. Rawling[98], M. Raymond[35], A.L. Read[131], N.P. Readioff[56], M. Reale[65a,65b], D.M. Rebuzzi[68a,68b], A. Redelbach[174], G. Redlinger[29], R. Reece[143], R.G. Reed[32c], K. Reeves[42], L. Rehnisch[19], J. Reichert[134], D. Reikher[158], A. Reiss[97], C. Rembser[35], H. Ren[15d], M. Rescigno[70a], S. Resconi[66a], E.D. Resseguie[134], S. Rettie[172], E. Reynolds[21], O.L. Rezanova[120b,120a], P. Reznicek[140], E. Ricci[73a,73b], R. Richter[113], S. Richter[44], E. Richter-Was[81b], O. Ricken[24], M. Ridel[133], P. Rieck[113], C.J. Riegel[179], O. Rifki[44], M. Rijssenbeek[152], A. Rimoldi[68a,68b], M. Rimoldi[20], L. Rinaldi[23b], G. Ripellino[151], B. Ristić[87], E. Ritsch[35], I. Riu[14], J.C. Rivera Vergara[144a], F. Rizatdinova[126], E. Rizvi[90], C. Rizzi[14], R.T. Roberts[98], S.H. Robertson[101,ad], D. Robinson[31], J.E.M. Robinson[44], A. Robson[55], E. Rocco[97], C. Roda[69a,69b], Y. Rodina[99], S. Rodriguez Bosca[171], A. Rodriguez Perez[14], D. Rodriguez Rodriguez[171], A.M. Rodríguez Vera[165b], S. Roe[35], C.S. Rogan[57], O. Røhne[131], R. Röhrig[113], C.P.A. Roland[63], J. Roloff[57], A. Romaniouk[110], M. Romano[23b,23a], N. Rompotis[88], M. Ronzani[122], L. Roos[133], S. Rosati[70a], K. Rosbach[50], N-A. Rosien[51], B.J. Rosser[134], E. Rossi[44], E. Rossi[72a,72b], E. Rossi[67a,67b], L.P. Rossi[53b], L. Rossini[66a,66b], J.H.N. Rosten[31], R. Rosten[14], M. Rotaru[27b], J. Rothberg[145], D. Rousseau[129], D. Roy[32c], A. Rozanov[99], Y. Rozen[157], X. Ruan[32c], F. Rubbo[150], F. Rühr[50], A. Ruiz-Martinez[171], Z. Rurikova[50], N.A. Rusakovich[77], H.L. Russell[101], J.P. Rutherfoord[7], E.M. Rüttinger[44,m], Y.F. Ryabov[135], M. Rybar[170], G. Rybkin[129], S. Ryu[6], A. Ryzhov[121], G.F. Rzehorz[51], P. Sabatini[51], G. Sabato[118], S. Sacerdoti[129], H.F-W. Sadrozinski[143], R. Sadykov[77], F. Safai Tehrani[70a], P. Saha[119], M. Sahinsoy[59a], A. Sahu[179], M. Saimpert[44], M. Saito[160], T. Saito[160], H. Sakamoto[160], A. Sakharov[122,am], D. Salamani[52], G. Salamanna[72a,72b], J.E. Salazar Loyola[144b], P.H. Sales De Bruin[169], D. Salihagic[113,*], A. Salnikov[150], J. Salt[171], D. Salvatore[40b,40a], F. Salvatore[153], A. Salvucci[61a,61b,61c], A. Salzburger[35], J. Samarati[35], D. Sammel[50], D. Sampsonidis[159], D. Sampsonidou[159], J. Sánchez[171], A. Sanchez Pineda[64a,64c], H. Sandaker[131], C.O. Sander[44], M. Sandhoff[179], C. Sandoval[22], D.P.C. Sankey[141], M. Sannino[53b,53a], Y. Sano[115], A. Sansoni[49], C. Santoni[37], H. Santos[137a], I. Santoyo Castillo[153], A. Santra[171], A. Sapronov[77], J.G. Saraiva[137a,137d], O. Sasaki[79], K. Sato[166], E. Sauvan[5], P. Savard[164,av], N. Savic[113], R. Sawada[160], C. Sawyer[141], L. Sawyer[93,ak], C. Sbarra[23b], A. Sbrizzi[23a], T. Scanlon[92], J. Schaarschmidt[145], P. Schacht[113], B.M. Schachtner[112], D. Schaefer[36], L. Schaefer[134], J. Schaeffer[97], S. Schaepe[35], U. Schäfer[97], A.C. Schaffer[129], D. Schaile[112], R.D. Schamberger[152], N. Scharmberg[98], V.A. Schegelsky[135], D. Scheirich[140], F. Schenck[19], M. Schernau[168], C. Schiavi[53b,53a], S. Schier[143], L.K. Schildgen[24], Z.M. Schillaci[26], E.J. Schioppa[35], M. Schioppa[40b,40a], K.E. Schleicher[50], S. Schlenker[35], K.R. Schmidt-Sommerfeld[113], K. Schmieden[35], C. Schmitt[97], S. Schmitt[44], S. Schmitz[97], J.C. Schmoeckel[44], U. Schnoor[50], L. Schoeffel[142], A. Schoening[59b], E. Schopf[132], M. Schott[97], J.F.P. Schouwenberg[117], J. Schovancova[35], S. Schramm[52], A. Schulte[97], H-C. Schultz-Coulon[59a], M. Schumacher[50], B.A. Schumm[143], Ph. Schune[142], A. Schwartzman[150], T.A. Schwarz[103], Ph. Schwemling[142], R. Schwienhorst[104], A. Sciandra[24], G. Sciolla[26], M. Scornajenghi[40b,40a], F. Scuri[69a], F. Scutti[102], L.M. Scyboz[113], C.D. Sebastiani[70a,70b], P. Seema[19], S.C. Seidel[116], A. Seiden[143], T. Seiss[36], J.M. Seixas[78b], G. Sekhniaidze[67a], K. Sekhon[103], S.J. Sekula[41], N. Semprini-Cesari[23b,23a], S. Sen[47], S. Senkin[37], C. Serfon[131], L. Serin[129], L. Serkin[64a,64b], M. Sessa[58a], H. Severini[125], F. Sforza[167], A. Sfyrla[52], E. Shabalina[51], J.D. Shahinian[143], N.W. Shaikh[43a,43b], L.Y. Shan[15a], R. Shang[170], J.T. Shank[25], M. Shapiro[18], A.S. Sharma[1], A. Sharma[132], P.B. Shatalov[109], K. Shaw[153], S.M. Shaw[98], A. Shcherbakova[135], Y. Shen[125], N. Sherafati[33], A.D. Sherman[25], P. Sherwood[92], L. Shi[155,ar], S. Shimizu[79], C.O. Shimmin[180], Y. Shimogama[176], M. Shimojima[114], I.P.J. Shipsey[132], S. Shirabe[85], M. Shiyakova[77], J. Shlomi[177], A. Shmeleva[108], D. Shoaleh Saadi[107], M.J. Shochet[36], S. Shojaii[102], D.R. Shope[125], S. Shrestha[123], E. Shulga[110], P. Sicho[138], A.M. Sickles[170], P.E. Sidebo[151], E. Sideras Haddad[32c], O. Sidiropoulou[35], A. Sidoti[23b,23a], F. Siegert[46], Dj. Sijacki[16], J. Silva[137a], M. Silva Jr.[178], M.V. Silva Oliveira[78a], S.B. Silverstein[43a], S. Simion[129], E. Simioni[97], M. Simon[97], R. Simoniello[97], P. Sinervo[164], N.B. Sinev[128], M. Sioli[23b,23a], G. Siragusa[174], I. Siral[103], S.Yu. Sivoklokov[111], J. Sjölin[43a,43b], P. Skubic[125], M. Slater[21], T. Slavicek[139], M. Slawinska[82], K. Sliwa[167], R. Slovak[140], V. Smakhtin[177], B.H. Smart[5], J. Smiesko[28a], N. Smirnov[110], S.Yu. Smirnov[110], Y. Smirnov[110], L.N. Smirnova[111], O. Smirnova[94], J.W. Smith[51], M. Smizanska[87], K. Smolek[139], A. Smykiewicz[82], A.A. Snesarev[108], I.M. Snyder[128], S. Snyder[29], R. Sobie[173,ad], A.M. Soffa[168], A. Soffer[158], A. Søgaard[48], D.A. Soh[155], G. Sokhrannyi[89], C.A. Solans Sanchez[35], M. Solar[139], E.Yu. Soldatov[110], U. Soldevila[171], A.A. Solodkov[121], A. Soloshenko[77], O.V. Solovyanov[121], V. Solovyev[135], P. Sommer[146], H. Son[167], W. Song[141], W.Y. Song[165b], A. Sopczak[139], F. Sopkova[28b], C.L. Sotiropoulou[69a,69b], S. Sottocornola[68a,68b], R. Soualah[64a,64c,j], A.M. Soukharev[120b,120a], D. South[44], B.C. Sowden[91], S. Spagnolo[65a,65b], M. Spalla[113], M. Spangenberg[175], F. Spanò[91], D. Sperlich[19], T.M. Spieker[59a], R. Spighi[23b], G. Spigo[35], L.A. Spiller[102], D.P. Spiteri[55], M. Spousta[140], A. Stabile[66a,66b], R. Stamen[59a], S. Stamm[19], E. Stanecka[82], R.W. Stanek[6], C. Stanescu[72a], B. Stanislaus[132], M.M. Stanitzki[44], B. Stapf[118], S. Stapnes[131], E.A. Starchenko[121], G.H. Stark[36], J. Stark[56], S.H Stark[39], P. Staroba[138],

P. Starovoitov[59a], S. Stärz[35], R. Staszewski[82], M. Stegler[44], P. Steinberg[29], B. Stelzer[149], H.J. Stelzer[35], O. Stelzer-Chilton[165a], H. Stenzel[54], T.J. Stevenson[153], G.A. Stewart[35], M.C. Stockton[35], G. Stoicea[27b], P. Stolte[51], S. Stonjek[113], A. Straessner[46], J. Strandberg[151], S. Strandberg[43a,43b], M. Strauss[125], P. Strizenec[28b], R. Ströhmer[174], D.M. Strom[128], R. Stroynowski[41], A. Strubig[48], S.A. Stucci[29], B. Stugu[17], J. Stupak[125], N.A. Styles[44], D. Su[150], J. Su[136], S. Suchek[59a], Y. Sugaya[130], M. Suk[139], V.V. Sulin[108], M.J. Sullivan[88], D.M.S. Sultan[52], S. Sultansoy[4c], T. Sumida[83], S. Sun[103], X. Sun[3], K. Suruliz[153], C.J.E. Suster[154], M.R. Sutton[153], S. Suzuki[79], M. Svatos[138], M. Swiatlowski[36], S.P. Swift[2], A. Sydorenko[97], I. Sykora[28a], T. Sykora[140], D. Ta[97], K. Tackmann[44,aa], J. Taenzer[158], A. Taffard[168], R. Tafirout[165a], E. Tahirovic[90], N. Taiblum[158], H. Takai[29], R. Takashima[84], E.H. Takasugi[113], K. Takeda[80], T. Takeshita[147], Y. Takubo[79], M. Talby[99], A.A. Talyshev[120b,120a], J. Tanaka[160], M. Tanaka[162], R. Tanaka[129], B.B. Tannenwald[123], S. Tapia Araya[144b], S. Tapprogge[97], A. Tarek Abouelfadl Mohamed[133], S. Tarem[157], G. Tarna[27b,e], G.F. Tartarelli[66a], P. Tas[140], M. Tasevsky[138], T. Tashiro[83], E. Tassi[40b,40a], A. Tavares Delgado[137a,137b], Y. Tayalati[34e], A.C. Taylor[116], A.J. Taylor[48], G.N. Taylor[102], P.T.E. Taylor[102], W. Taylor[165b], A.S. Tee[87], P. Teixeira-Dias[91], H. Ten Kate[35], J.J. Teoh[118], S. Terada[79], K. Terashi[160], J. Terron[96], S. Terzo[14], M. Testa[49], R.J. Teuscher[164,ad], S.J. Thais[180], T. Theveneaux-Pelzer[44], F. Thiele[39], D.W. Thomas[91], J.P. Thomas[21], A.S. Thompson[55], P.D. Thompson[21], L.A. Thomsen[180], E. Thomson[134], Y. Tian[38], R.E. Ticse Torres[51], V.O. Tikhomirov[108,ao], Yu.A. Tikhonov[120b,120a], S. Timoshenko[110], P. Tipton[180], S. Tisserant[99], K. Todome[162], S. Todorova-Nova[5], S. Todt[46], J. Tojo[85], S. Tokár[28a], K. Tokushuku[79], E. Tolley[123], K.G. Tomiwa[32c], M. Tomoto[115], L. Tompkins[150,r], K. Toms[116], B. Tong[57], P. Tornambe[50], E. Torrence[128], H. Torres[46], E. Torró Pastor[145], C. Tosciri[132], J. Toth[99,ac], F. Touchard[99], D.R. Tovey[146], C.J. Treado[122], T. Trefzger[174], F. Tresoldi[153], A. Tricoli[29], I.M. Trigger[165a], S. Trincaz-Duvoid[133], M.F. Tripiana[14], W. Trischuk[164], B. Trocmé[56], A. Trofymov[129], C. Troncon[66a], M. Trovatelli[173], F. Trovato[153], L. Truong[32b], M. Trzebinski[82], A. Trzupek[82], F. Tsai[44], J.C-L. Tseng[132], P.V. Tsiareshka[105], A. Tsirigotis[159], N. Tsirintanis[9], V. Tsiskaridze[152], E.G. Tskhadadze[156a], I.I. Tsukerman[109], V. Tsulaia[18], S. Tsuno[79], D. Tsybychev[152,163], Y. Tu[61b], A. Tudorache[27b], V. Tudorache[27b], T.T. Tulbure[27a], A.N. Tuna[57], S. Turchikhin[77], D. Turgeman[177], I. Turk Cakir[4b,u], R.T. Turra[66a], P.M. Tuts[38], E. Tzovara[97], G. Ucchielli[23b,23a], I. Ueda[79], M. Ughetto[43a,43b], F. Ukegawa[166], G. Unal[35], A. Undrus[29], G. Unel[168], F.C. Ungaro[102], Y. Unno[79], K. Uno[160], J. Urban[28b], P. Urquijo[102], P. Urrejola[97], G. Usai[8], J. Usui[79], L. Vacavant[99], V. Vacek[139], B. Vachon[101], K.O.H. Vadla[131], A. Vaidya[92], C. Valderanis[112], E. Valdes Santurio[43a,43b], M. Valente[52], S. Valentinetti[23b,23a], A. Valero[171], L. Valéry[44], R.A. Vallance[21], A. Vallier[5], J.A. Valls Ferrer[171], T.R. Van Daalen[14], H. Van der Graaf[118], P. Van Gemmeren[6], J. Van Nieuwkoop[149], I. Van Vulpen[118], M. Vanadia[71a,71b], W. Vandelli[35], A. Vaniachine[163], P. Vankov[118], R. Vari[70a], E.W. Varnes[7], C. Varni[53b,53a], T. Varol[41], D. Varouchas[129], K.E. Varvell[154], G.A. Vasquez[144b], J.G. Vasquez[180], F. Vazeille[37], D. Vazquez Furelos[14], T. Vazquez Schroeder[35], J. Veatch[51], V. Vecchio[72a,72b], L.M. Veloce[164], F. Veloso[137a,137c], S. Veneziano[70a], A. Ventura[65a,65b], M. Venturi[173], N. Venturi[35], V. Vercesi[68a], M. Verducci[72a,72b], C.M. Vergel Infante[76], C. Vergis[24], W. Verkerke[118], A.T. Vermeulen[118], J.C. Vermeulen[118], M.C. Vetterli[149,av], N. Viaux Maira[144b], M. Vicente Barreto Pinto[52], I. Vichou[170,*], T. Vickey[146], O.E. Vickey Boeriu[146], G.H.A. Viehhauser[132], S. Viel[18], L. Vigani[132], M. Villa[23b,23a], M. Villaplana Perez[66a,66b], E. Vilucchi[49], M.G. Vincter[33], V.B. Vinogradov[77], A. Vishwakarma[44], C. Vittori[23b,23a], I. Vivarelli[153], S. Vlachos[10], M. Vogel[179], P. Vokac[139], G. Volpi[14], S.E. von Buddenbrock[32c], E. Von Toerne[24], V. Vorobel[140], K. Vorobev[110], M. Vos[171], J.H. Vossebeld[88], N. Vranjes[16], M. Vranjes Milosavljevic[16], V. Vrba[139], M. Vreeswijk[118], T. Šfiligoj[89], R. Vuillermet[35], I. Vukotic[36], T. Ženiš[28a], L. Živković[16], P. Wagner[24], W. Wagner[179],

J. Wagner-Kuhr[112], H. Wahlberg[86], S. Wahrmund[46], K. Wakamiya[80], V.M. Walbrecht[113], J. Walder[87], R. Walker[112], S.D. Walker[91], W. Walkowiak[148], V. Wallangen[43a,43b], A.M. Wang[57], C. Wang[58b,e], F. Wang[178], H. Wang[18], H. Wang[3], J. Wang[154], J. Wang[59b], P. Wang[41], Q. Wang[125], R.-J. Wang[133], R. Wang[58a], R. Wang[6], S.M. Wang[155], W.T. Wang[58a], W. Wang[15c,ae], W.X. Wang[58a,ae], Y. Wang[58a,al], Z. Wang[58c], C. Wanotayaroj[44], A. Warburton[101], C.P. Ward[31], D.R. Wardrope[92], A. Washbrook[48], P.M. Watkins[21], A.T. Watson[21], M.F. Watson[21], G. Watts[145], S. Watts[98], B.M. Waugh[92], A.F. Webb[11], S. Webb[97], C. Weber[180], M.S. Weber[20], S.A. Weber[33], S.M. Weber[59a], A.R. Weidberg[132], B. Weinert[63], J. Weingarten[45], M. Weirich[97], C. Weiser[50], P.S. Wells[35], T. Wenaus[29], T. Wengler[35], S. Wenig[35], N. Wermes[24], M.D. Werner[76], P. Werner[35], M. Wessels[59a], T.D. Weston[20], K. Whalen[128], N.L. Whallon[145], A.M. Wharton[87], A.S. White[103], A. White[8], M.J. White[1], R. White[144b], D. Whiteson[168], B.W. Whitmore[87], F.J. Wickens[141], W. Wiedenmann[178], M. Wielers[141], C. Wiglesworth[39], L.A.M. Wiik-Fuchs[50], F. Wilk[98], H.G. Wilkens[35], L.J. Wilkins[91], H.H. Williams[134], S. Williams[31], C. Willis[104], S. Willocq[100], J.A. Wilson[21], I. Wingerter-Seez[5], E. Winkels[153], F. Winklmeier[128], O.J. Winston[153], B.T. Winter[50], M. Wittgen[150], M. Wobisch[93], A. Wolf[97], T.M.H. Wolf[118], R. Wolff[99], M.W. Wolter[82], H. Wolters[137a,137c], V.W.S. Wong[172], N.L. Woods[143], S.D. Worm[21], B.K. Wosiek[82], K.W. Woźniak[82], K. Wraight[55], M. Wu[36], S.L. Wu[178], X. Wu[52], Y. Wu[58a], T.R. Wyatt[98], B.M. Wynne[48], S. Xella[39], Z. Xi[103], L. Xia[175], D. Xu[15a], H. Xu[58a,e], L. Xu[29], T. Xu[142], W. Xu[103], B. Yabsley[154], S. Yacoob[32a], K. Yajima[130], D.P. Yallup[92], D. Yamaguchi[162], Y. Yamaguchi[162], A. Yamamoto[79], T. Yamanaka[160], F. Yamane[80], M. Yamatani[160], T. Yamazaki[160], Y. Yamazaki[80], Z. Yan[25], H.J. Yang[58c,58d], H.T. Yang[18], S. Yang[75], Y. Yang[160], Z. Yang[17], W-M. Yao[18], Y.C. Yap[44], Y. Yasu[79], E. Yatsenko[58c,58d], J. Ye[41], S. Ye[29], I. Yeletskikh[77], E. Yigitbasi[25], E. Yildirim[97], K. Yorita[176], K. Yoshihara[134], C.J.S. Young[35], C. Young[150], J. Yu[8], J. Yu[76], X. Yue[59a], S.P.Y. Yuen[24], B. Zabinski[82], G. Zacharis[10], E. Zaffaroni[52], R. Zaidan[14], A.M. Zaitsev[121,an], T. Zakareishvili[156b], N. Zakharchuk[33], J. Zalieckas[17], S. Zambito[57], D. Zanzi[35], D.R. Zaripovas[55], S.V. Zeißner[45], C. Zeitnitz[179], G. Zemaityte[132], J.C. Zeng[170], Q. Zeng[150], O. Zenin[121], D. Zerwas[129], M. Zgubič[132], D.F. Zhang[58b], D. Zhang[103], F. Zhang[178], G. Zhang[58a], G. Zhang[15b], H. Zhang[15c], J. Zhang[6], L. Zhang[15c], L. Zhang[58a], M. Zhang[170], P. Zhang[15c], R. Zhang[58a], R. Zhang[24], X. Zhang[58b], Y. Zhang[15d], Z. Zhang[129], P. Zhao[47], Y. Zhao[58b,129,aj], Z. Zhao[58a], A. Zhemchugov[77], Z. Zheng[103], D. Zhong[170], B. Zhou[103], C. Zhou[178], L. Zhou[41], M.S. Zhou[15d], M. Zhou[152], N. Zhou[58c], Y. Zhou[7], C.G. Zhu[58b], H.L. Zhu[58a], H. Zhu[15a], J. Zhu[103], Y. Zhu[58a], X. Zhuang[15a], K. Zhukov[108], V. Zhulanov[120b,120a], A. Zibell[174], D. Zieminska[63], N.I. Zimine[77], S. Zimmermann[50], Z. Zinonos[113], M. Zinser[97], M. Ziolkowski[148], G. Zobernig[178], A. Zoccoli[23b,23a], K. Zoch[51], T.G. Zorbas[146], R. Zou[36], M. Zur Nedden[19], L. Zwalinski[35]

[1] *Department of Physics, University of Adelaide, Adelaide; Australia*
[2] *Physics Department, SUNY Albany, Albany NY; United States of America*
[3] *Department of Physics, University of Alberta, Edmonton AB; Canada*
[4] *Department of Physics[(a)], Ankara University, Ankara; Istanbul Aydin University[(b)], Istanbul; Division of Physics[(c)], TOBB University of Economics and Technology, Ankara; Turkey*
[5] *LAPP, Université Grenoble Alpes, Université Savoie Mont Blanc, CNRS/IN2P3, Annecy; France*
[6] *High Energy Physics Division, Argonne National Laboratory, Argonne IL; United States of America*
[7] *Department of Physics, University of Arizona, Tucson AZ; United States of America*
[8] *Department of Physics, University of Texas at Arlington, Arlington TX; United States of America*
[9] *Physics Department, National and Kapodistrian University of Athens, Athens; Greece*
[10] *Physics Department, National Technical University of Athens, Zografou; Greece*
[11] *Department of Physics, University of Texas at Austin, Austin TX; United States of America*

JHEP05(2019)041

[12] *Bahcesehir University*[(a)], *Faculty of Engineering and Natural Sciences, Istanbul; Istanbul Bilgi University*[(b)], *Faculty of Engineering and Natural Sciences, Istanbul; Department of Physics*[(c)], *Bogazici University, Istanbul; Department of Physics Engineering*[(d)], *Gaziantep University, Gaziantep; Turkey*
[13] *Institute of Physics, Azerbaijan Academy of Sciences, Baku; Azerbaijan*
[14] *Institut de Física d'Altes Energies (IFAE), Barcelona Institute of Science and Technology, Barcelona; Spain*
[15] *Institute of High Energy Physics*[(a)], *Chinese Academy of Sciences, Beijing; Physics Department*[(b)], *Tsinghua University, Beijing; Department of Physics*[(c)], *Nanjing University, Nanjing; University of Chinese Academy of Science (UCAS)*[(d)], *Beijing; China*
[16] *Institute of Physics, University of Belgrade, Belgrade; Serbia*
[17] *Department for Physics and Technology, University of Bergen, Bergen; Norway*
[18] *Physics Division, Lawrence Berkeley National Laboratory and University of California, Berkeley CA; United States of America*
[19] *Institut für Physik, Humboldt Universität zu Berlin, Berlin; Germany*
[20] *Albert Einstein Center for Fundamental Physics and Laboratory for High Energy Physics, University of Bern, Bern; Switzerland*
[21] *School of Physics and Astronomy, University of Birmingham, Birmingham; United Kingdom*
[22] *Centro de Investigaciónes, Universidad Antonio Nariño, Bogota; Colombia*
[23] *Dipartimento di Fisica e Astronomia*[(a)], *Università di Bologna, Bologna; INFN Sezione di Bologna*[(b)]*; Italy*
[24] *Physikalisches Institut, Universität Bonn, Bonn; Germany*
[25] *Department of Physics, Boston University, Boston MA; United States of America*
[26] *Department of Physics, Brandeis University, Waltham MA; United States of America*
[27] *Transilvania University of Brasov*[(a)], *Brasov; Horia Hulubei National Institute of Physics and Nuclear Engineering*[(b)], *Bucharest; Department of Physics*[(c)], *Alexandru Ioan Cuza University of Iasi, Iasi; National Institute for Research and Development of Isotopic and Molecular Technologies*[(d)], *Physics Department, Cluj-Napoca; University Politehnica Bucharest*[(e)], *Bucharest; West University in Timisoara*[(f)], *Timisoara; Romania*
[28] *Faculty of Mathematics*[(a)], *Physics and Informatics, Comenius University, Bratislava; Department of Subnuclear Physics*[(b)], *Institute of Experimental Physics of the Slovak Academy of Sciences, Kosice; Slovak Republic*
[29] *Physics Department, Brookhaven National Laboratory, Upton NY; United States of America*
[30] *Departamento de Física, Universidad de Buenos Aires, Buenos Aires; Argentina*
[31] *Cavendish Laboratory, University of Cambridge, Cambridge; United Kingdom*
[32] *Department of Physics*[(a)], *University of Cape Town, Cape Town; Department of Mechanical Engineering Science*[(b)], *University of Johannesburg, Johannesburg; School of Physics*[(c)], *University of the Witwatersrand, Johannesburg; South Africa*
[33] *Department of Physics, Carleton University, Ottawa ON; Canada*
[34] *Faculté des Sciences Ain Chock*[(a)], *Réseau Universitaire de Physique des Hautes Energies — Université Hassan II, Casablanca; Centre National de l'Energie des Sciences Techniques Nucleaires (CNESTEN)*[(b)], *Rabat; Faculté des Sciences Semlalia*[(c)], *Université Cadi Ayyad, LPHEA-Marrakech; Faculté des Sciences*[(d)], *Université Mohamed Premier and LPTPM, Oujda; Faculté des sciences*[(e)], *Université Mohammed V, Rabat; Morocco*
[35] *CERN, Geneva; Switzerland*
[36] *Enrico Fermi Institute, University of Chicago, Chicago IL; United States of America*
[37] *LPC, Université Clermont Auvergne, CNRS/IN2P3, Clermont-Ferrand; France*
[38] *Nevis Laboratory, Columbia University, Irvington NY; United States of America*
[39] *Niels Bohr Institute, University of Copenhagen, Copenhagen; Denmark*
[40] *Dipartimento di Fisica*[(a)], *Università della Calabria, Rende; INFN Gruppo Collegato di Cosenza*[(b)], *Laboratori Nazionali di Frascati; Italy*
[41] *Physics Department, Southern Methodist University, Dallas TX; United States of America*

JHEP05(2019)041

[42] *Physics Department, University of Texas at Dallas, Richardson TX; United States of America*
[43] *Department of Physics*[(a)]*, Stockholm University; Oskar Klein Centre*[(b)]*, Stockholm; Sweden*
[44] *Deutsches Elektronen-Synchrotron DESY, Hamburg and Zeuthen; Germany*
[45] *Lehrstuhl für Experimentelle Physik IV, Technische Universität Dortmund, Dortmund; Germany*
[46] *Institut für Kern- und Teilchenphysik, Technische Universität Dresden, Dresden; Germany*
[47] *Department of Physics, Duke University, Durham NC; United States of America*
[48] *SUPA — School of Physics and Astronomy, University of Edinburgh, Edinburgh; United Kingdom*
[49] *INFN e Laboratori Nazionali di Frascati, Frascati; Italy*
[50] *Physikalisches Institut, Albert-Ludwigs-Universität Freiburg, Freiburg; Germany*
[51] *II. Physikalisches Institut, Georg-August-Universität Göttingen, Göttingen; Germany*
[52] *Département de Physique Nucléaire et Corpusculaire, Université de Genève, Genève; Switzerland*
[53] *Dipartimento di Fisica*[(a)]*, Università di Genova, Genova; INFN Sezione di Genova*[(b)]*; Italy*
[54] *II. Physikalisches Institut, Justus-Liebig-Universität Giessen, Giessen; Germany*
[55] *SUPA — School of Physics and Astronomy, University of Glasgow, Glasgow; United Kingdom*
[56] *LPSC, Université Grenoble Alpes, CNRS/IN2P3, Grenoble INP, Grenoble; France*
[57] *Laboratory for Particle Physics and Cosmology, Harvard University, Cambridge MA; United States of America*
[58] *Department of Modern Physics and State Key Laboratory of Particle Detection and Electronics*[(a)]*, University of Science and Technology of China, Hefei; Institute of Frontier and Interdisciplinary Science and Key Laboratory of Particle Physics and Particle Irradiation (MOE)*[(b)]*, Shandong University, Qingdao; School of Physics and Astronomy*[(c)]*, Shanghai Jiao Tong University, KLPPAC-MoE, SKLPPC, Shanghai; Tsung-Dao Lee Institute*[(d)]*, Shanghai; China*
[59] *Kirchhoff-Institut für Physik*[(a)]*, Ruprecht-Karls-Universität Heidelberg, Heidelberg; Physikalisches Institut*[(b)]*, Ruprecht-Karls-Universität Heidelberg, Heidelberg; Germany*
[60] *Faculty of Applied Information Science, Hiroshima Institute of Technology, Hiroshima; Japan*
[61] *Department of Physics*[(a)]*, Chinese University of Hong Kong, Shatin, N.T., Hong Kong; Department of Physics*[(b)]*, University of Hong Kong, Hong Kong; Department of Physics and Institute for Advanced Study*[(c)]*, Hong Kong University of Science and Technology, Clear Water Bay, Kowloon, Hong Kong; China*
[62] *Department of Physics, National Tsing Hua University, Hsinchu; Taiwan*
[63] *Department of Physics, Indiana University, Bloomington IN; United States of America*
[64] *INFN Gruppo Collegato di Udine*[(a)]*, Sezione di Trieste, Udine; ICTP*[(b)]*, Trieste; Dipartimento Politecnico di Ingegneria e Architettura*[(c)]*, Università di Udine, Udine; Italy*
[65] *INFN Sezione di Lecce*[(a)]*; Dipartimento di Matematica e Fisica*[(b)]*, Università del Salento, Lecce; Italy*
[66] *INFN Sezione di Milano*[(a)]*; Dipartimento di Fisica*[(b)]*, Università di Milano, Milano; Italy*
[67] *INFN Sezione di Napoli*[(a)]*; Dipartimento di Fisica*[(b)]*, Università di Napoli, Napoli; Italy*
[68] *INFN Sezione di Pavia*[(a)]*; Dipartimento di Fisica*[(b)]*, Università di Pavia, Pavia; Italy*
[69] *INFN Sezione di Pisa*[(a)]*; Dipartimento di Fisica E. Fermi*[(b)]*, Università di Pisa, Pisa; Italy*
[70] *INFN Sezione di Roma*[(a)]*; Dipartimento di Fisica*[(b)]*, Sapienza Università di Roma, Roma; Italy*
[71] *INFN Sezione di Roma Tor Vergata*[(a)]*; Dipartimento di Fisica*[(b)]*, Università di Roma Tor Vergata, Roma; Italy*
[72] *INFN Sezione di Roma Tre*[(a)]*; Dipartimento di Matematica e Fisica*[(b)]*, Università Roma Tre, Roma; Italy*
[73] *INFN-TIFPA*[(a)]*; Università degli Studi di Trento*[(b)]*, Trento; Italy*
[74] *Institut für Astro- und Teilchenphysik, Leopold-Franzens-Universität, Innsbruck; Austria*
[75] *University of Iowa, Iowa City IA; United States of America*
[76] *Department of Physics and Astronomy, Iowa State University, Ames IA; United States of America*
[77] *Joint Institute for Nuclear Research, Dubna; Russia*
[78] *Departamento de Engenharia Elétrica*[(a)]*, Universidade Federal de Juiz de Fora (UFJF), Juiz de Fora; Universidade Federal do Rio De Janeiro COPPE/EE/IF*[(b)]*, Rio de Janeiro; Universidade Federal de São João del Rei (UFSJ)*[(c)]*, São João del Rei; Instituto de Física*[(d)]*, Universidade de São Paulo, São Paulo; Brazil*

JHEP05(2019)041

[79] *KEK, High Energy Accelerator Research Organization, Tsukuba; Japan*
[80] *Graduate School of Science, Kobe University, Kobe; Japan*
[81] *AGH University of Science and Technology[(a)], Faculty of Physics and Applied Computer Science, Krakow; Marian Smoluchowski Institute of Physics[(b)], Jagiellonian University, Krakow; Poland*
[82] *Institute of Nuclear Physics Polish Academy of Sciences, Krakow; Poland*
[83] *Faculty of Science, Kyoto University, Kyoto; Japan*
[84] *Kyoto University of Education, Kyoto; Japan*
[85] *Research Center for Advanced Particle Physics and Department of Physics, Kyushu University, Fukuoka; Japan*
[86] *Instituto de Física La Plata, Universidad Nacional de La Plata and CONICET, La Plata; Argentina*
[87] *Physics Department, Lancaster University, Lancaster; United Kingdom*
[88] *Oliver Lodge Laboratory, University of Liverpool, Liverpool; United Kingdom*
[89] *Department of Experimental Particle Physics, Jožef Stefan Institute and Department of Physics, University of Ljubljana, Ljubljana; Slovenia*
[90] *School of Physics and Astronomy, Queen Mary University of London, London; United Kingdom*
[91] *Department of Physics, Royal Holloway University of London, Egham; United Kingdom*
[92] *Department of Physics and Astronomy, University College London, London; United Kingdom*
[93] *Louisiana Tech University, Ruston LA; United States of America*
[94] *Fysiska institutionen, Lunds universitet, Lund; Sweden*
[95] *Centre de Calcul de l'Institut National de Physique Nucléaire et de Physique des Particules (IN2P3), Villeurbanne; France*
[96] *Departamento de Física Teorica C-15 and CIAFF, Universidad Autónoma de Madrid, Madrid; Spain*
[97] *Institut für Physik, Universität Mainz, Mainz; Germany*
[98] *School of Physics and Astronomy, University of Manchester, Manchester; United Kingdom*
[99] *CPPM, Aix-Marseille Université, CNRS/IN2P3, Marseille; France*
[100] *Department of Physics, University of Massachusetts, Amherst MA; United States of America*
[101] *Department of Physics, McGill University, Montreal QC; Canada*
[102] *School of Physics, University of Melbourne, Victoria; Australia*
[103] *Department of Physics, University of Michigan, Ann Arbor MI; United States of America*
[104] *Department of Physics and Astronomy, Michigan State University, East Lansing MI; United States of America*
[105] *B.I. Stepanov Institute of Physics, National Academy of Sciences of Belarus, Minsk; Belarus*
[106] *Research Institute for Nuclear Problems of Byelorussian State University, Minsk; Belarus*
[107] *Group of Particle Physics, University of Montreal, Montreal QC; Canada*
[108] *P.N. Lebedev Physical Institute of the Russian Academy of Sciences, Moscow; Russia*
[109] *Institute for Theoretical and Experimental Physics of the National Research Centre Kurchatov Institute, Moscow; Russia*
[110] *National Research Nuclear University MEPhI, Moscow; Russia*
[111] *D.V. Skobeltsyn Institute of Nuclear Physics, M.V. Lomonosov Moscow State University, Moscow; Russia*
[112] *Fakultät für Physik, Ludwig-Maximilians-Universität München, München; Germany*
[113] *Max-Planck-Institut für Physik (Werner-Heisenberg-Institut), München; Germany*
[114] *Nagasaki Institute of Applied Science, Nagasaki; Japan*
[115] *Graduate School of Science and Kobayashi-Maskawa Institute, Nagoya University, Nagoya; Japan*
[116] *Department of Physics and Astronomy, University of New Mexico, Albuquerque NM; United States of America*
[117] *Institute for Mathematics, Astrophysics and Particle Physics, Radboud University Nijmegen/Nikhef, Nijmegen; Netherlands*
[118] *Nikhef National Institute for Subatomic Physics and University of Amsterdam, Amsterdam; Netherlands*
[119] *Department of Physics, Northern Illinois University, DeKalb IL; United States of America*

120 Budker Institute of Nuclear Physics and NSU[(a)], SB RAS, Novosibirsk; Novosibirsk State University Novosibirsk[(b)]; Russia
121 Institute for High Energy Physics of the National Research Centre Kurchatov Institute, Protvino; Russia
122 Department of Physics, New York University, New York NY; United States of America
123 Ohio State University, Columbus OH; United States of America
124 Faculty of Science, Okayama University, Okayama; Japan
125 Homer L. Dodge Department of Physics and Astronomy, University of Oklahoma, Norman OK; United States of America
126 Department of Physics, Oklahoma State University, Stillwater OK; United States of America
127 Palacký University, RCPTM, Joint Laboratory of Optics, Olomouc; Czech Republic
128 Center for High Energy Physics, University of Oregon, Eugene OR; United States of America
129 LAL, Université Paris-Sud, CNRS/IN2P3, Université Paris-Saclay, Orsay; France
130 Graduate School of Science, Osaka University, Osaka; Japan
131 Department of Physics, University of Oslo, Oslo; Norway
132 Department of Physics, Oxford University, Oxford; United Kingdom
133 LPNHE, Sorbonne Université, Paris Diderot Sorbonne Paris Cité, CNRS/IN2P3, Paris; France
134 Department of Physics, University of Pennsylvania, Philadelphia PA; United States of America
135 Konstantinov Nuclear Physics Institute of National Research Centre "Kurchatov Institute", PNPI, St. Petersburg; Russia
136 Department of Physics and Astronomy, University of Pittsburgh, Pittsburgh PA; United States of America
137 Laboratório de Instrumentação e Física Experimental de Partículas — LIP[(a)]; Departamento de Física[(b)], Faculdade de Ciências, Universidade de Lisboa, Lisboa; Departamento de Física[(c)], Universidade de Coimbra, Coimbra; Centro de Física Nuclear da Universidade de Lisboa[(d)], Lisboa; Departamento de Física[(e)], Universidade do Minho, Braga; Departamento de Física Teorica y del Cosmos[(f)], Universidad de Granada, Granada (Spain); Dep Física and CEFITEC of Faculdade de Ciências e Tecnologia[(g)], Universidade Nova de Lisboa, Caparica; Portugal
138 Institute of Physics of the Czech Academy of Sciences, Prague; Czech Republic
139 Czech Technical University in Prague, Prague; Czech Republic
140 Charles University, Faculty of Mathematics and Physics, Prague; Czech Republic
141 Particle Physics Department, Rutherford Appleton Laboratory, Didcot; United Kingdom
142 IRFU, CEA, Université Paris-Saclay, Gif-sur-Yvette; France
143 Santa Cruz Institute for Particle Physics, University of California Santa Cruz, Santa Cruz CA; United States of America
144 Departamento de Física[(a)], Pontificia Universidad Católica de Chile, Santiago; Departamento de Física[(b)], Universidad Técnica Federico Santa María, Valparaíso; Chile
145 Department of Physics, University of Washington, Seattle WA; United States of America
146 Department of Physics and Astronomy, University of Sheffield, Sheffield; United Kingdom
147 Department of Physics, Shinshu University, Nagano; Japan
148 Department Physik, Universität Siegen, Siegen; Germany
149 Department of Physics, Simon Fraser University, Burnaby BC; Canada
150 SLAC National Accelerator Laboratory, Stanford CA; United States of America
151 Physics Department, Royal Institute of Technology, Stockholm; Sweden
152 Departments of Physics and Astronomy, Stony Brook University, Stony Brook NY; United States of America
153 Department of Physics and Astronomy, University of Sussex, Brighton; United Kingdom
154 School of Physics, University of Sydney, Sydney; Australia
155 Institute of Physics, Academia Sinica, Taipei; Taiwan
156 E. Andronikashvili Institute of Physics[(a)], Iv. Javakhishvili Tbilisi State University, Tbilisi; High Energy Physics Institute[(b)], Tbilisi State University, Tbilisi; Georgia
157 Department of Physics, Technion, Israel Institute of Technology, Haifa; Israel

JHEP05(2019)041

[158] *Raymond and Beverly Sackler School of Physics and Astronomy, Tel Aviv University, Tel Aviv; Israel*
[159] *Department of Physics, Aristotle University of Thessaloniki, Thessaloniki; Greece*
[160] *International Center for Elementary Particle Physics and Department of Physics, University of Tokyo, Tokyo; Japan*
[161] *Graduate School of Science and Technology, Tokyo Metropolitan University, Tokyo; Japan*
[162] *Department of Physics, Tokyo Institute of Technology, Tokyo; Japan*
[163] *Tomsk State University, Tomsk; Russia*
[164] *Department of Physics, University of Toronto, Toronto ON; Canada*
[165] *TRIUMF[(a)], Vancouver BC; Department of Physics and Astronomy[(b)], York University, Toronto ON; Canada*
[166] *Division of Physics and Tomonaga Center for the History of the Universe, Faculty of Pure and Applied Sciences, University of Tsukuba, Tsukuba; Japan*
[167] *Department of Physics and Astronomy, Tufts University, Medford MA; United States of America*
[168] *Department of Physics and Astronomy, University of California Irvine, Irvine CA; United States of America*
[169] *Department of Physics and Astronomy, University of Uppsala, Uppsala; Sweden*
[170] *Department of Physics, University of Illinois, Urbana IL; United States of America*
[171] *Instituto de Física Corpuscular (IFIC), Centro Mixto Universidad de Valencia — CSIC, Valencia; Spain*
[172] *Department of Physics, University of British Columbia, Vancouver BC; Canada*
[173] *Department of Physics and Astronomy, University of Victoria, Victoria BC; Canada*
[174] *Fakultät für Physik und Astronomie, Julius-Maximilians-Universität Würzburg, Würzburg; Germany*
[175] *Department of Physics, University of Warwick, Coventry; United Kingdom*
[176] *Waseda University, Tokyo; Japan*
[177] *Department of Particle Physics, Weizmann Institute of Science, Rehovot; Israel*
[178] *Department of Physics, University of Wisconsin, Madison WI; United States of America*
[179] *Fakultät für Mathematik und Naturwissenschaften, Fachgruppe Physik, Bergische Universität Wuppertal, Wuppertal; Germany*
[180] *Department of Physics, Yale University, New Haven CT; United States of America*
[181] *Yerevan Physics Institute, Yerevan; Armenia*

[a] *Also at Borough of Manhattan Community College, City University of New York, NY; United States of America*
[b] *Also at California State University, East Bay; United States of America*
[c] *Also at Centre for High Performance Computing, CSIR Campus, Rosebank, Cape Town; South Africa*
[d] *Also at CERN, Geneva; Switzerland*
[e] *Also at CPPM, Aix-Marseille Université, CNRS/IN2P3, Marseille; France*
[f] *Also at Département de Physique Nucléaire et Corpusculaire, Université de Genève, Genève; Switzerland*
[g] *Also at Departament de Fisica de la Universitat Autonoma de Barcelona, Barcelona; Spain*
[h] *Also at Departamento de Física Teorica y del Cosmos, Universidad de Granada, Granada (Spain); Spain*
[i] *Also at Departamento de Física, Instituto Superior Técnico, Universidade de Lisboa, Lisboa; Portugal*
[j] *Also at Department of Applied Physics and Astronomy, University of Sharjah, Sharjah; United Arab Emirates*
[k] *Also at Department of Financial and Management Engineering, University of the Aegean, Chios; Greece*
[l] *Also at Department of Physics and Astronomy, University of Louisville, Louisville, KY; United States of America*

[m] Also at Department of Physics and Astronomy, University of Sheffield, Sheffield; United Kingdom
[n] Also at Department of Physics, California State University, Fresno CA; United States of America
[o] Also at Department of Physics, California State University, Sacramento CA; United States of America
[p] Also at Department of Physics, King's College London, London; United Kingdom
[q] Also at Department of Physics, St. Petersburg State Polytechnical University, St. Petersburg; Russia
[r] Also at Department of Physics, Stanford University; United States of America
[s] Also at Department of Physics, University of Fribourg, Fribourg; Switzerland
[t] Also at Department of Physics, University of Michigan, Ann Arbor MI; United States of America
[u] Also at Giresun University, Faculty of Engineering, Giresun; Turkey
[v] Also at Graduate School of Science, Osaka University, Osaka; Japan
[w] Also at Hellenic Open University, Patras; Greece
[x] Also at Horia Hulubei National Institute of Physics and Nuclear Engineering, Bucharest; Romania
[y] Also at II. Physikalisches Institut, Georg-August-Universität Göttingen, Göttingen; Germany
[z] Also at Institucio Catalana de Recerca i Estudis Avancats, ICREA, Barcelona; Spain
[aa] Also at Institut für Experimentalphysik, Universität Hamburg, Hamburg; Germany
[ab] Also at Institute for Mathematics, Astrophysics and Particle Physics, Radboud University Nijmegen/Nikhef, Nijmegen; Netherlands
[ac] Also at Institute for Particle and Nuclear Physics, Wigner Research Centre for Physics, Budapest; Hungary
[ad] Also at Institute of Particle Physics (IPP); Canada
[ae] Also at Institute of Physics, Academia Sinica, Taipei; Taiwan
[af] Also at Institute of Physics, Azerbaijan Academy of Sciences, Baku; Azerbaijan
[ag] Also at Institute of Theoretical Physics, Ilia State University, Tbilisi; Georgia
[ah] Also at Instituto de Física Teórica de la Universidad Autónoma de Madrid; Spain
[ai] Also at Istanbul University, Dept. of Physics, Istanbul; Turkey
[aj] Also at LAL, Université Paris-Sud, CNRS/IN2P3, Université Paris-Saclay, Orsay; France
[ak] Also at Louisiana Tech University, Ruston LA; United States of America
[al] Also at LPNHE, Sorbonne Université, Paris Diderot Sorbonne Paris Cité, CNRS/IN2P3, Paris; France
[am] Also at Manhattan College, New York NY; United States of America
[an] Also at Moscow Institute of Physics and Technology State University, Dolgoprudny; Russia
[ao] Also at National Research Nuclear University MEPhI, Moscow; Russia
[ap] Also at Physics Dept, University of South Africa, Pretoria; South Africa
[aq] Also at Physikalisches Institut, Albert-Ludwigs-Universität Freiburg, Freiburg; Germany
[ar] Also at School of Physics, Sun Yat-sen University, Guangzhou; China
[as] Also at The City College of New York, New York NY; United States of America
[at] Also at The Collaborative Innovation Center of Quantum Matter (CICQM), Beijing; China
[au] Also at Tomsk State University, Tomsk, and Moscow Institute of Physics and Technology State University, Dolgoprudny; Russia
[av] Also at TRIUMF, Vancouver BC; Canada
[aw] Also at Universita di Napoli Parthenope, Napoli; Italy
[*] Deceased

JHEP05(2019)041